INTELLIGENT VENTILATED WINDOW PERFORMANCE AND FURTHER IMPROVEMENTS: A CASE STUDY IN A DANISH PRIMARY SCHOOL

MASTER THESIS PROJECT

Indoor Environmental and Energy Engineering
Department of Civil Engineering
Aalborg University

AALBORG UNIVERSITY
DENMARK

Marta Bonet Arbos, Leire Chavarri Remiro and Aleksandra Maria Tutaj

Supervisors: Per Kvols Heiselberg, Chen Zhang and Hicham Johra
Collaboration with: VentilationsVinduet
June 2019

AALBORG UNIVERSITY
STUDENT REPORT

MSc at School of Engineering and Science
Thomas Manns Vej 23
9220 Aalborg Øst

Title:

Intelligent ventilated window performance and further improvements: a case study in a Danish Primary School

Project:

Master Thesis

Project period:

September 2018 - June 2019

Participants:

Marta Bonet Arbos
Leire Chávarri Remiro
Aleksandra Maria Tutaj

Supervisors:

Per Kvols Heiselberg
Chen Zhang
Hicham Johra

Synopsis:

Indoor environment of the buildings has a major impact on the health and well-being of the occupants. Therefore, it is necessary to design a ventilation system that provides enough fresh air to remove the contaminants, providing comfortable indoor conditions. This project presents a ventilated window during a case study in Ødis Primary School - Kolding Kommune, Denmark. The ventilated window aims to improve the indoor climate avoiding a decentralized ventilation system. This clean and passive solution works by the combination of natural driving forces and mechanical or natural exhaust in the rooms.The main advantage is the ability to adapt to different indoor and outdoor conditions due to their dynamic working modes which significantly impact their functionality. Further experiments of the window performance in Aalborg University laboratory give an extended analysis of the window possible behaviour. Eventually, the application of a suggested control strategy could achieve a more efficient ventilation system.
The project is implemented in partnership with Ventilationsvinduet Company (Horn Group).

Pages: 139
Finished: 7th June 2019

Acknowledgements

Major thanks are directed towards our supervisors Per Kvols Heiselberg, Chen Zhang and Hicham Johra from Aalborg University for their cooperation, assistance and guidance through this project.

We would like to thank the laboratory technician Lars Isbach Poulsen for the technical help with the experimental setup and the rest of technicians at Aalborg University for all their assistance in the test facility. A thank you is also addressed to Hicham Johra for providing all-round assistance during the planning and execution of the measurements.

A special thanks to Ødis School, all the kids and teachers that had the patience and consideration with the equipment during the six months of the measurement in the classrooms. Also to Kenneth Munk Kock, the technical service manager at the school who has always been available for us.

Moreover, we would like to thank our colleges for their support, good working environment throughout the master education.

Last, but not least, we appreciate Poul Horn and Aidas Janulis from *Ventilationsvinduet* company for involving us in the project, allowing us to understand and test their designs.

Abstract

Buildings in a need of renovation represent a large energy consumption source. However, it is no longer enough to focus just on the energy framework of buildings without particular interest in the indoor environment. Windows are one of the building elements on the façade that, if adequately sized, can provide with appropriate visual comfort, heat gains and natural ventilation. Nevertheless, natural ventilated buildings cannot always provide with the required temperature and ventilation rate and in addition its control is always user dependent. For this reason, this paper focuses on the performance and indoor environment provided by two different designs of ventilated windows. This technology allows a self-controlled ventilation where the air supplied to the room is at a higher temperature than the air outdoors. In addition, its dynamic working modes can adapt to the different indoor and outdoor conditions.

Influence of the window performance in indoor environment in a primary school is analyzed. Results show that the window performance is enhanced the most together with a mechanical extraction. With regards to the thermal performance, the height of the cavity and the inclusion of blinds between the panes improve the ability of preheating the air. However, this phenomena is negatively affected by high flow rates. In terms of indoor comfort, a first window design does not provide with enough ventilation and suitable control strategy to remove the excessive CO_2 concentrations reported in the rooms. Consequently, a new window design together with a suggested control strategy aims to address the problem of poor air quality at the school.

Further studies will permit to test the suggested control strategy and prove that ventilated windows are a solution that can serve high and variable occupancy loads and avoid a decentralized ventilation system. There is a large potential in which ventilated windows would be an effective solution. However, it is crucial for their effectiveness to have a controlled mechanical exhaust, a window design that enhances the temperature rise through the window and assure a system with enough number of windows in order provide an optimal air flow rate.

Preface

This Master Thesis is conducted by group 1.216-2 of the Master of Science program at Aalborg University, Indoor Environmental and Energy Engineering. The report is titled *Intelligent ventilated window performance and further improvements: a case study in a Danish Primary School*. It has been written in the period from September 2018 to June 2019 and covers 50 ECTS points.

Reading guide

All of the symbols, acronyms, abbreviations are listed in the chapter , named Nomenclature. Literature references used in this report are collected in a chapter named 'Bibliography', and uses the Harvard method for sorting. Equations, figures and tables are referenced under the given chapter. For instance, the second equation in chapter one will be named as equation 1.2. The decimal separator is represented with a "." Limits from regulations on figures are represented as straight horizontal or vertical red line. In addition, some data is represented by boxplots. The definition and criteria by which the boxplots are created can be found in Appendix C.1.

The report is divided into the main report and the appendices. The main report is a representation of the considerations, used methods and results while in the appendix remains the documentation and any extra information that is considered important for the understanding of this project. Appendices are named by capital letters. For instance, the second appendix is denoted as B.

Aleksandra Maria Tutaj	Leire Chavarri Remiro	Marta Bonet Arbos

Nomenclature

Symbol	Description	Unit
A	Area	m^2
ACH	Air changer per hour	1/h
AHR	Active Heat Recovery	[-]
$ANOVA$	Analysis of Variance	
c	CO_2 concentration in the room	m^3/m^3
c_0	CO_2 concentration in the room at t=0	m^3/m^3
c_e	CO_2 concentration in the exhaust	ppm
c_i	CO_2 concentration in the inlet	m^3/m^3
$CLO - mode$	Valves closed	
$C - mode$	Valves in cooling mode	
C_{out}	CO_2 concentration outside	ppm
C_{oz}	CO_2 concentration in the occupied zone	ppm
cp	Specific heat capacity of the air	J/kg· K
ΔP	Pressure difference	Pa
DF	Daylight Factor	%
DR	Draught Rate	%
HR	Heat Recovery	[-]
$HVAC$	Heating Ventilation and Air Conditioning	
I_e	Illuminance outside	lux
I_i	Illuminance inside	lux
LT	Light Transmittance	%
$Mech.Vent$	Mechanical ventilation	
N	Amount of people	[-]
$Nat.Vent$	Natural ventilation	
occ	Occupancy	
OZ	Occupied Zone	
P	Pressure	Pa
P_1	Pole of anemometers next to the window	
P_2	Pole of anemometers in the occupied zone	
$P_{2.1}$	Pole of anemometers in front of the door	
$PH - mode$	Valves in preheating mode	

continues in next page

PHR	Passive Heat recovery	[-]
$q_{actual-DE}$	Actual air flow rate by dilution equation	l/s
q_b	Ventilation rate from building emissions	l/s per m^2
q_{cav}	Air flow through the cavity	l/s
$q_{optimal-DE}$	Optimal air flow by dilution equation	l/s
$Q_{recovered}$	Heat recovered	W
q_s	Air flow rate supplied	l/s
q_{tot}	Total air flow rate	l/s
q_w	Air flow through the window	l/s
$R1$	Room 1	
$R2$	Room 2	
Rad	Solar Radiation	W/m^2
RH	Relative Humidity	%
RH_w	Average of the relative humidity	%
ρ	Density of air	kg/m^3
SA	Sensitivity Analysis	
t	Time	h
T_1	Average of bottom cavities temperature	°C
T_2	Average of top cavities temperature	°C
Ta	Local air temperature	°C
T_{BOT}	Temperature at the bottom part of the cavity	°C
$Temp.$	Temperature	°C
T_{IN}	Temperature in the room	°C
T_{OUT}	Temperature outside	°C
T_{TOP}	Temperature at the top part of the cavity	°C
T_u	Local mean air velocity	m/s
U	Thermal transmittance	W/m$^2\cdot$ K
V	Volume	m^3
Va	Local turbulence intensity	%
VAV	Variable Air Volume	
VOC	Volatile Organic Compounds	
$WT1$	Window Type 1	
$WT2$	Window Type 2	
ε_c	Concentration effectiveness	[-]

Contents

1 Introduction

Buildings are the main source of energy consumption and emissions, resulting in approximately 40% of the total energy consumption and 36% of the CO_2 emissions in the European Union. Nowadays, around 35% of buildings in the EU are over 50 years old and energy inefficient [European Commission, 2019]. Therefore, the need for building renovation is receiving increased attention, due to aging of the construction [Jensen et al., 2018]. Building materials and services are reaching their lifespan.

Moreover, building adjustment to modern standard became a challenge for the building stock. New directives, published by the European Union, demand an increased energy performance by the current building stocks [Hamid et al., 2018]. In order to adjust to these strategies, the building renovation is relevant and necessary action [Almeida and Ferreira, 2017]. By renovating the building stock, the total energy consumption of the EU can be reduced by 5-6% and CO_2 emission reduced by about 5% [European Commission, 2019]. Hence, limitation on the harmful climate impact is assessed [Jensen et al., 2018].

In addition, the improvement of the energy performance of buildings can ensure a more affordable housing [Jensen et al., 2018]. More importantly, due to a better indoor climate, health, comfort and well-being is improved. Consequently, the quality of life and social sustainability of the occupants is enhanced [European Commission, 2019]. The above mentioned are the general provisions of proper thermal conditions and indoor climate in buildings [BR 18, 2018]. When dealing with buildings occupied by the children, these becomes a matter of significant importance.

Nowadays, the renovation of old buildings uses an integrated approach with focus not only on the thermal insulation, airtightness and heat recovery, but also on an optimal use of sustainable technologies. For instance, the application of passive solar gains, passive cooling, daylighting and natural ventilation [Heiselberg, 1999]. It has been observed that retrofitting of existing buildings that are originally designed with natural ventilation, have a negative effect on the indoor climate and residents well-being. This is due to the fact that in order to reduce their energy consumption, buildings become highly air-tight [Kamendere et al., 2015]. However, the installation of a mechanical ventilation system is often a more complex procedure. It is of higher cost and it can create high disturbances to the occupants during the process. Additionally, buildings with low ceiling become an issue for the ducts system fitting [Kamendere et al., 2015].

As the energy-efficient ventilation system is a prerequisite for low energy consumption [Heiselberg, 2002], it is crucial to choose wisely the ventilation strategy. The design of energy-efficient ventilation system in educational buildings has become a question of using either natural or mechanical systems [Heiselberg, 2002]. The school institutions and the teaching rooms are exposed to high density occupancy and several variations during the day. In that manner, it is challenging to provide with an adequate ventilation rate relaying only on natural ventilation strategies. Moreover, with natural ventilation by itself, an efficient level of performance cannot be guaranteed. As Heiselberg [2002] says, in the majority of cases, the most beneficial would be a combination of natural and mechanical ventilation systems adapted to indoor and outdoor conditions.

Speaking of systems that can be adjusted to the mentioned conditions, the ventilated window is introduced. This is a passive technology that was mainly aimed for the renovation sector, especially in old buildings without energy efficient ventilation systems [Heiselberg et al., 2013]. This window can be used to reduce the energy demand and improve the indoor comfort environment [Liu et al., 2017].

This report focuses on the ventilated window produced by the company *VentilationsVinduet*. It consists of a double glazed window with a ventilated air gap in between. The key difference from a conventional window is the dynamic working principle. It allows to supply with fresh air at different temperatures depending on the outdoor conditions. The working principle for the categorized functionalities are presented in Figure 1.1.

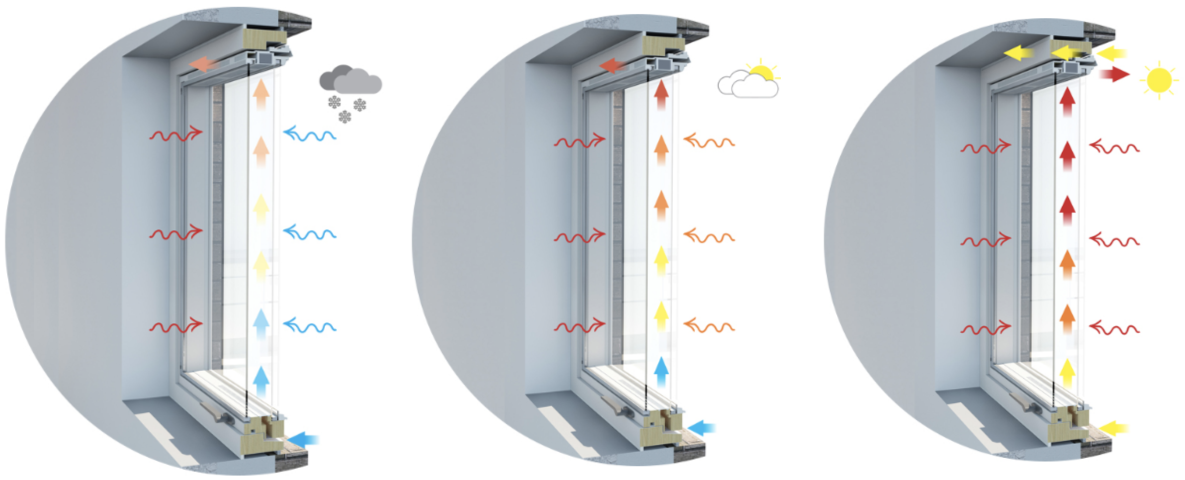

(a) *(b)* *(c)*

Figure 1.1: Working principle of the ventilated windows designed by [Horn Group, 2019].

If cold outdoor conditions occurs, as shows Figure 1.1a, an inlet opening allows the air to enter to the cavity while it is warmed up by heat transfer from the building and solar radiation. If this situation happens in a sunny day, solar radiation becomes the main source to heat up the air, still maintaining an influence of the building heat losses on that process, as it can be seen in Figure 1.1b. However, it can happen that the air within the air cavity is warm enough to be supplied indoors. In that case, Figure 1.1c presents an option of bypassing the air from outdoors, directly to the internal space. At the same time, a circulation of air through the cavity avoids excessive overheating by sending the air outside again when room conditions are already warm.

The ventilated window influences positively on the occupants comfort in contrast to a conventional window. Preheating the air before being supplied indoors, results in minimizing the risk of draught and reducing discomfort of the occupants. Additionally, even though windows are one of the weakest building envelope components in terms of heat losses, it is the only element that apart from heat losses, also contributes with heat gains. This window design pursues an aesthetic design exploiting these features.

In general, it is a remarkable solution that can serve a broad market. The main application could be in buildings that need renovation where natural ventilation strategies becomes insufficient. Moreover, it can improve newly erected buildings to avoid costly decentralized ventilation system.

1.1 Aim of the study

This project focuses on the analysis of the performance of the ventilated window and its influence on the indoor environment. The onsite investigation of the indoor environment takes place in two of the classrooms of the primary school located in Ødis Primary School, Kolding Kommune, Denmark. Building users notified the following problems: overheating, draught, glare and not comfortable air quality. Through an experimental analysis, the preceding stated problems are evaluated.

The aim of the project is to analyze the indoor comfort in the classrooms and understand the main problems that arise when the ventilation system consist of a ventilated window. Two window designs are tested. A passively controlled window is studied first and a second design that is electronically controlled. For this reason, it is important to asses the performance of both windows in terms of comfort, efficient design and an optimal control strategy that could fit for a high density occupancy such as a school.

The main objectives that the following project pursues are summarized below:

1. How does the window influence the indoor environment under the existing conditions?
2. How the surrounding conditions are affecting the window performance?
3. What is the visual comfort provided by the windows?
4. What is the optimal control strategy design to provide comfortable indoor environment in the classrooms?

2

Literature Review

In this chapter, literature review regarding ventilated window and indoor environment in school is presented. The aim of this chapter is to explain the current state of art on the ventilated window. The following review presents some of the most relevant studies and experiments that are addressed and outlined. Many topics concerning energy transfer, airflow through the double glass and air temperature have been investigated to expand the knowledge within these subjects. Furthermore, based on the studies, the explanation of an expected and necessary control strategy from the window itself is included. At last, the review about indoor environment in schools is presented. The problems that can possibly occur in school and their assessment method.

2.1 Ventilated Window Benchmark

A ventilated window consists of a double sheet ventilated glass window. It is a passive natural ventilation, which means a solution based on the use of natural forces. The gap between panes is supplied with fresh air from outside. By the incident solar radiation on the window's surface, the air is heated up creating a buoyancy effect. This heat is transferred from the glass to the air by convection, makes the flow to be induced upwards. In the end, air is supplied to the room at a higher temperature than outdoors. This heat transfer by convection depends on the solar radiation, internal loads, glass surface area and the air flow velocity.

Figure 2.1 presents the ventilated window technology which offers preheating, cooling and bypass mode. It permits the air to move in different paths by its dynamic working modes. From the intake of fresh air in the bottom part, the air moves up through the cavity and thereby gets preheated and transferred indoors. This strategy is named preheating mode. The technology and the idea of preheating the air is also the main principle for multiple skin facades systems [Markussen, 2007]. Nonetheless, only when warm outdoor conditions are experienced, the air in the cavity can be returned outside, instead to the internal space. Thereby, the circulated air is again preheated, but pushed outdoors in cooling mode. This air path eludes heat transfer from the inner pane, avoiding overheating the internal space. The last functionality offered by the window is bypass mode. It allows the ambient air to go directly from outside to inside by an opening in the upper part. It is useful when there is no need for the outdoor air to be warmed up. It can be transferred straight from outside.

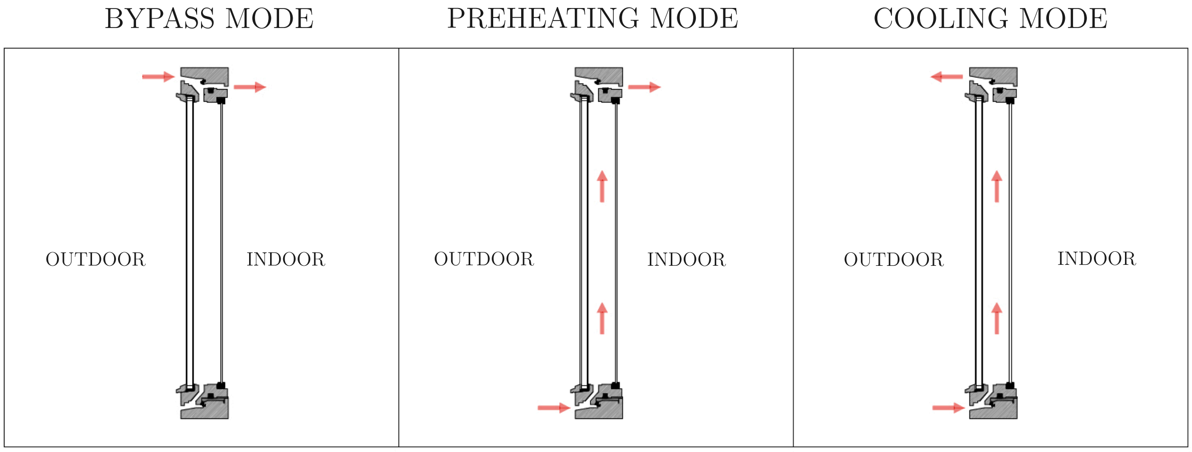

Figure 2.1: Ventilation window principles and working modes.

The EU CLIMAWIN project by Heiselberg et al. [2013] was a collaboration between several research partners with the goal of developing a high performance window based on these operating modes. In that research, 15 different ventilated window typologies were tested in which different panes, shadings and glazing configurations were analyzed. Simulations about the window performance using WIS software were carried out for four orientations and four locations representing north, south, east and west in Europe. The evaluation of window typologies was carried out first based on lowering the energy consumption from heating and cooling demand. Furthermore, the window giving the best thermal comfort in terms of internal surface temperature and supply air temperature was investigated.

Overall, out of the all 15 tested samples, three typologies were selected whose configurations are presented in Figure 2.2. Results showed that for all four climate references a ventilated window is able to improve the indoor climate compared to a traditional window. With regards to the design of the layers configuration, the position of the single glazing is preferably on the internal side in terms of inlet air temperature. Fact visible in all three selected samples. In terms of energy consumption, is slightly better on the external side. However, the positioning of a low emissivity coating on the pane is preferably on the outer glass, as sample 1 and sample 13 shows.

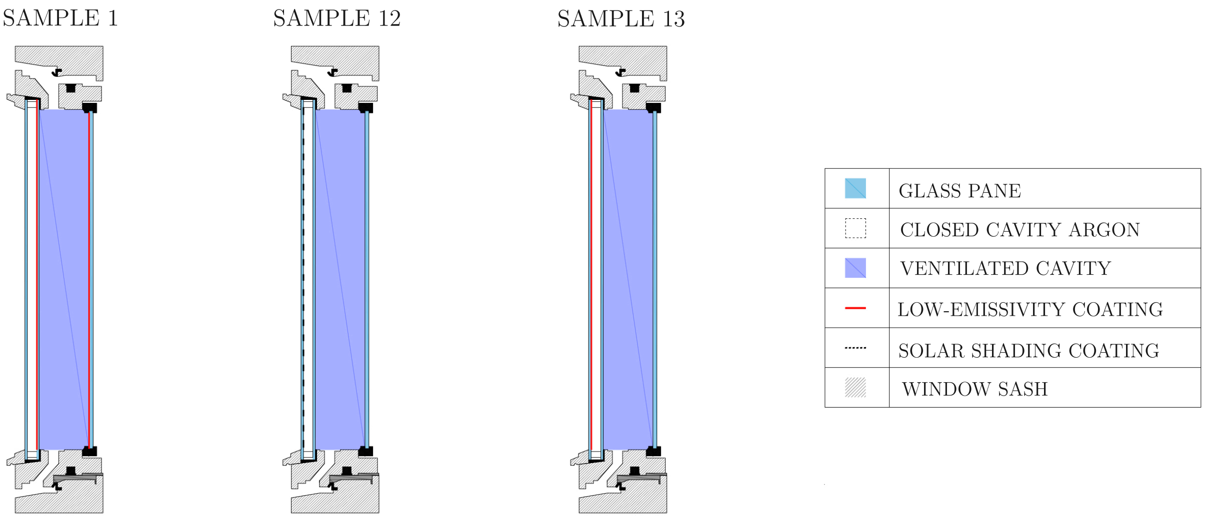

Figure 2.2: Selected window samples with different configurations from article Liu et al. [2017].

Sample 12 was concluded to be the most beneficial window typology during summer. Solar control glass helps to block out solar radiation preventing possible overheating in summer. For a better indoor performance it was sample 1. In terms of indoor environment sample 13 and sample 1 provide the same comfort levels. However, sample 13 performed slightly worse in energy performance but it was cheaper [Liu et al., 2017]. They have the same structure, except for a double low emissivity layer in sample 1. For this reason, it reduces the energy consumption. From the selected samples it is important to highlight that all closed cavities are filled with Argon, not air. Simulations from Heiselberg et al. [2013] showed that they performed better.

Another relevant study by Appelfeld and Svendsen [2011] aimed to determine the thermal transmittance of a ventilated window by using a hot-box. The window was exposed to eight different airflow rates between 1.3 l/s to 8 l/s. Results showed that the energy efficiency is dependent on air flow rate. It decreases with higher ventilation rates. In that case study, a maximum of 6 l/s showed that the ventilated window was no longer beneficial. High air flows increased heat losses due to the increased window thermal transmittance, making it larger than the amount of energy regained by preheating. The investigation concluded that the heat was mainly exchanged in the frame and it suggested not to use ventilated windows in buildings with high required ventilation rates and small number of windows. In addition to the experimental work, the article formed a unified methodology for the assessment of the energy performance and the heat transmittance. The traditional static U-value of a window is no longer applicable once the air is circulating through the gap. Heat losses are dependent on the air conditions.

Furthermore, with regards to the window thermal performance, the report from Carlos et al. [2011] describes a numerical simulations. Additionally, an experiment was conducted on the south façade during winter season. Air flow rate, outdoor air temperature and solar irradiance were varied with the aim to predict the temperature rise (difference between outdoor and supplied temperature) and the useful energy of the delivered air. These results were validated by comparing them with the numerical simulations. Overall, the study states that the heat balance of the window changes due to the temperature variation between outdoor and indoor. Heat balance increases when solar radiation increases, plus the lower flow rate, the higher heat balance is achieved. The study by Carlos et al. [2010] supports the working principle of a ventilated window by proving that it is able to supply preheated air even in winter time, recovering part of the heat losses from indoors and by transferring solar radiation into heat gains.

2.1.1 Control Automation

Due to the ability to change modes to preheating, cooling or bypass of a ventilated window, it is of a high importance to incorporate a control strategy that adapts to the indoor comfort of the occupants and outdoor conditions. Especially, if it is supported by a mechanical exhaust ventilation system that can assure a minimum ventilation rate [Markussen, 2007]. Natural ventilation system is a sustainable an clean technology that when efficiently controlled, it is well accepted by the users [Heiselberg, 2002]. Heiselberg et al. [2013] describes the development of the electronic operation of an auto-regulated natural ventilation system for a high performance window. In addition, it includes automatic controlled blinds. Overall, the ventilated window became a common practice and popular solution for the housing [Carlos et al., 2011]. However, the implementation of the system adding automatic control is not yet well documented and more research in that area is required.

2.2 Indoor Environment in Schools

Indoor environment in schools started to be a priority since the raising awareness of the relationship between environment, health and academic performance. With regards to schools in Denmark, ICIEE-DTU [2019] has conducted researches about the impact of indoor environment factors on human comfort, health and productivity. This is an issue because in Denmark most of the school buildings are ventilated by natural manner, system which could produce a risk of poor indoor environment associated with an insufficient ventilation rate and supported by the lack of any mechanical ventilation system.

Between energy efficiency in buildings and indoor environment quality, more emphasis is being given to energy efficiency. Nowadays, the absence of any standard or reference document relating to the appropriate design of classrooms is worsening the situation [Singh et al., 2019]. Moreover, most pupils spend over 30% of their life in schools and about 70% of that time inside a classroom during school days [Hou et al., 2015]. Identifying the key hazards to which children are exposed due to their special vulnerability, it is an obligation to avoid the risk of sick building syndrome symptoms. Children are more prone to be affected by air pollution than other age groups due to their underdeveloped immune systems and higher intake volumes of air per kilogram of body mass [Trompetter et al., 2018].

Through the Indoor Air Pollution in Schools Project by Carrer et al. [2002], highlighted the need for a EU program aiming to provide a healthy school environment [Kalimeri et al., 2016]. Poor indoor air quality (IAQ) has long been recognized as a cause of occupant discomfort, adverse health effects, increased absenteeism and degraded cognitive performance [Johnson et al., 2018].

Student performance depends on the ability to concentrate and on attendance levels, both closely related to the indoor environment. The study of Menå and Larsen [2010] states with a statistical significance that reducing the temperature setpoint from 25 °C to 20°C and doubling ventilation rate from 5 to 10 l/s per person, the academical performance of the students is increased.

Poor indoor air quality may be a consequence of air pollution. This research by Menå and Larsen [2010] on the field, compares results of measured CO_2 concentrations and temperatures from similar experiments performed simultaneously in schools from Denmark, Norway and Sweden. The same equipment was used, giving usable CO_2 data from 743 classrooms in 330 schools. From the participating classrooms, 56% measured CO_2 concentrations higher than a 1000 ppm in Danish schools, whereas only between 16-21% of them were above the limit in Norway and Sweden, respectively. One explanation can be found in the type of ventilation; less than half of the participating Danish schools had mechanical ventilation, as opposed to more than 90% in Sweden and almost 80% in Norway.

Different approaches and strategies are suggested when poor indoor air quality is reported. More usage of natural ventilation, changing to mechanical ventilation or building renovation improving the enclosure with higher quality materials [Almeida et al., 2015].

Natural ventilation is the most common ventilation type in Danish schools [ICIEE-DTU, 2019]. Ventilation is often relying only on cracks in the facade and on manual opening of windows. In Denmark, which has a temperate climate, windows are not opened regularly during the winter season. It means that ventilation is poor during the heating season in many naturally ventilated schools.

Figure 2.3 shows a diagram where the most repeated concepts mentioned in researches about indoor environment in school are listed. Highlighted in red are the ones selected and further studied in this project. This report focuses on why there is a poor indoor environment more than the consequences from it.

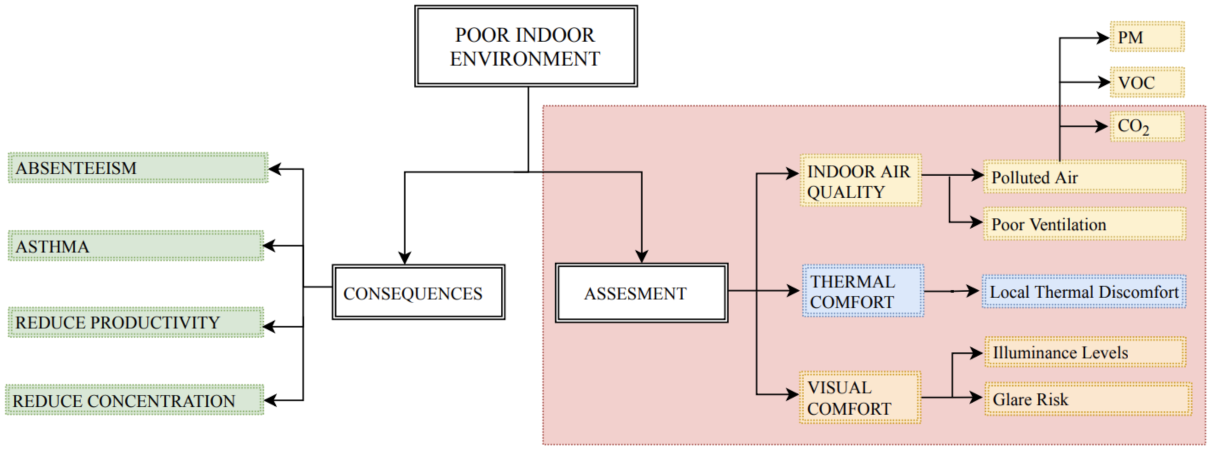

Figure 2.3: Diagram of the main ideas from researches about Indoor Environment in Schools.

The goal is to achieve healthy, comfortable and productive indoor environments, with minimal energy consumption. Although saving energy is important, it should not compromise the health and well-being of children. It is worth mentioning that nonexistent research has been found about the effect of ventilated windows for educational buildings.

3

Problem Statement

This project is a case study based on the work from Liu et al. [2017], according to the description of the window working modes and its impact on indoor conditions. Once the theoretical background of the window functionalities is investigated, an experimental assessment of the window is studied. In this chapter, the methodology of the thesis is explained.

The ventilated window has proven to be highly influential on energy and heating demand for the building renovation sector. However, these have not been thoroughly investigated with a real case study approach for this window design. As a result, this thesis aims to study the above mentioned performance. The concerned windows were installed in Ødis School in Kolding, Denmark, as a pilot project for the company *VentilationsVinduet*. The design of the ventilated window opens up a whole new possibilities for establishing good indoor climate with minimal work required.

Based on the perception of the users in the classrooms, several problems have been experienced in the school. Among them, lack of fresh air in the rooms, glare problems, issues with too high CO_2 level and overheating.

3.1 Assessment Method

The project is divided into two parts. The first stage of this project concerns the first window design - window type 1 (WT1) installed in the school during the winter season. Detailed analysis of the indoor conditions includes CO_2 concentration level, daily occupancy profile, air temperature, air velocity, indoor temperature, relative humidity, window air temperatures, air flow rate exhaust and visual comfort in the classrooms. Additionally, the different working principle are investigated as a part of the experimental analysis.

The second stage includes an analysis of an improved design - window type 2 (WT2), which is expected to contribute to a better indoor environment and visual comfort. The presumption relies on the electronic controlled design. Experimental tests are performed in Aalborg University laboratory. Its purpose is to study the supplied air flow rate per cavity, pressure drop correlation, heat recovery rate and visual comfort. In addition, a sensor test for the electronic control is made. The aim is to verify if the sensors are acceptable and precise enough for measuring the indoor environment conditions. Lastly, a control strategy design for the school is proposed with the objective to enhance its indoor environment.

Figure 3.1 outlines the methodology for the following master thesis. The report is divided into three analysis. At the flowchart the organization of this research is visualized: introduction and conditions present the background on the report and defines the specific goals to be addressed, while framing this investigation. Experimental analysis includes the theory behind the investigations and both empirical analysis for window type 1 and 2. The last analysis is called recapitulation, including discussion, suggest further improvements and the conclusion, which are the overall assessment.

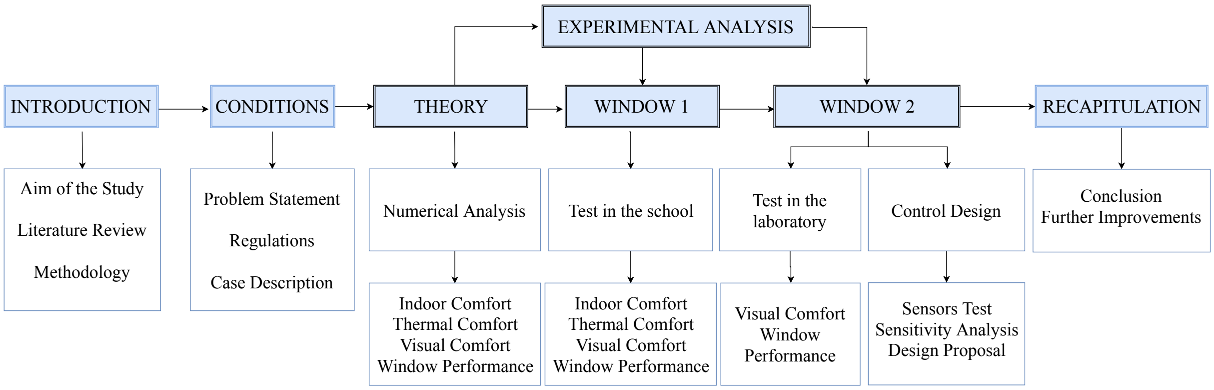

Figure 3.1: Methodology chart of the following project.

Figure 3.2 shows the systematic approach to plan the execution of the measurements. The following diagram focusing on indoor conditions, outdoor condition and window performance has been used :

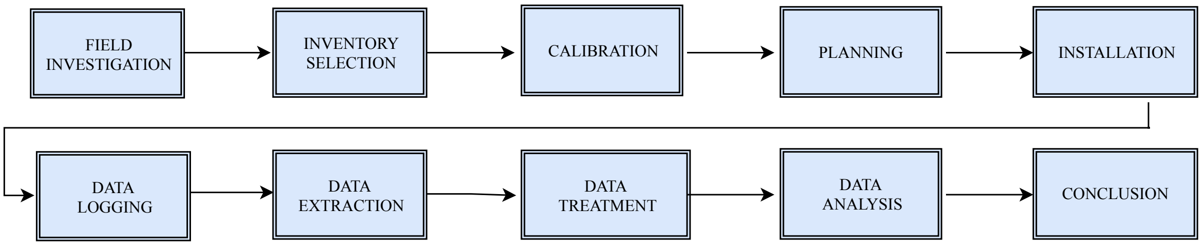

Figure 3.2: Diagram of the project approach.

Therefore, measurements for indoor and outdoor conditions from WT1 and WT2, respectively are the key to explain how the system works. This leads to the possibility to compare results and use them to suggest improvements of the system operation, such as the control strategy. Overall, by the end of the study, the following report wishes to answers the following concerns:

- Analyze the window performance based on the indoor and outdoor conditions.
- Test window working modes and its capability to adjust to changes in the environment.
- Ascertain window capacity to supply minimum air flow rate for the occupancy.
- Investigate the air velocity in the occupied zone to prevent risk of draft causing discomfort.
- Study the visual comfort levels to prevent glare problems while allowing the maximum daylight.
- Check if the indoor levels meet the standards and regulations.
- Evaluate the sensors used in the electronically controlled window.
- Suggest a final proposal for a control strategy.

3.2 Limitation

Due to the finite period time of this project, the study covers the problems to a limited extend. In that manner, limitation are listed below:

1. Experimental analysis WT1 is performed only during heating season.
2. Analysis of the indoor environment in the school with WT2 is not included.
3. Energy performance of the building is not calculated.
4. Detail analysis of the air flow distribution in the air gap of the window is not assessed.
5. Control strategy implementation is not included.

3.3 Regulations

In order to provide a safety, healthy and comfortable conditions of the occupants, the indoor environmental conditions must comply with the designed regulations and standards. The criteria is based on several standards applicable for the following case. In the Table 3.1 description and regulations are listed.

Table 3.1: Standards and building regulations applicable to this project.

Category	**Document**	**Restriction**	**Value**
General	[DS/EN 15251, 2007, Table 1]	Category applicability	I
	[Vorre et al., 2017, p. 32]	Winter period	Nov - Mar
	[Vorre et al., 2017, p. 32]	Summer period	May - Sep
Indoor	[BR 18, 2018, Section 447 (2)]	Max CO_2 of the indoor air	$\leqslant$1000 ppm
Air Quality	[BR 18, 2018, Section 447 (2)]	Min. air supply & extract	5 l/s/per + 0.35 $l/s/m^2$
Thermal	[Vorre et al., 2017, Table 3]	Temp. tolerance, winter	50h > 25°C
Comfort	[DS 1752, 2001, Table 1]	Operative temp, winter	22.0 +/- 1.0
	[DS 1752, 2001, Table A2]	Vertical Air Temp. Diff.	<2 °C
	[ISO 7730, 2005, Table A1]	Draught Risk	<10%
RH	[DS 1752, 2001, A3.8]	Relative Humidity	30% - 70%
Visual Comfort	[BR 15, 2015, Section 6.5.2 (1)]	Daylight Factor in working area	$\leqslant$ 2 %

4

Case Study

In this chapter, the conditions of the case study are explained. The main focus of the case study is the ventilated window performance in two classrooms located in Ødis primary school. The school building, its surroundings and detailed explanation of the classrooms are defined. Additionally, detailed explanation about the ventilated windows (WT1-WT2) including working conditions and valves positioning for the different working modes.

4.1 Introduction

The background of the following project started with the CLIMAWIN project, previously described in Section 2.1. The idea was to develop an energy efficient window, which could provide acceptable indoor environment and thermal comfort for the occupants. In that case, these windows could be a solution for the renovation of the buildings, where the decentralized ventilation system installation is avoided.

The window design was developed in collaboration between Aalborg University - active member of the CLIMAWIN project, and the producer Horn Group - *VentilationsVinduet* company. The ventilated windows was installed in the Ødis primary school, as a part of the school renovation.

4.2 Building Description

The building chosen for the case study is located in Steppingvej 14, 6580 Vamdrup, Ødis, Kolding Kommune, Denmark. The building accommodates the school for the teaching and educational purposes. In the study, only two classrooms are undergoing the renovation: classroom 1 (R1) and classroom 2 (R2). As the building interacts with the outdoor environment, analysis of the building and its surroundings is necessary. The location of the school has been examined regarding the influence of the environment. These are the main observations: rural area, green zone, non-heavy traffic and no industries nearby. The building is a two storey building with a basement. The classrooms: R1 and R2 are located on the ground floor. Their windows are facing directly the south-east orientation. There is no shade event of shading from trees or surrounding buildings.

Figure 4.1 is a replica from the original floor plan, where the location of the school and orientation of the classroom is presented. Highlighted, in the floor plan are the classrooms chosen for the analysis.

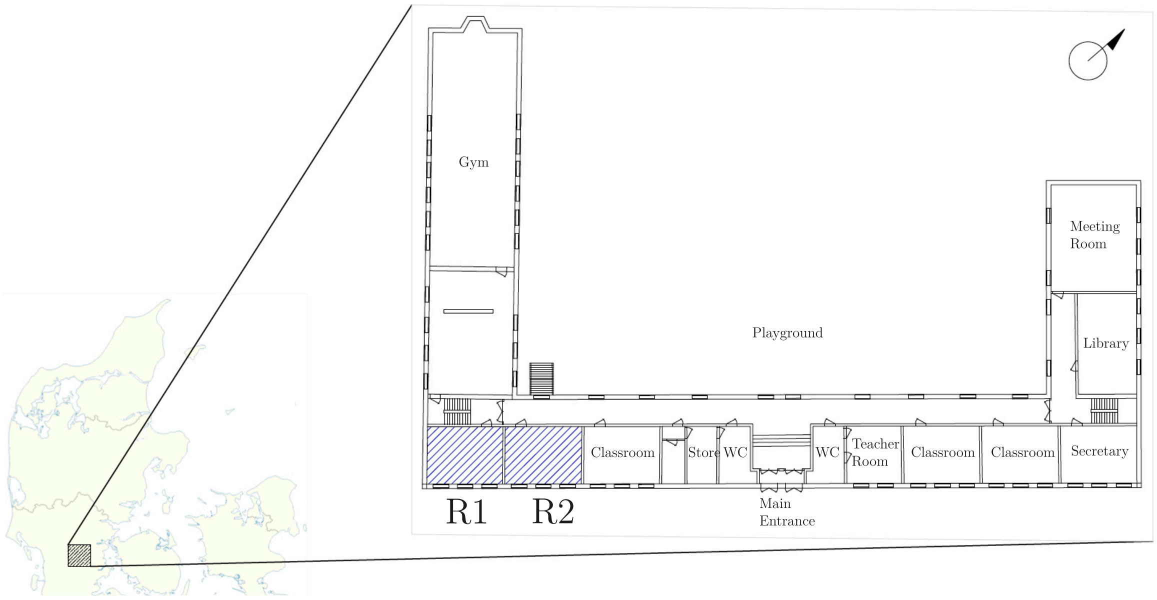

Figure 4.1: Building location and floor plan distribution of Ødis Primary School.

The school was build in 1960s, and represents the typical danish construction. The external wall is a brick construction with a thickness of 330 mm. The thickness of insulation in building construction in the sixties was low, sometimes as little as 30 mm only [Hannoudi et al., 2016]. According to the 1961 Building Regulations, the maximum heat transfer coefficient for an external wall brick was approximately 0.99 W/m^2 [Hannoudi et al., 2016]. However, documentation about the building construction has not been available. Therefore, it is not known if the building has undergone any renovation. Windows installed in 60's, should be double-glazed with a minimum distance of 12 mm between them in accordance to the 1961 building regulations. The approximate heat transfer coefficient of the glazing part is 2.9 W/m^2 ·K, whereas nowadays it is reduced up to 1.5 W/m^2 ·K [BR 18, 2018]. The internal walls in the school have the thickness 180 mm.

4.3 Classrooms Conditions

The evaluated classrooms, accommodate 15 students from fifth grade in for Room 1 and 13 student from sixth grade in Room 2. They are all between 10-11 years old. Students occupy the classrooms, every week day between 8:00h and 16:00h, with an exceptions for Wednesdays, which are days with field activities. It is expected, that children stay in the classroom during the lessons and leave the room during the break. The lessons take 45 min, having 10 min break in between on average.

Figure 4.2 and Figure 4.3 present a 3D sketch determining the room dimensions, the internal space distribution, the door position, the number of windows per room and its location on the wall facing outside and the ventilation extraction. It is also highlighted in red the occupied zone, further explained its application in the numerical analysis.

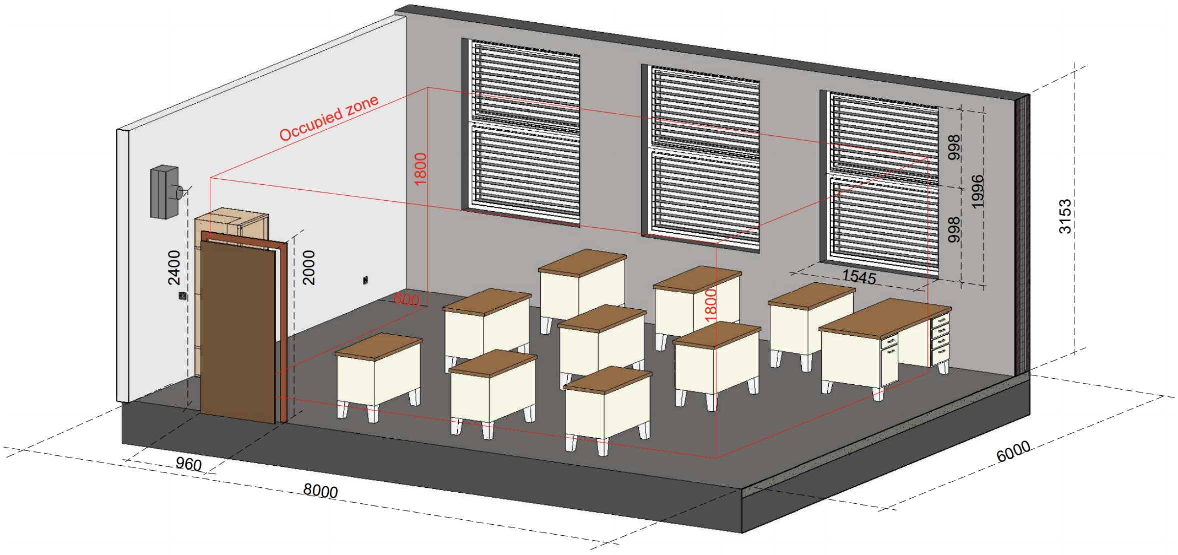

Figure 4.2: 3D model of the Room 1 and dimensions [mm].

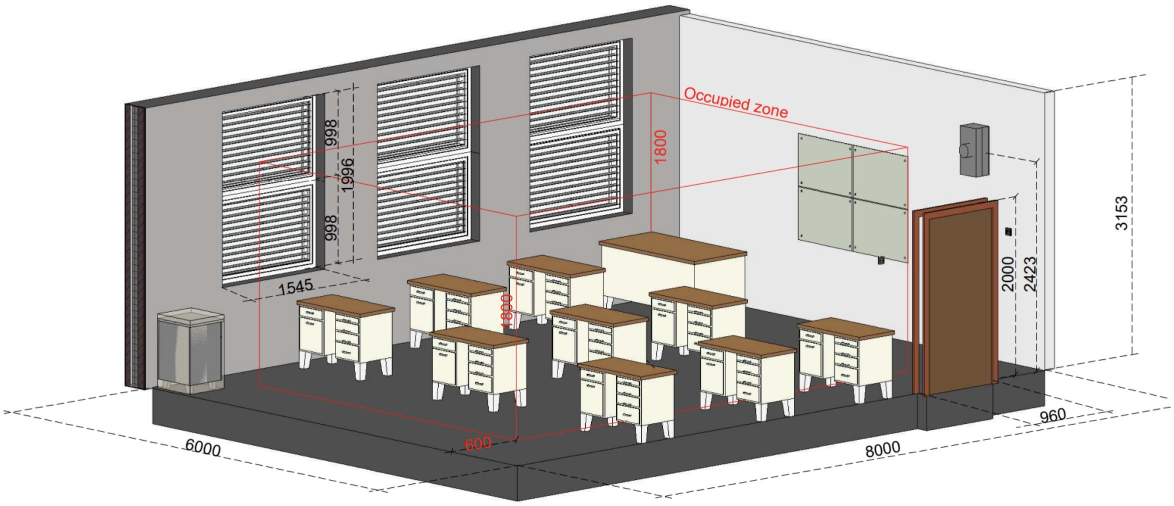

Figure 4.3: 3D model of the Room 2 and its dimensions [mm].

In Table 4.1 conditions that influences on the systems operation, window performance and indoor environment are summarized. There are some main differences in the operation of the room, each system and characteristics are explained in the following subsections.

Table 4.1: Summary of rooms conditions in Ødis Primary School.

	Characteristics				Systems			
	Windows	Room Area	Room Height	Occupancy	Exhaust	Heating	Lighting	Shading
Room 1	6	48 m^2	3.1 m	13 people	Natural	Radiators	Auto	Manual
Room 2	3	48 m^2	3.1 m	15 people	Mechanical	Radiators	Auto	Electrical

4.3.1 Ventilation System-Exhaust

Both rooms have the same number and type of windows with same outdoor conditions and surroundings. The main difference between Room 1 and Room 2 is the ventilation strategy. Room 1 has the natural ventilation with an extraction through a chimney, operating for 24 hours, while Room 2 has a mechanical extraction. There are no specification regarding the operation of the mechanical extraction.

4.3.2 Heating System

Based on the information from Building Council registration [Kolding Kommune, 2019], the school has a central heating system from a geothermal heat pump. It is supplemented by a natural gas boiler. Inlet flow temperature is approximately 45°C from the geothermal heat pump, while the gas fire is controlled by an outdoor compensation curve manually supervised. The analyzed rooms have 3 radiators each, placed beneath the windows. The radiators can be controlled by the users by thermostats. The heating system schedule is not known.

4.3.3 Lighting System

The analyzed rooms are equipped with artificial lighting system. Each room has six fluorescent lights, which are controlled both automatically and manually. When the sensor detects the movement, the lights turn on, however, they can be operated manually by the on/off switch.

4.3.4 Shading System

The venetian blinds are chosen as the shading system for the classrooms. The venetian blinds are placed inside the cavity for both rooms and they consist of many horizontal slats, made of aluminum. The slats are connected with a string and can be rotated up to 170°to avoid the daylight or can be pulled up so that the entire window is clear. The most common position of the blinds is with the slat tilted horizontally. In both rooms the slats are identical, however, their control is different in each room.

In Room 1 the blinds are operated manually. That means the user can adjust the position of the blinds accordingly to their needs. The blinds can be positioned up and down by the use of the string. In Room 2 the blinds are operated mechanically. The system, by the use of a switch, allows to move the blinds up and down. The switch moves them all at the same time, with no possibility of moving them independently. It is also important to highlight that poor interaction of the users to change the position of the blinds has been reported. For example, the top windows cannot be easily reached and are constantly down in a horizontally tilted position.

4.3.5 Other Heat Loads

In term of heat loads, both rooms have one electrical tech board, a projector and each student has a laptop.

4.4 Windows System Description

The aim of this section is to explain the windows design and its working strategy. As there are 2 types of windows, which are different in terms of design and working principles, each window is explained individually. The window type 1 (WT1) is the initial design on which the case study in school is performed, shown in Figure 4.4. After renovation, window type 2 (WT2) is installed which it is an improved design with an electrical control strategy, shown in Figure 4.5.

Figure 4.4: Inside view of the window type 1 (WT1), located in the Ødis school.

Figure 4.5: Inside view of the window type 2 (WT2), located in the AAU laboratory.

Figure 4.6 shows the layout Window Type 1. It consist of two windows located on top of each other with the same dimensions. Each of them has one cavity, which can be opened individually. There is no internal connection between them for the air to pass through. Figure 4.7 show the Window type 2. WT2 is composed of 3 cavities. Two bottom cavities (Cavity 1 and Cavity 2) are the same size, only the top cavity (Cavity 3) is different. All of the cavities of WT2, share a common sash. The bottom cavities can be opened manually, while there is no possibility to open the cavity 3. The air goes through each cavity, therefore, there is no internal connection between them.

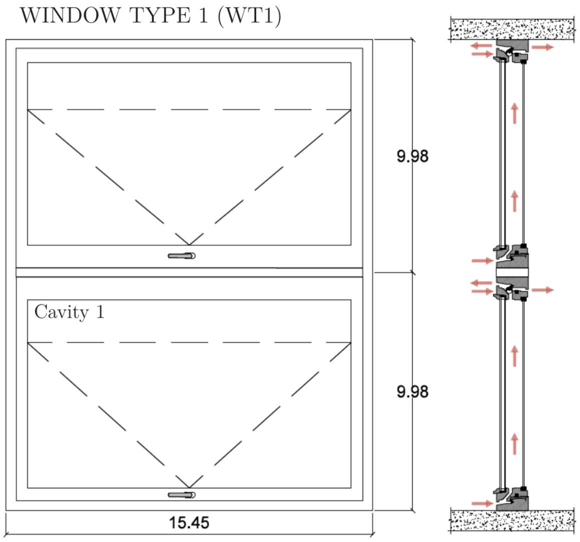

Figure 4.6: Front view of WT1 2D, section where cavities show possible air ventilation air path and dimensions [dm].

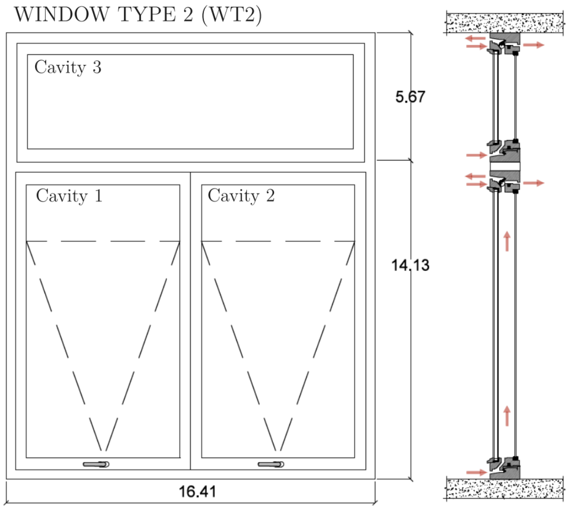

Figure 4.7: Front view of the WT2 2D, section where cavities show possible air ventilation air path and dimensions [dm].

As presented on the figures above, each cavity has 3 possibilities of air movement, depending on the working mode of the window. That means, the air can be supplied by: preheating, bypass or cooling option. Overall, there are several differences between two window types. There are different different number of actuators, number of valves, openings and working modes for each cavity. Detailed description of each window types is explained in the following subsection 4.4.1 for WT1 and subsection 4.4.2 for WT2.

4.4.1 Window Type 1 (WT1)

First each material and its layer configuration is introduced. The window is a the triple glazing with an external insulated glass unit (IGU) which consists of a double-pane with a sealed space in between them filled with Argon, and a low emissivity coating for an optimal window performance. Argon located in between the cavity, reduces the heat transfer through the window and it is preferable to air. Argon is a better insulator and it does not compromise the amount of light that enters to the room, in contrast to air that contains moisture that can condense inside the glass. The air moves through the internal sealed cavity between two glazing units. The inner pane is a 6 mm floating glass. The inlet is located in the bottom part of the window in between the two glazing units. The supply to the room is possible through two openings located at the top part of the window. The window working modes are controlled by a top-mounted thermal expansion valve. Its control strategy is further explained in the Table 4.3. In addition, a venetian blind is located inside the air cavity. It is the chosen shading option by the supplier. The venetian blinds purpose is to protect the building occupants from solar radiation, avoid glare, and contribute to better preheating capacity of the air.

Figure 4.8 shows a section of the window configuration with all the explained layers:

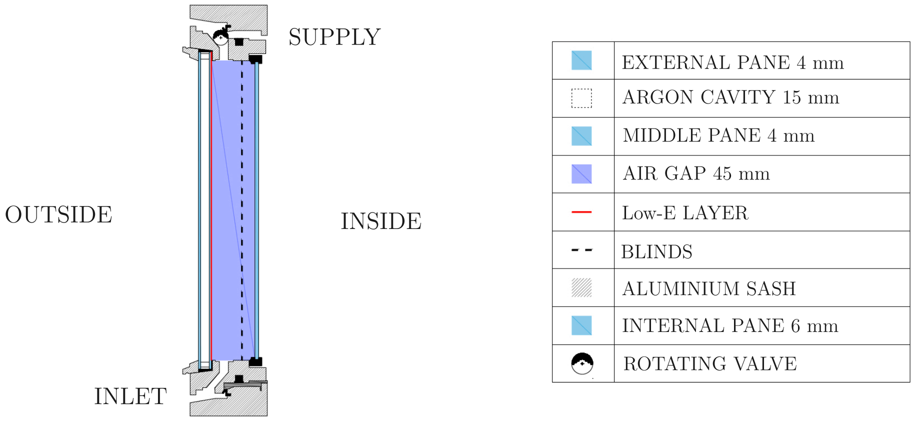

Figure 4.8: Window types in 2D and sections, where cavities show possible air path.

Table 4.2 summarizes glazing, frame and window dimensions for the window - WT1. The values are expressed in meters for height and width and m^2 for the areas. The glazing represents 69.9% of the window area.

Table 4.2: Dimensions from the tested Window - WT1 in meters.

Glazing			**Frame**			**Total**		
Height	Width	Area	Height	Width	Area	Height	Width	Area
0.791	1.365	1.079	-	-	0.462	0.998	1.545	1.542

Figure 4.9 shows a 3D model of the window type 1. Five window openings are presented: three facing outside and two that supplies to the internal space.

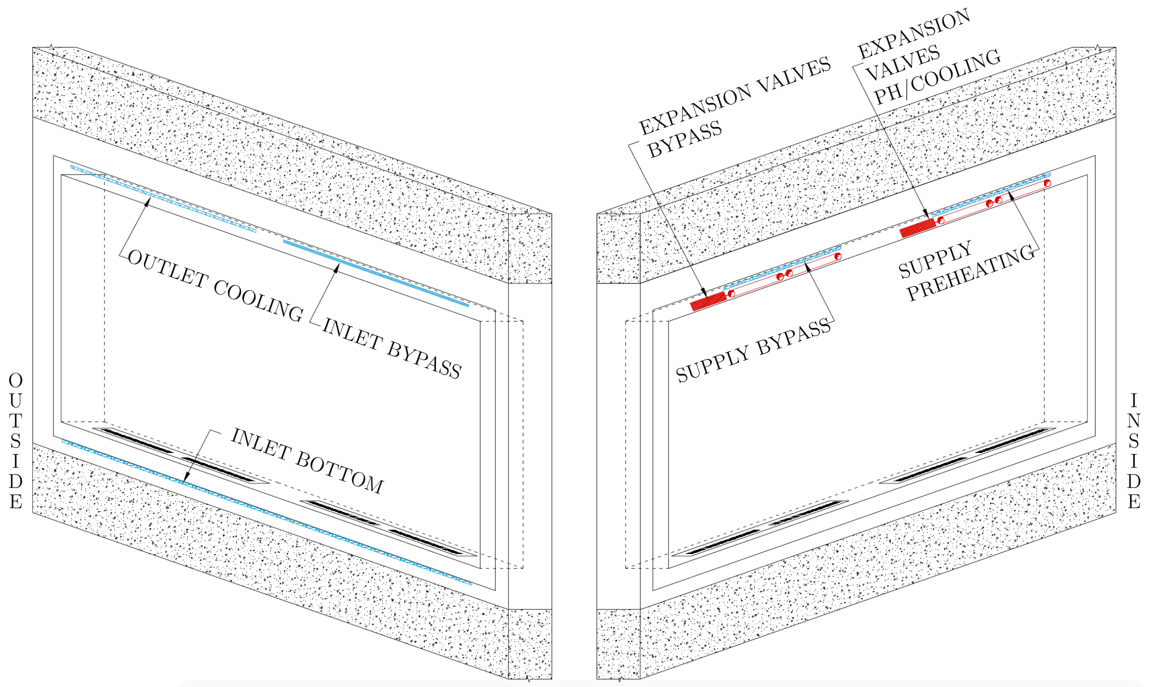

Figure 4.9: Window openings placed in between the air cavity of WT1.

Inlet bottom is the opening that connects the air cavity with the exterior, so the air moves from the outside to the air gap. The two openings in the upper part: *Outlet cooling* and *Inlet bypass* corresponds to the link between the outside top part of the cavity and indoor space. The actuator and thermal expansion valves are located in between the cavity. It is essential for the good understanding of the window performance to know in which working mode it is. The valves can work independently in different working modes, they are not connected. One valve can only work in bypass mode and the other one in preheating cooling. Possible working modes combinations is explained in Figure 4.13.

Table 4.3 presents the criteria and the setpoints by which the rotation of the valves changes. It is a thermal expansion valve, meaning that a gas under pressure induces a rotation of the valves above a certain temperature. T_{TOP} is defined as the temperature at the top of the cavity and T_{OUT} as the temperature at the temperature outside.

Table 4.3: Working modes and its properties for the window WT1.

Preheating Mode $T_{TOP} > 12°C$	**Cooling Mode** $T_{TOP} > 30°C$	**Bypass Mode** $T_{OUT} > 15°C$
The ambient air from *inlet bottom* moves to *supply preheating*. Purpose is to supply warmer air heated up by solar radiation and building's heat losses.	The ambient air from *inlet bottom* circulates to *outlet cooling*. The purpose is to minimize solar gains by ventilating the cavity.	The ambient air from *inlet bypass* to *supply bypass*.The purpose is to supply the ambient air with directly indoors.
Closed: $T_{TOP} < 12°C$, too low temperatures, no air supply to the room.		

Depending on the angular position of the valves, the working mode is defined. The positioning of the valves is induced by wind and thermal buoyancy forces. They work passively, no electrical motor is required to activate the movement of the valves due to the thermal expansion.

Focusing on valve rotation, it can be rotated 360°. There are four main different valves positions, resulting in four window behaviour. Each of the position has its operational range in degrees. Figure 4.10 shows the pictures from these positions of the valve. Figure 4.11 is a representation of the operational ranges.

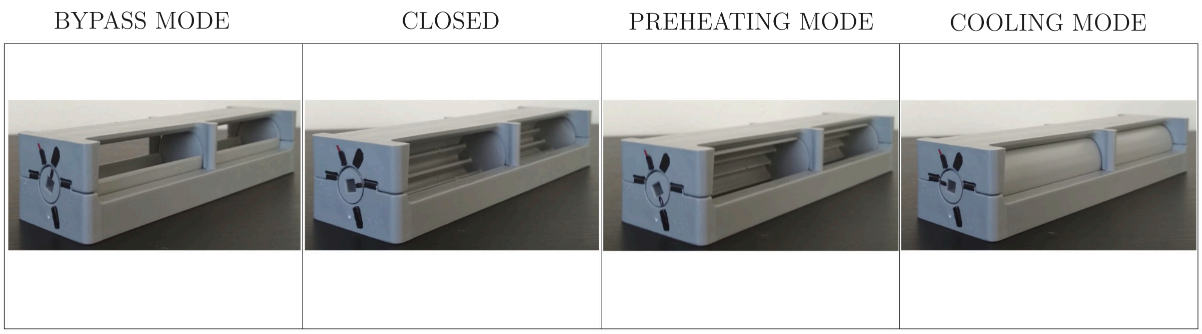

Figure 4.10: Pictures of the different position of the valves.

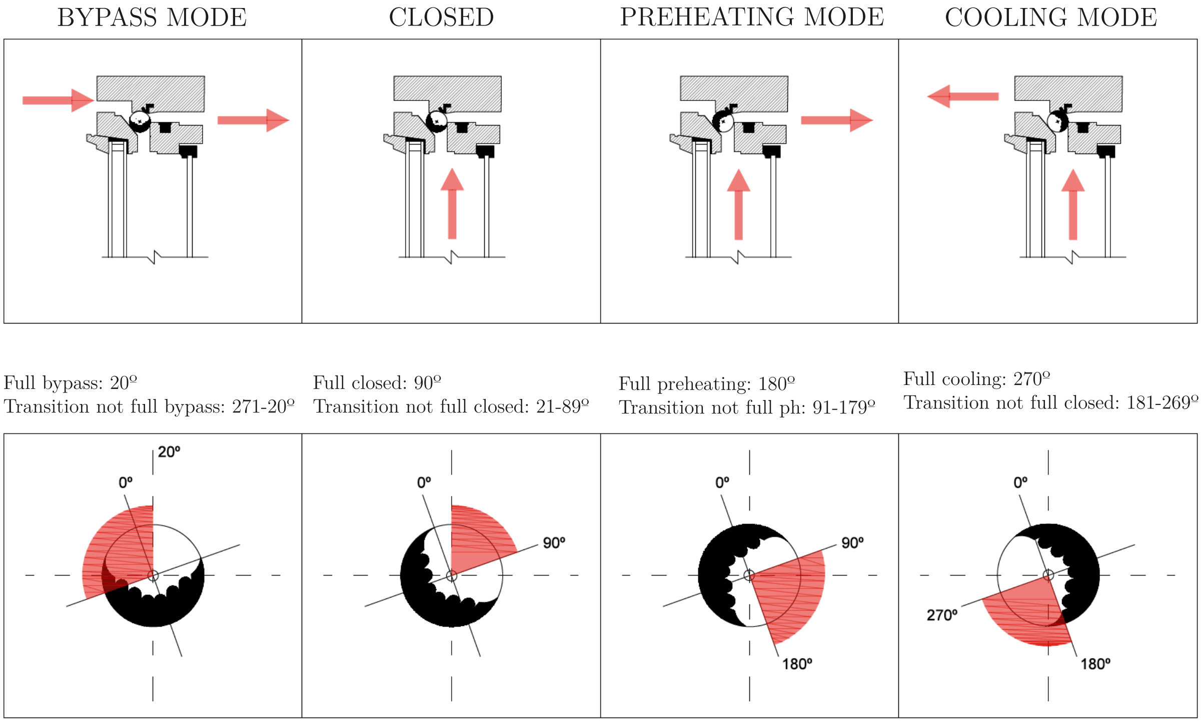

Figure 4.11: Different valve position and transition for the window modes.

Figure 4.12 shows the location of the valves. On the left bypass valve, in the middle the thermal expansion valve and on the right the preheating/cooling rotating valve.

Figure 4.12: Valves in window type 1.

Figure 4.13 presents the combination of the different working modes. It is important to highlight that the same valve operates both preheating and cooling mode whereas the other valve works only in bypass. These valves operate accordingly to the temperature in the cavity. When the valves are closed, there is no air supply to the room but there is still air circulating through the cavity, as the inlet of the window is always open. On the figure below, the closed-bypass mode is not shown. That is due to the improbability of outside being more than 15 °C while the temperature inside the cavity is less than 12 °C.

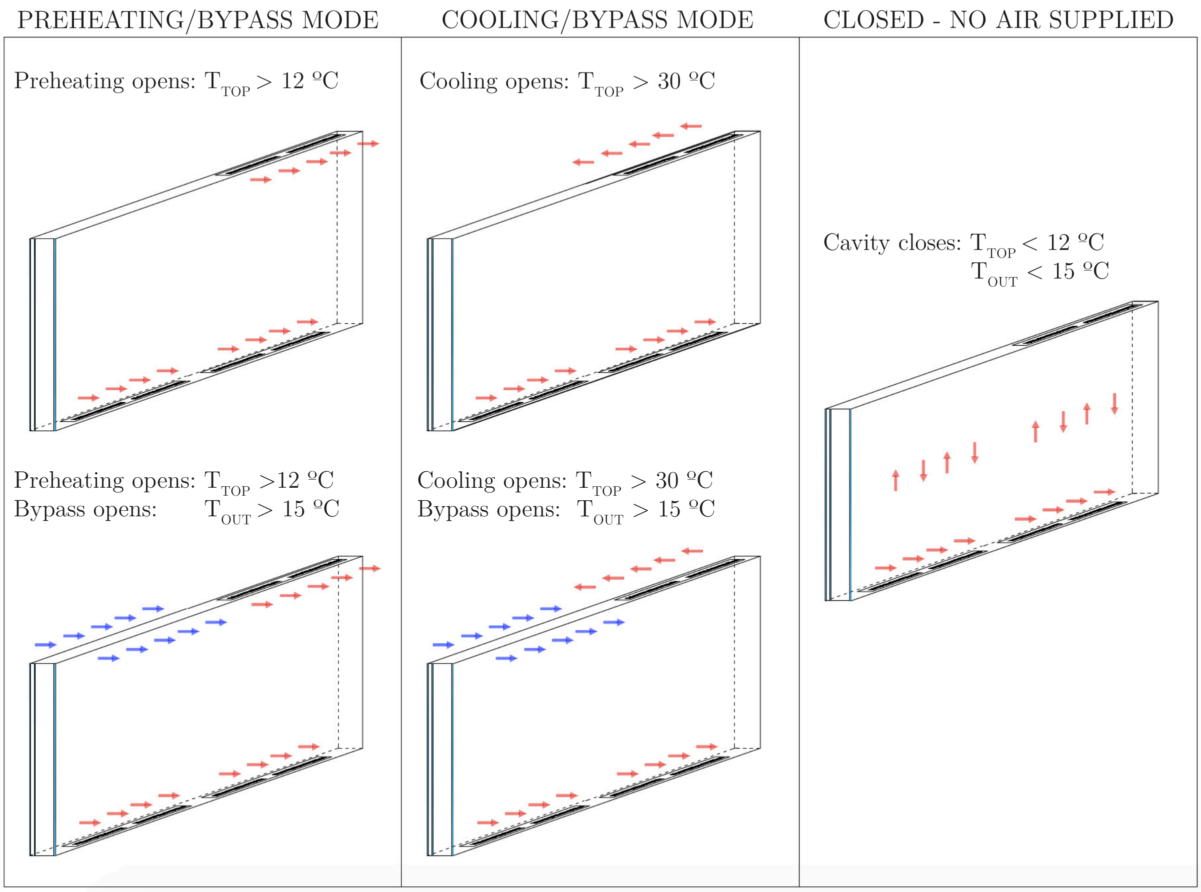

Figure 4.13: Functioning of the ventilated window by the two different modes.

4.4.2 Window Type 2 (WT2)

The window type 2 is divided into 3 cavities in which glazing represents 78.9% of the window area. The dimensions of the window are presented in the Table 4.4. Layers, materials and thickness of the window are identical to the WT1, as previously explained on Figure 4.8.

Table 4.4: Dimensions from the tested window - WT2 in meters.

Glazing 1			**Glazing 2**			**Glazing 3**		
Height	Width	Area	Height	Width	Area	Height	Width	Area
1.211	0.685	0.829	1.211	0.685	0,92	0.418	1.449	0.605
Total Glazing			**Total Frame**			**Total Window**		
Height	Width	Area	Height	Width	Area	Height	Width	Area
-	-	2.264	-	-	0.604	1.449	1.980	2.869

However, the operation of the window is different, since the WT2 is automatized. That means that the rotation of the valves is dependent on a motor/actuator. The bottom cavities have one motor/actuator placed on top of the cavity. However, as the top cavity as it is wider, it has 2 sets of motor and vales. The supply to the window is located on the bottom of the cavity. On the Figure 4.14 the WT2 openings are presented.

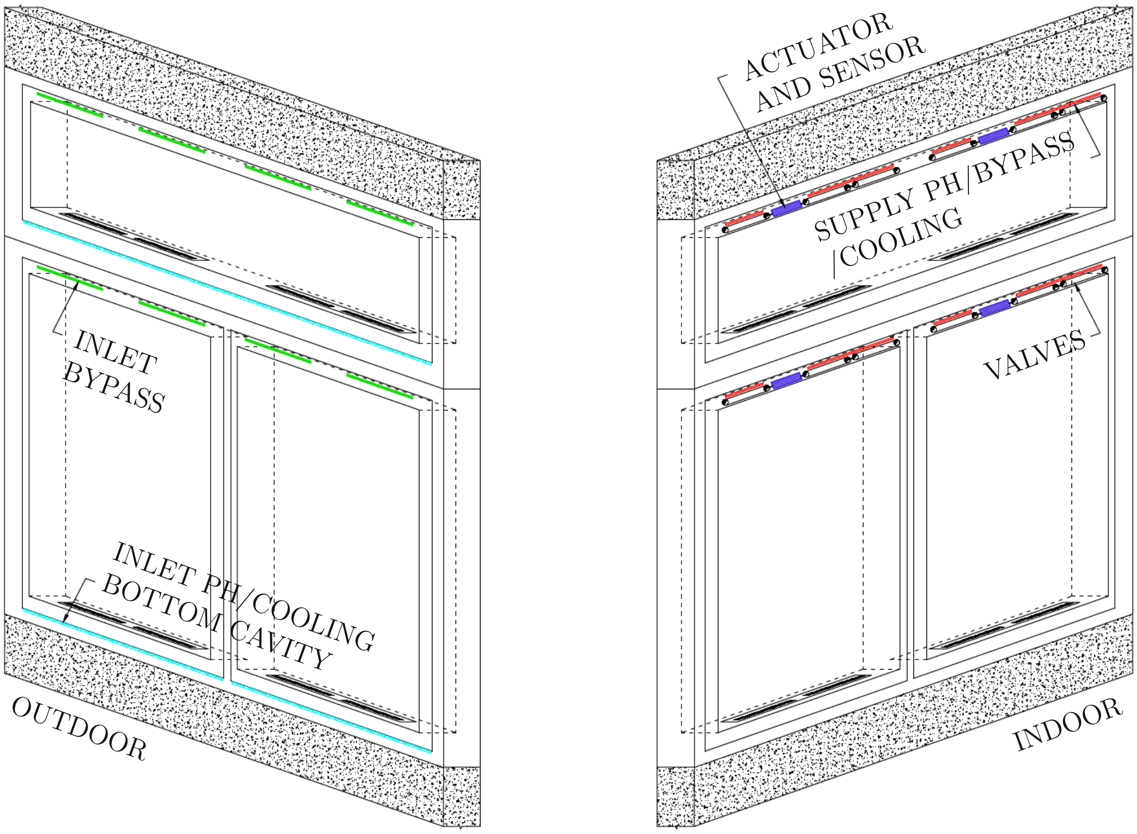

Figure 4.14: Sketch of window openings in the air cavity of the WT2.

Figure 4.15 shows the location of the valves and electronics in the top cavity.

Figure 4.15: Location of the valves and electronic in the top cavity.

The working modes of the WT2 are the same as described in the Figure 4.10. There are four different modes: preheating, cooling, bypass and closed. Nevertheless, as the rotation of the valves is dependent on the automatic control strategy, all the valves can rotate to any working mode. A sensor located inside the room measures the indoor environment and sends this information to a unit that decides, together with the measurements from sensor located at the cavities, the position of the valve.

The choice of the shading device in the Window Type 2 is described in the further section of the report. The decision about it is taken after the experimental analysis on the visual comfort, Section 7.2.

5

Numerical Analysis

The aim of this section is to approach through the numerical analysis the answers to the questions from Section 1.1. The numerical analysis presents the equations used to estimate the indoor environment and window performance. In addition, the regulations that define a good indoor comfort are described.

All the theoretical investigation and calculations raised here, are further investigated as a real case study from Chapter 6 about window type 1 in the school to Chapter 7 about window type 2 in Aalborg University Laboratory.

5.1 Indoor Environment

Indoor environment is referred to the quality of a space in relation to the health and comfort of the occupants. There are needs that must be satisfied, resulting from determined factors, including room temperatures, light or air quality, among others. They are studied for Room 1 and Room 2. The question to be answered is as follows:

> *"How does the window influence the indoor environment under the existing conditions?"*

This evaluation of long term indicators is based on design criteria, calculations and long term measurements [DS/EN 15251, 2007, p. 21]. In each of the following section the chosen procedure is explained. The list of the parameters measured in the school to evaluate the indoor environment are specified in the Appendix A.1.

5.1.1 Indoor Air Quality

Indoor air quality (IAQ) is referred as a representation of pollutants that affect health, comfort and performance of occupants, being consequently and indirectly related to the ventilation rate [DS/EN 15251, 2007]. Measurements for the ventilation rates (per person per m^2) can be derived using CO_2 measurements, only when people are the main pollutant source [DS/EN 15251, 2007, p. 24]. Therefore, the measurements concerning the amount of carbon dioxide concentrated in the air are measured. From the regulation explained in Table 3.1 a good air quality is defined when the amount of CO_2 level in the air does not exceed 1000 ppm.

Ventilation effectiveness

The carbon dioxide concentration can be used as an indicator of air quality. Ventilation effectiveness, also referred as the Contaminant Removal Effectiveness (CRE), is an indicator of how fast an airbone contaminant is removed from the space. In addition, it also refers to the type of air flow pattern in the room [Skistad, 2004, p. 22]. The CRE,ε_c, is defined by the Equation 5.1:

$$\varepsilon_c = \frac{C_e - C_{out}}{C_{oz} - C_{out}} \tag{5.1}$$

C_e	Concentration of CO_2 at the exhaust [ppm]
C_{out}	Concentration of CO_2 outdoor [ppm]
C_{oz}	Concentration of CO_2 at the occupied zone [ppm]

The occupied zone is the area established in which people occupy the space. According to [Skistad, 2004, p. 6], it is defined as the area 1 m from walls that contain windows, doors or radiation and 0.6 m from the rest of the walls. Its height is 1.3 m if people inside it are sitting and 1.8 m if standing.

Table 5.1 presents the interpretation of the results from CRE calculations:

Table 5.1: Indication of Contaminant Removal Effectiveness results [Skistad, 2004].

Concentration Effectiveness		
$\varepsilon_c \ll 1$	$\varepsilon_c = 1$	$\varepsilon_c > 1$
Need to increase air flow rate	Perfect mixing ventilation	Start displacement ventilation

5.1.2 Air Flow Calculations

How effectively the windows removes air pollutants and excessive temperature in the classroom is essential to determinate if the windows supply enough air flow. Air changes per hour (ACH) is a measure of the air volume added to or removed from a space which is defined by the Equation 5.2.

$$n = \frac{\sum q_s}{V} \tag{5.2}$$

n	Air changes per hour, ACH [1/h]
q_s	air flow rate supplied [m^3/h]
V	classroom volume [m^3]

Maximum Ventilation Flow Rate

The air flow rate is defined according to the maximum and minimum air flow rate design for the school based on the regulations. These calculations are based on the recommended design criteria using the required ventilation for people and building component [DS/EN 15251, 2007, B1.2]. Values are extracted from [BR 15, 2015, Section 6.1.3.1]. By the design criteria the number of the occupants in the room is 24 people [DS 1752, 2001, Table 1]. Equation 5.3 calculates the maximum flow rate needed in the classroom.

$$q_{tot} = q_p \cdot N + q_B \cdot A = 136.8\ l/s \tag{5.3}$$

q_{tot}	maximum air flow rate in the classroom [l/s]
q_w	maximum air flow rate per window [l/s]
q_{cav}	maximum air flow rate per cavity [l/s]
q_p	ventilation rate from occupants, q_p=5 [l/s per pers]
q_B	ventilation rate from building emissions, q_B=0.35 [l/s per m^2]
A	Room area [m^2]
N	Number of occupants, N=0.5·A [-]

The maximum air flow rate for the classroom in accordance to BR 15 [2015] is 136.8 l/s. After the renovation, the number of the windows change from six to three and from one cavity per window to three. Results from the calculations are shown in Table 5.2.

Table 5.2: Maximum air flow rate per type of window according to regulations.

		WT1	**WT2**
Flow Rate window	q_w [l/s]	22.8	45.6
Flow Rate cavity	q_{cav} [l/s]	22.8	15.2

Minimum Ventilation Flow Rate

This calculation follows the same standards and regulations as the previous maximum air flow rate, but calculated using the real averaged amount of students in the classrooms which is 15. Based on the Equation 5.3, the results from the minimum air flow rate per type of window is described in Table 5.3.

$$q_{tot} = q_p \cdot n + q_B \cdot A = 91.8\ l/s$$

Table 5.3: Minimum air flow rate per type of window according to regulations.

		WT1	**WT2**
Flow Rate window	q_w [l/s]	15.3	30.6
Flow Rate cavity	q_{cav} [l/s]	15.3	10.2

Dilution Equation

In addition, not exceeding the maximum CO_2 concentration recommended in the classroom is also a requirement. Therefore, the dilution equation is applied to obtain the air flow rate necessary for a day during 8 hours in which the CO_2 concentration rises to not more than 1000 ppm according to the following formula:

$$c = (\frac{q_s}{n \cdot V}) \cdot [1 - (1/e^{n \cdot t})] + (c_0 - c_i) \cdot (1/e^{n \cdot t}) + c_i \tag{5.4}$$

c	carbon dioxide concentration in the room [m^3/m^3]
q_s	carbon dioxide supplied to the room [m^3/h]
n	number of air changes per hour, ACH [1/h]
V	volume of the room [m^3]
t	time [h]
c_0	carbon dioxide concentration in the room at start, t = 0 [m^3/m^3]
c_i	carbon dioxide concentration at the exhaust [m^3/m^3]

Solving for n, ACH and applying Equation 5.2:

$$q_{tot} = 209.23 \ l/s$$

Table 5.4: Maximum air flow rate per type of window according to the dilution equation.

		WT1	**WT2**
Flow Rate window	q_w [l/s]	34.87	69.74
Flow Rate cavity	q_{cav} [l/s]	34.87	23.24

As the maximum air flow rate from the dilution equation is higher and therefore, more restrictive than the one stated by regulations from Equation 5.3, it has been selected as the maximum air flow rate and multiplied by a 1.2 safety coefficient for the experimental analysis.

5.1.3 Relative Humidity

Air humidity in occupied spaces has an influence on the thermal sensation. Relative humidity is the ratio between the current absolute humidity to the highest possible humidity, which depends on the current air temperature. A reading value of 100% of relative humidity means totally saturated, that the air cannot hold more water vapor. Desired values between 30-70 % of relative humidity ensure that no condensation is occurring [DS 1752, 2001, A3.8].

Table 5.5 defines the possible ranges. Low humidity could result in sensation of skin irritation or dry eyes. Besides, too high values could have the consequence of growth moulds or other fungi due to moisture.

Table 5.5: Relative Humidity ranges for the evaluation for indoor air humidity in R1 and R2.

Relative Humidity		
Uncomfortable Range	Comfortable Range	Uncomfortable Range
0-30%	30-70%	70-100%

5.1.4 Thermal Comfort

Indoor temperature is influenced by internal heat loads, such as number of occupants and any heat sources in the room. External heat loads such as solar radiation, also contribute to the heat gain in the room.

The data evaluated in this calculation has to be taken in the occupied zone. According to the mentioned standards, the percentage of time in which the temperatures are within each category is used as a design indicator of comfort categories. These ones can be seen in Table 5.6.

Table 5.6: Operative temperature ranges for calculations for cooling and heating energy.

Operative Temperature [°C] - Heating season						
Cat. -IV	Cat. -III	Cat. -II	Cat. I	Cat. +II	Cat. +III	Cat. +IV
< 19	$19 \leq T < 20$	$20 \leq T < 21$	$21 \leq T < 23$	$23 \leq T < 24$	$24 \leq T < 25$	≥ 25

Local Thermal Discomfort

Draught is defined as the unwanted local cooling of the body caused by air movements [Skistad, 2004]. It makes the occupants feel uncomfortable due to too high velocities or low temperatures of the air supplied. The maximum % of dissatisfied people form draught rate is 10 %. Therefore, this discomfort may be expressed as the percentage of people predicted to be dissatisfied by draught [ISO 7730, 2005, p. 12] using the following formula:

$$DR = (34 - T_a) \cdot (V_a - 0.05)^{0.62} \cdot (0.37 \cdot V_a \cdot T_u + 3.14) \tag{5.5}$$

T_a	Local air temperature [°C]
T_u	Local mean air velocity [m/s]
V_a	Local turbulence intensity [%]

Large vertical air temperature differences between head and ankles, 1.1 and 0.1 m above the floor level, during a short period of time can create an unwanted local cooling of the body, generating discomfort. Therefore, the maximum allowed vertical air temperature gradient is 2°C. [DS 1752, 2001, p. 19].

5.2 Window Performance

The aim of this section is to study the functionality of the ventilated window and understand its limitations and performance under different scenarios. Pressure drop explanation and equations for the heat recovery and total heat recovered are presented. Summarizing this behavior, the question aroused is the one as follows:

How the surrounding conditions are affecting the window performance?

5.2.1 Pressure drop

The purpose of the pressure drop analysis is to find the relation between the air flow capacity and pressure drop, and find the differences at different working modes. This part is purely an investigation performed in the Aalborg University Laboratory.

5.2.2 Heat Recovery

Heat recovery is defined as the ability of the window to supply air at a higher temperature than the ambient. It only occurs when preheating mode is in use. Fresh air goes through the cavity driven by buoyancy and wind forces while it is heated due to solar or/and internal heat contributions. This allows the window to supply warmer air than the outside temperature avoiding uncomfortable temperatures. The equation defining heat recovery is expressed by:

$$HR = \frac{T_{TOP} - T_{OUT}}{T_{IN} - T_{OUT}} \tag{5.6}$$

T_{TOP}	Temperature supplied to the room [°C]
T_{OUT}	Temperature outside [°C]
T_{IN}	Indoor temperature [°C]

It is a coefficient that determines how much a ventilated window under certain conditions is able to preheat the air over the room temperature. It does not take into account the amount of air flow supplied. The different ranges that define the HR are found in the following table:

Table 5.7: Heat Recovery

Heat Recovery		
$HR < 1$	$HR = 0$	$HR > 1$
$T_{TOP} < T_{IN}$	$T_{TOP} = T_{OUT}$	$T_{TOP} > T_{IN}$

The heat recovery calculation is divided into Active Heat Recovery (AHR) and Passive Heat Recovery (PHR).

Passive Heat Recovery

PHR is defined as the heat recovered by the influence of heat transmissions from the building to the window. The intention is to obtain a regression between the difference T$_{IN}$-T$_{OUT}$ temperature and T$_{TOP}$-T$_{OUT}$ air temperature during solar radiation time.

Active Heat Recovery

AHR is defined as the heat transmissions from solar radiation and internal heat gains.

Heat Recovered

The useful heat recovered corresponds to the heat saved by the ventilated window in comparison to a conventional window. It is defined by the following equation:

$$Q_r = c_p \cdot \rho \cdot q_{cav} \cdot \Delta T \tag{5.7}$$

Q_r	Heat recovered [W]
c_p	Heat capacity of the air [J/kg·K]
q_{cav}	Flow rate through the cavity [m^3/s]
ΔT	Outlet rise between upper cavity and outside [°C]
ρ	Density of air [kg/m^3]

5.3 Visual Comfort

Well-daylight space is indispensable to provide a comfortable visual environment. Furthermore, exceeding the amount of luxes or insufficient daylight in a room could negatively impact on the students performance. It is of interest to answer the following question:

What is the visual comfort provided by the windows?

Equation 5.8 defines the ratio between outdoor and indoor illuminance at the same height on an horizontal plane at 0.8 m above the floor level. Required DF requirements are documented in [BR 15, 2015, Section 6.5.2 (1)]. Measurements have to be performed during an overcast day.

$$DF = \frac{I_i}{I_e} \cdot 100\% \tag{5.8}$$

I_i	Illuminance due to daylight inside [lux]
I_e	Illuminance due to daylight on a horizontal plane outside [lux]

A minimum daylight factor 2 % is required BR 15 [2015]. The assessment of the glare has been done qualitatively. Excessive contrast, meaning big differences between the field of view and the eye could result in creating discomfort.

6

Experimental Analysis - School WT1

This chapter focuses on analyzing comfort criteria for the evaluation of indoor environment quality. Air quality, thermal comfort, window performance and visual comfort are presented analyzing the experimental data logged in the school.

Previous to the analysis explanation, an introduction about the methodology and the equipment used is needed. It is to introduce devices location in the classrooms and at the window. More information about the measurement plan can be found in Appendix A. The summary of the equipment used is listed below:

1. Exhaust air temperature and flow rate - Lindab flow meter x2
2. Indoor conditions CO_2, Temperature and Relative Humidity - IC-meters x4
3. Occupancy and door open/closed - Cameras x4
4. Data Logger - Grant x1
   a) Solar Radiation - Pyranometer x1
   b) Temperature in the window - Thick type K Thermocouples x4
5. Air velocity and air temperature - Anemometers x8
6. Lux in the working area - Luxmeters x2

Figure 6.1 presents the position of the thermocouples and pyranometer. T_{OUT} is referred to outdoor temperature, T_{BOT} is bottom inner part of the cavity temperature, T_{TOP} is the upper inner part of the cavity and RAD, solar radiation on the vertical surface of the façade.

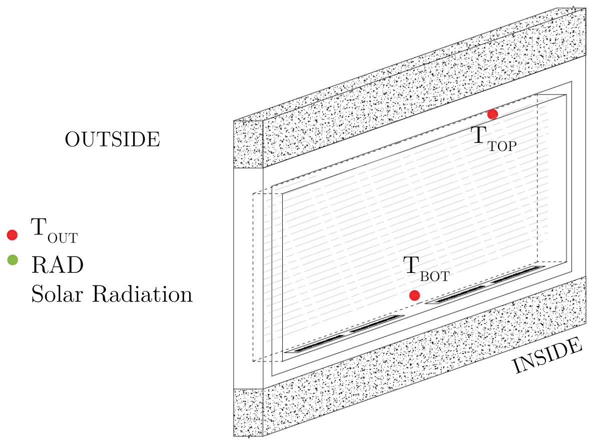

Figure 6.1: 3D window measured points.

Figure 6.2 and Figure 6.3 present the 3D model of the two analyzed classrooms with the corresponding equipment and dimensions. Thermocouples installed at the window are highlighted in red in Room 2.

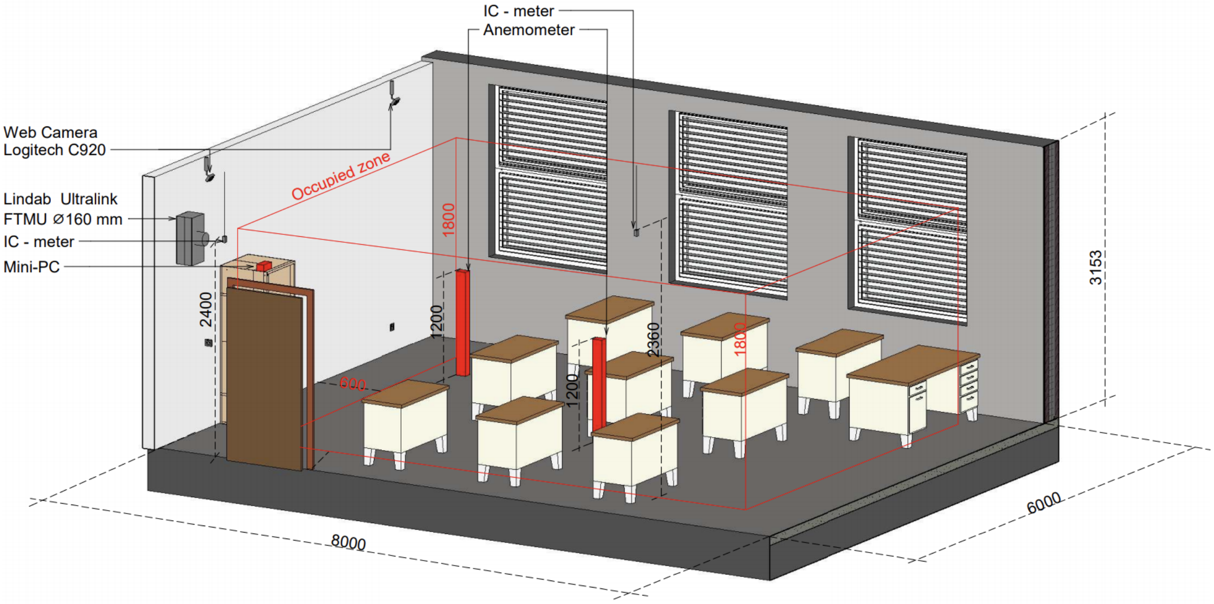

Figure 6.2: 3D model with the equipment of the Room 1.

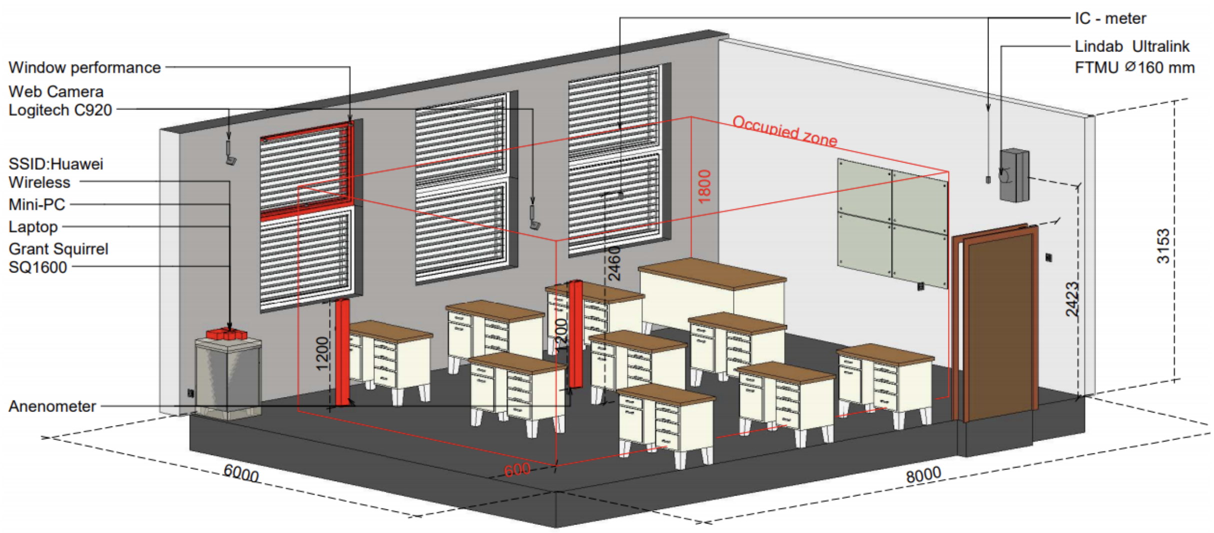

Figure 6.3: 3D model with the equipment of the Room 2.

In the Appendix A there is a brief description of the measurement plan and the reasoning why data has been logged during different duration in time. Every study provides a table where parameter, unit, definition, instrument, duration of time and name point is shown. This nomenclatures is further used in the calculations and data analysis in this chapter. Furthermore, the pictures showing all the equipment positioned in the classrooms and outside are included.

6.1 Methodology

Overall, this analysis is performed during heating season between 18-Dec 2018 to 1-March 2019. The Christmas holidays took place between 22-Dec 2018 to 3-Jan and winter holidays between 9-Feb to 17-Feb. Data from each classroom and one outdoors location has been collected. The school operated normally during this time period, except for the 26-Jan to 29-Jan when the heating system was stalled giving low temperatures in the school. These days have been excluded from the statistical analysis.

All devices result in data for a period of 74 days, 40 schooldays without considering weekends and holidays. All measurements collected at the explained locations are analyzed in this chapter. The measuring points are listed in detail in Appendix A. From all data-set, averages from 5 min, 10 min and hourly mean values have been used in the calculations and the following analysis. real time-step for the logged data, averaged data.

Table 6.1: Logging and averaging of data from all devices used.

Device	2 sec	10 sec	1 min	5 min	10 min	1 hour
Lindabs						
Grant						
IC-meters						
Cameras						
Anemometers						

Figure 6.4 shows the diagram of the measurements from which the methodology is structured, dividing the recorded data in indoor conditions, window performance and outdoor conditions. The general indoor climate evaluation during the heating season at the school takes place for the period of time between 18 Dec - 1 March. However, the local thermal discomfort analysis consists of three representative days (21st, 22nd and 23rd January). In addition, visual comfort measurements is described by instantaneous measurements with lux meters for an overcast sky.

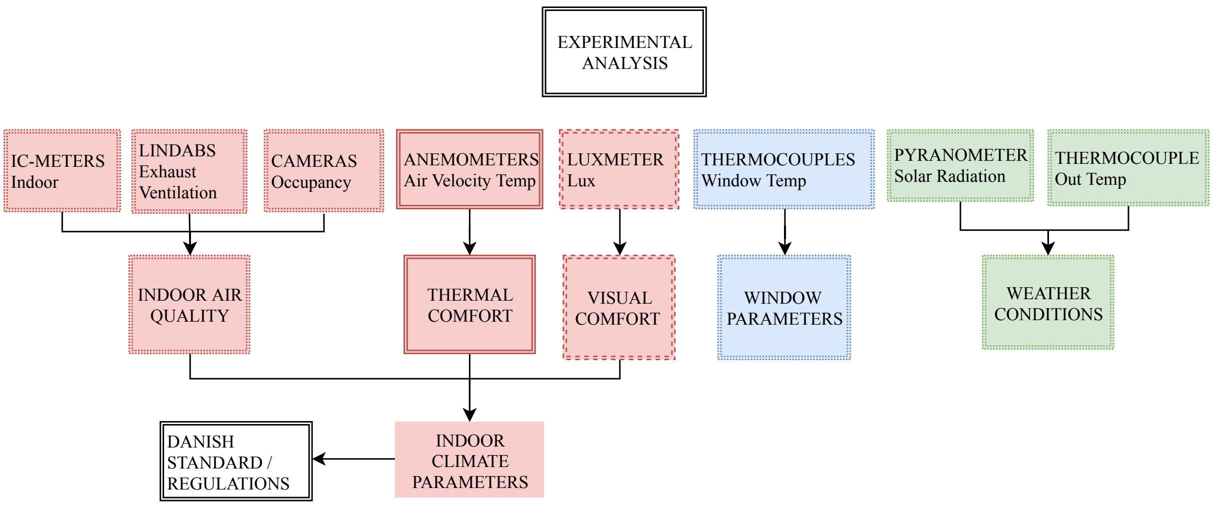

Figure 6.4: Diagram from measurements methodology used for Experimental Analysis at School.

6.2 Limitations and Assumptions

As the experiment has been carried out during normal school activities, the following limitations have been found during this experiment:

- As pictures from the cameras are taken every 5 min there is the possibility that some time the opened door has not been captured. Student headcount have been recorded for each picture.
- IC-meters have not been placed in the occupied zone at the breathing level (1.2 m above the floor level) due to the disturbance in the classrooms. This is why they have been suspended from the ceiling at 2.36 m above the floor level.
- Indoor environment is studied in both classrooms due to different user behavior, occupancy and ventilation system.

During the whole analysis, the following assumptions have been assumed, due to difficulties to be measured and to reach a robust conclusion. Simplifications are listed as follows:

- Occupied hours mean no weekends, no holidays and no period outside 8:00h - 16:00h.
- One window is monitored, however it is assumed that all of them work in the same way.
- No shadows from trees or surrounding buildings on the windows.
- All of the windows remain closed during the analysis.
- Curtains always opened, they are neglected in the analysis.
- Blinds always down and horizontally tilted.

6.3 Indoor Environment

Indoor environment first examines indoor air quality. Based on statistical analysis a correlation between CO_2 and the occupancy profile is investigated. Additionally, based on the carbon dioxide level, the amount of time students are outside the comfort ranges is calculated. Additionally, ventilation effectiveness and air flow calculations are included. The analysis of the local thermal discomfort test, draught risk and vertical air temperature gradient is calculated. Consequently, the study of the relative humidity levels and thermal comfort categories.

6.3.1 Indoor Air Quality

Comfort and occupants well-being are directly influenced by the indoor air quality in indoor spaces. In this manner, the CO_2 concentration in the classrooms is compared to the occupancy measured from the cameras to the designed occupancy from the schedule provided by the school.

CO_2 correlation with Occupancy

CO_2 level and the occupancy have been recorded every 5 min. Based on the data, the general daily profile has been developed both for the CO_2 concentration and the occupancy. For that purpose, data has been averaged by weekdays. That means every Mondays with occupants have been averaged together, creating a general daily Monday profile. The same has been done for the rest of the weekdays. Additionally, the general profile is further compared with the designed profile. Designed occupancy profile is defined by the classroom schedule.

It is assumed that during lectures, the classroom is occupied by the total number of kids, while during the break children are expected to leave the room. Figure 6.5 shows the comparison between the designed occupancy profiles and the CO_2 level for Room 2.

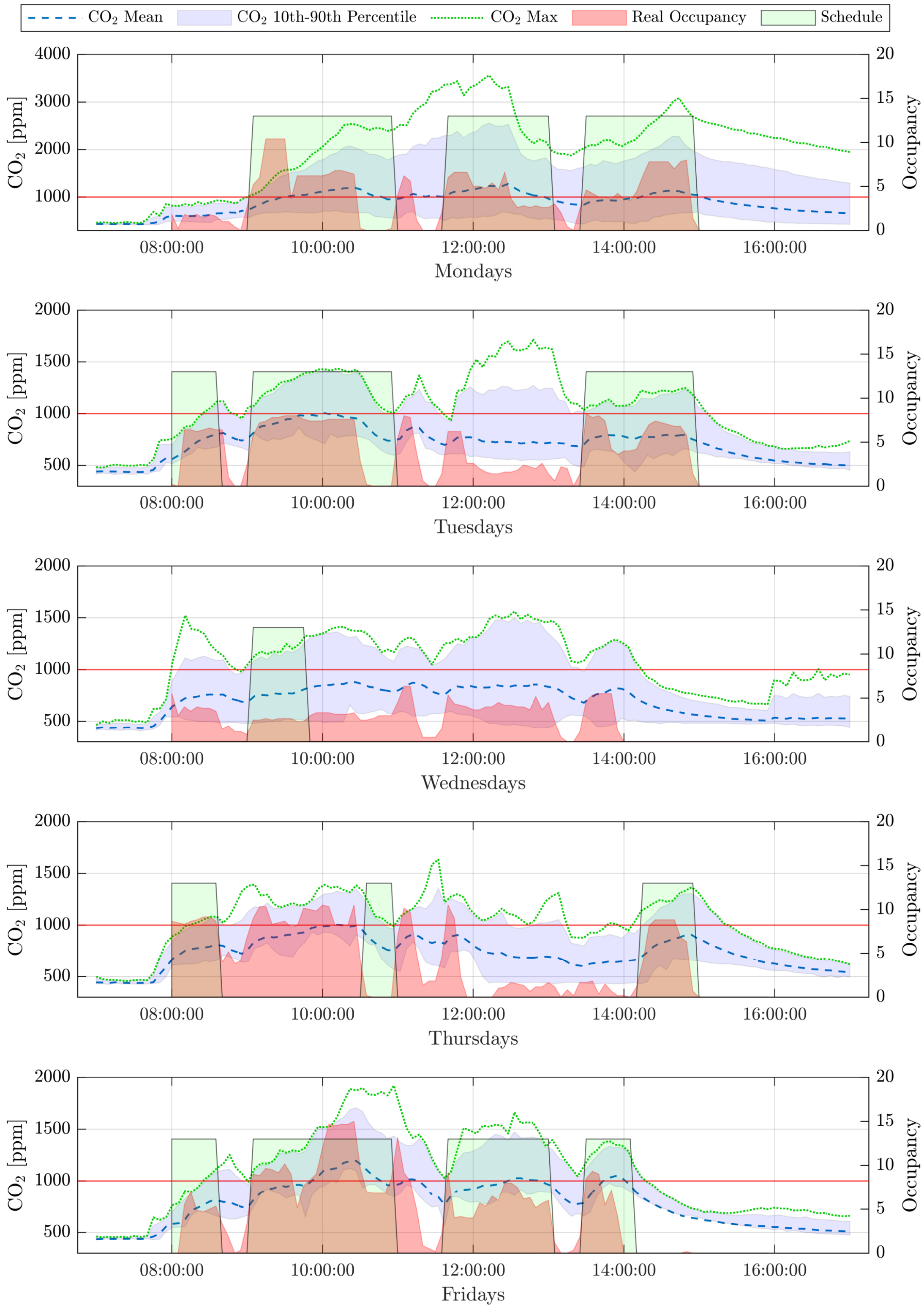

Figure 6.5: CO_2 level and occupancy profile in Room 2 (mechanical ventilation) during a typical winter week.

The figure above is the representation of the averaged profile of the CO_2 concentration together with 10th percentile and 90th percentile and its maximum values. This allows to observe the difference between the mean values and extreme conditions of the CO_2. The horizontal red line highlights the carbon dioxide threshold. These values should not exceed 1000 ppm.

By comparing the mean values of the CO_2 concentration, it can be concluded that Mondays and Fridays are the days with the highest level of concentration. The averaged profiles exceeds threshold stated by the BR 18 [2018]. With regards to the other weekdays, Tuesday and Thursday shows the same tendency with the highest peak of the CO_2 around 10:00 h. Yet, still maintaining the values below the limit. The CO_2 concentration on Wednesdays is the lowest during the entire week being correlated with low occupancy. Outside the working hours, the level stays around 500 ppm.

By looking at the maximum values, Mondays results are the highest among the whole week and reach almost 3500 ppm. The y-axis limit on Monday is set to 4000, while in rest of the week days it is 2000 ppm. However, the deviation from 90th percentile to maximum values is small, meaning that extreme situations with very high occupancy does not happen too often.

In terms of the occupancy profile, the tendency of the correlation between the weekdays is also applicable here. In accordance to the schedule, the kids are expected to be outside school on Wednesdays for additional activities. Most of the days, the highest peak of the occupancy occurs between 9:00 h - 11:00 h, when children have lectures for longer period of time and at the end of the day between 13:30 h - 15:00 h. During the following analysis, it is of interest to compare the real occupancy with the schedule, the so-called designed occupancy profile.

Very often, the buildings operation is designed in accordance to fixed schedules and for a generalized number of the occupants. However, as presented on the following example, the designed and general occupancy profile differ significantly. For 60% of the time, children are present in the classrooms when not expected. It is also important to mention that children spend time in the classrooms during the breaks, that is why the following number is high. Generally, outside the expected unoccupied time, there are 2 kids in the room on average. In terms of the amount of children in the classroom, on average, there are only 41% kids present. For example, on Mondays there should be 13 children, while there are only 5 on average. The variation of the occupancy is presented in the Figure C.3, where the 90th and 10th percentile is shown.

Appendix C.2.1 shows the same analysis but for Room 1, where the correlation between the occupancy and the CO_2 is similar in both cases.

All in all, it can be concluded that the occupancy and the CO_2 level are closely related and dependent on each other. In fact, as presented on the previous figure, the rise is quickly noticeable. Deeper analysis of the factor influential on the CO_2 increase is presented below. The analysis is based on the actual (raw data) for 5th and 25th of February. The Figure 6.6 shows not only the CO_2 and occupancy, but also the door position and temperature in the occupied zone.

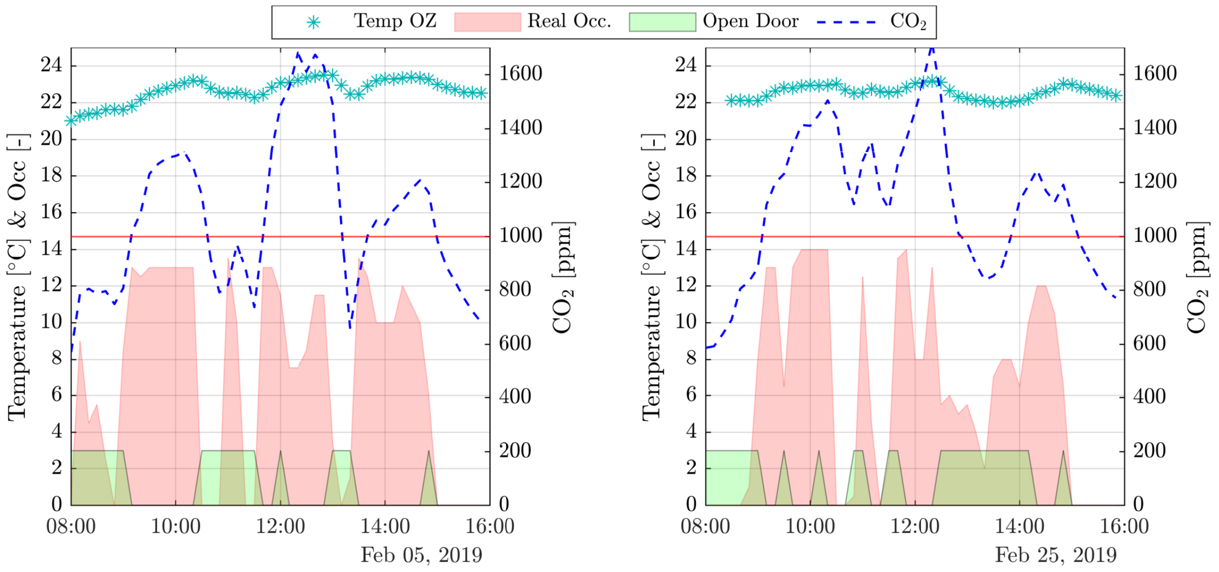

Figure 6.6: CO_2 level and occupancy correlation with door condition during typical winter day in Room 2.

It can be observed in the figure above that the occupancy and the CO_2 are tightly correlated. However, the big influence of the door position can be observed. When doors are closed, the rise of CO_2 is almost immediate. For instance, with the same occupancy of 13 people, the level of CO_2 with the doors closed is 1300 ppm, while with the door open it lowers up to 980 ppm, making the air flow exhaust through the corridor. It can be visible between 10:00 h - 12:00 h. However, between 12:00 h - 13:00 h, with the same occupancy, the level increases up to 1600 ppm. This could be explained by the uncertainties of the measurements or working modes of the windows. The recording time of the door opening and the occupancy has been recorded in 5 min time step. That means, all of the door openings might not have been noticed. That is why, the results with the same occupancy and door situation show different results in the CO_2 level. By looking at the results, in the figure presented to the right, the excessive level of CO_2 is reported for most of the day.

By looking into the temperature in the OZ, with very high CO_2, the OZ temperature also increases slightly. This is an expected behaviour as higher amount of people means higher CO_2, and higher heat loads.

However, it can be concluded that the CO_2 level reacts and is highly correlated with the occupancy. Also, it can be observed that the limit is exceeding for most of the time. Deeper analysis of the discomfort time caused by the CO_2 is presented in the following subsection.

Discomfort Time CO_2

In this section, the percentage of discomfort time from averaged data every 5 min is presented for both rooms. The discomfort time is defined by exceeding 1000 ppm limit. Figure 6.7 presents the data during occupied hours.

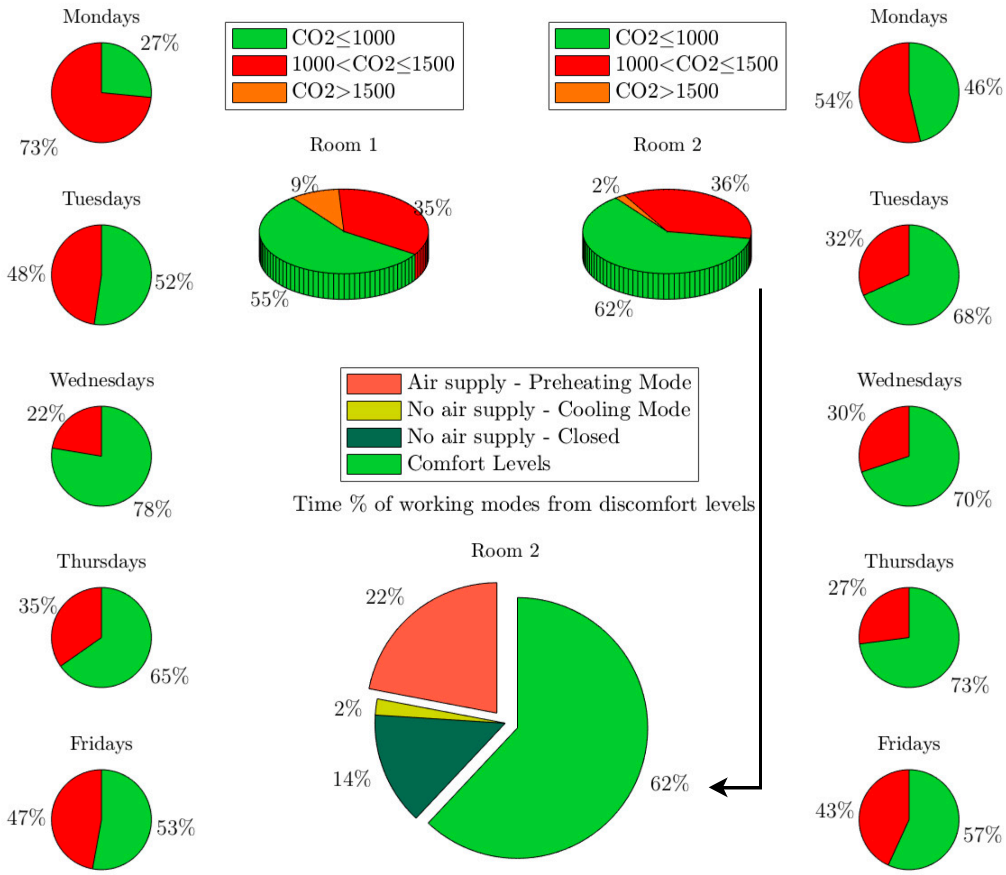

Figure 6.7: Percentage of time during occupied hours when CO_2 level is above 1000 ppm - data averaged every 5 min.

Based in the Figure 6.7 occupants spend almost 35-36% in the uncomfortable conditions. That is clearly an issue, since the children should be provided with the highest comfortable environment. The chart presented on the bottom part shows the influence of the different working modes on the discomfort level in room 2. That means that during the 36% of the discomfort time, 16% of the time there is no air supply to the room. Therefore, concluding in a poor control strategy of the valves.

In addition, the influence of the ventilation extraction, can be observed in the Figure above. Room 1 is driven by natural extraction and Room 2 by mechanical. Results show that the mechanical extraction increases the comfort level in the Room 2 by 7% of the time compared to the Room 1.

Ventilation Effectiveness

Ventilation effectiveness defined by Equation 5.1 uses data from the positions C_e and C_{oz}. The CO_2 concentration outdoors has been assumed to be 350 ppm, as it has been the minimum concentration reported in the room. Results are shown in Figure 6.8. This calculation takes data averaged every 5 min and only during occupied hours.

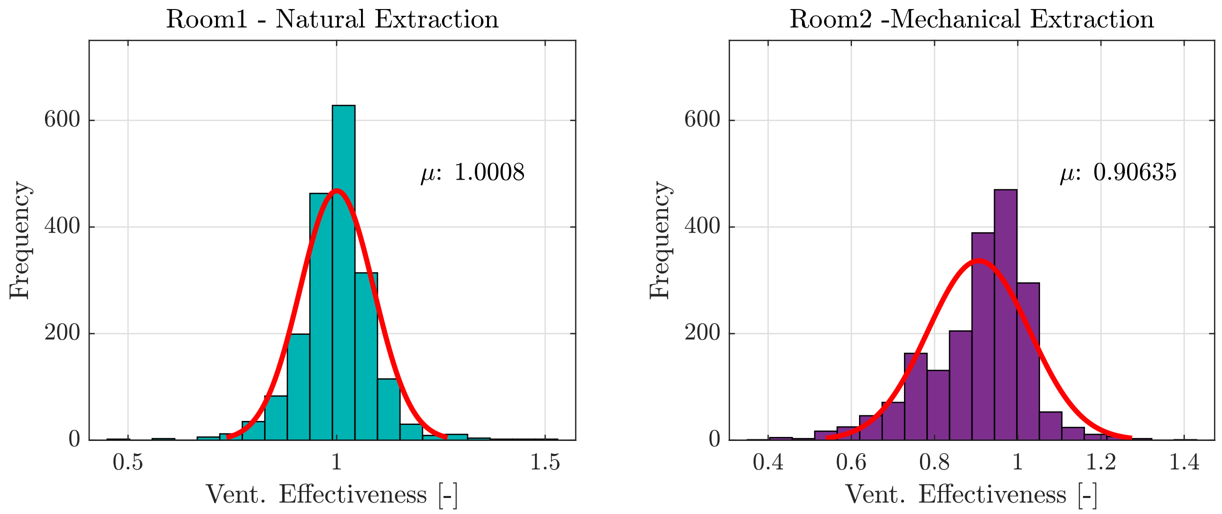

Figure 6.8: Ventilation Effectiveness during two case studies for both rooms.

The results show that the ventilation effectiveness is close to 1 in both rooms. This illustrates a mixing air distribution, where concentration in the occupied zone and the exhaust are very similar. In addition, Room 1 with natural extraction reports higher frequency of values closer to one, resembling a more defined normal distribution. Therefore, even though the Room 2 with mechanical extraction shows more time in the comfort range with regards the amount of CO_2 in contrast to Room 1 (as seen in Figure 6.8), Room 2 does not show a better ventilation effectiveness. This might be due to the fact that the IC-meter located in the occupied space is nearly as high as the one in the exhaust. Consequently, not fully representing the concentration at the breathing height but giving an idea of the ventilation strategy in the rooms.

Air Flow Calculations

As previously explained in Section 5.1.2, the carbon dioxide concentration can be used as an indicator of air quality and after a time, t. In this subsection an analysis of the air flow rate through the exhaust and the window is conducted. Due to the impossibility of measuring the real air flow rate coming through the windows in the school, the dilution equation is used. It is worth mentioning that the data from occupation, CO_2 and flow meters have been filtered. It is due to the fact that no occupancy or an open door the results would be unrealistic. This conditions for the filtration are summarized bellow:

- Data taken only when the window is supplying air (preheating mode),
- Data taken only when there is occupancy,
- Data taken only when the door is closed.

Figure 6.9 represents the difference in the results obtained calculating the dilution equation and the measured air flow rates at the exhausts. It can be seen how the results in both rooms from the dilution equation are more spread. This is due to people and CO_2 variability. In addition, in Room 1 with natural extraction the mean air flow from the Lindabs is lower than the results from the dilusion eq., therefore, resulting in a pressurized room. However, on the right-hand side in Room 2 where there is mechanical extraction, the room is underpressured, which does not help to avoid infiltration but it is more beneficial to make more flow rate go through the ventilated window.

By comparing both measured flow rates they are very different in range and values. From it can be seen that the flow meter at the exhaust differs more due to being driven by natural forces (5-40 l/s), whereas mechanical extraction sucks the air most of the times at a constant air flow rate (120 l/s).

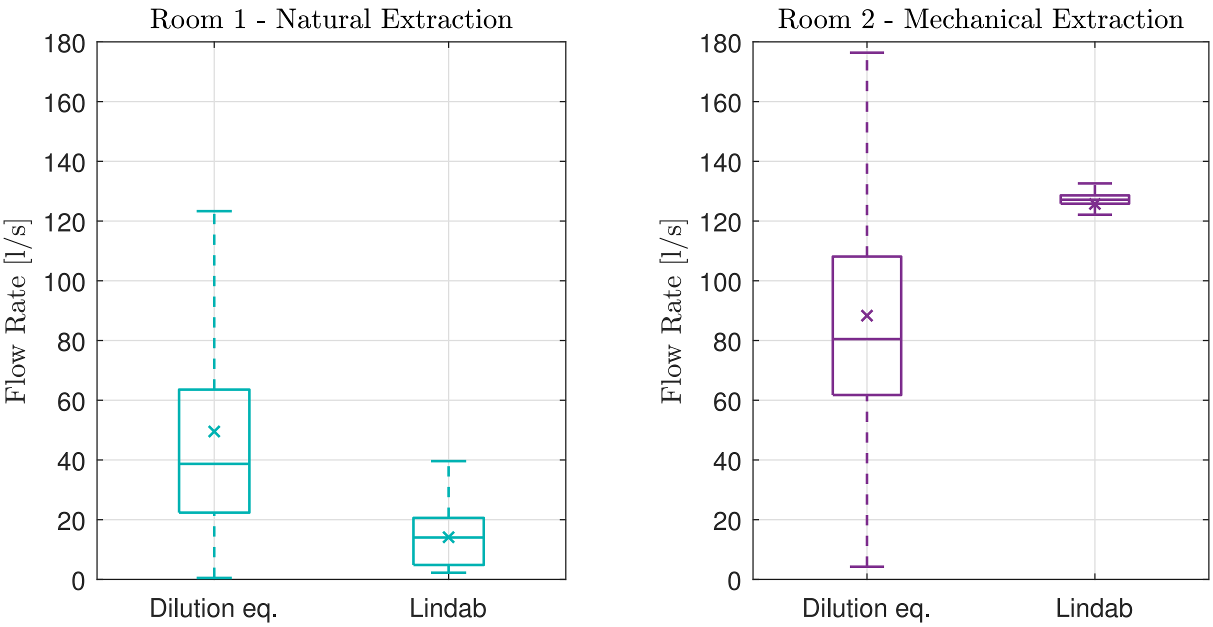

Figure 6.9: Comparison of the dilution equation results and Lindabs air flow rates.

Table 6.2 gives the mean values from both for the dilution equation results and flow meter measurements. It can be concluded results do not correlate. However, when comparing both dilution and flow meter mean values with the air flow capacity chart provided by *VentilationsVinduet*,(Table C.8), it can be seen that both are out of the range for a naturally driven window, whereas the dilution equation for the mechanical exhaust works as expected.

Table 6.2: Comparison of average values of air flow rates calculated and measured.

	Room 1	**Room 2**
	μ	μ
Dilution Equation q_{DE} [l/s]	48.3	88.3
Extraction q_e [l/s]	12.75	123.38

Now, a second analysis is conducted in order to estimate the proper air flow rate needed in the room from which CO_2 levels will not rise above 1000 ppm. For this analysis, one representative day for each room has been chosen. Due to the filtering explained at the beginning of this subsection there are lots of gaps in the results.

Figure 6.10 represents one day in each room. The actual CO_2 from IC-meters in the occupied zone is plotted, together with the corresponding air flow rate calculated by dilution equation, $q_{actual_{DE}}$. The optimal air flow rate from which the CO_2 level will not rise above 1000 ppm is the $q_{optimal_{DE}}$.

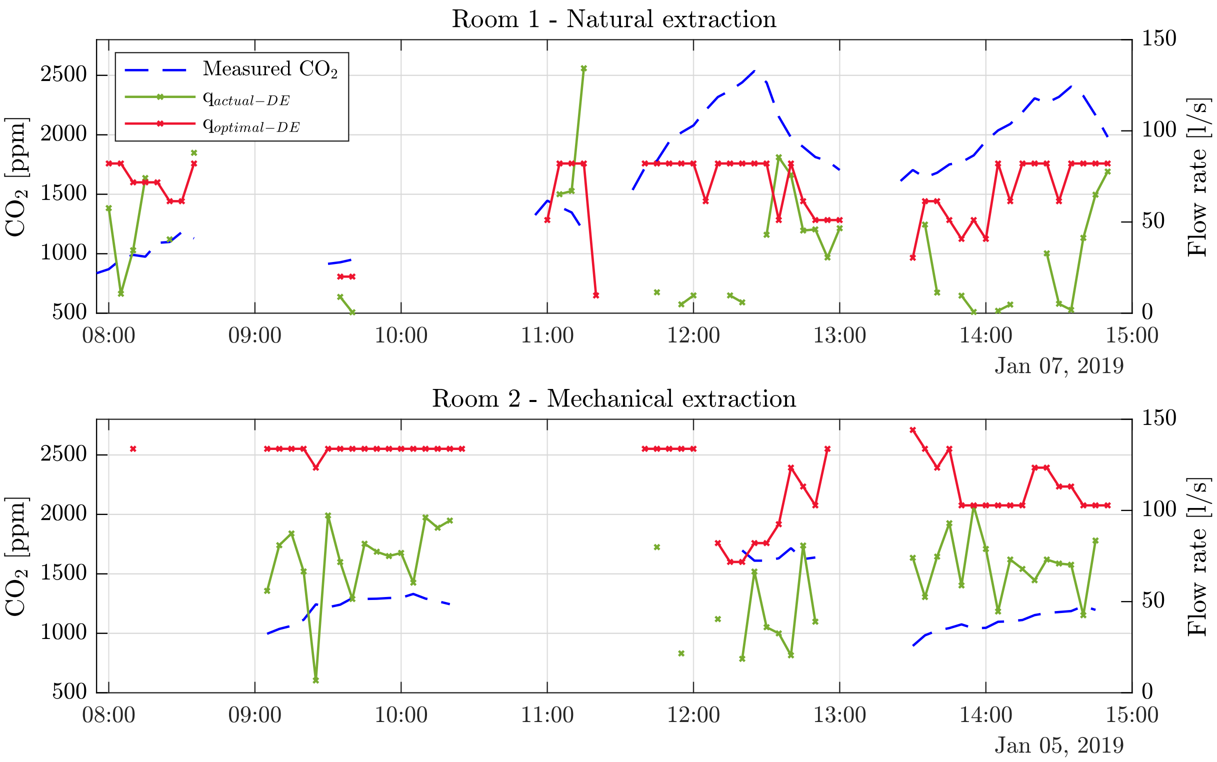

Figure 6.10: Actual CO_2 concentration, and actual flow and optimal air flow rate by dilution equation

Although Room 1 had an occupation of 7 people throughout the day, and Room 2 had an occupation of 13 people in the morning and 11 in the afternoon, from the Figure 6.10 it can be seen that the Room 1 is reporting higher CO_2 concentrations. This is due to the very low air flow rate supplied by the windows. Furthermore, it can be seen that most of the time the actual air flow rate is lower than the optimal, concluding that there is a need for the windows to supply more air flow and that a mechanical exhausts performs better than a natural driven one.

Consequently, the analysis of how much air flow rate would be needed in order not to overcome 1000 ppm during the occupied hours for a working day according to different occupations is represented in the Figure 6.11.

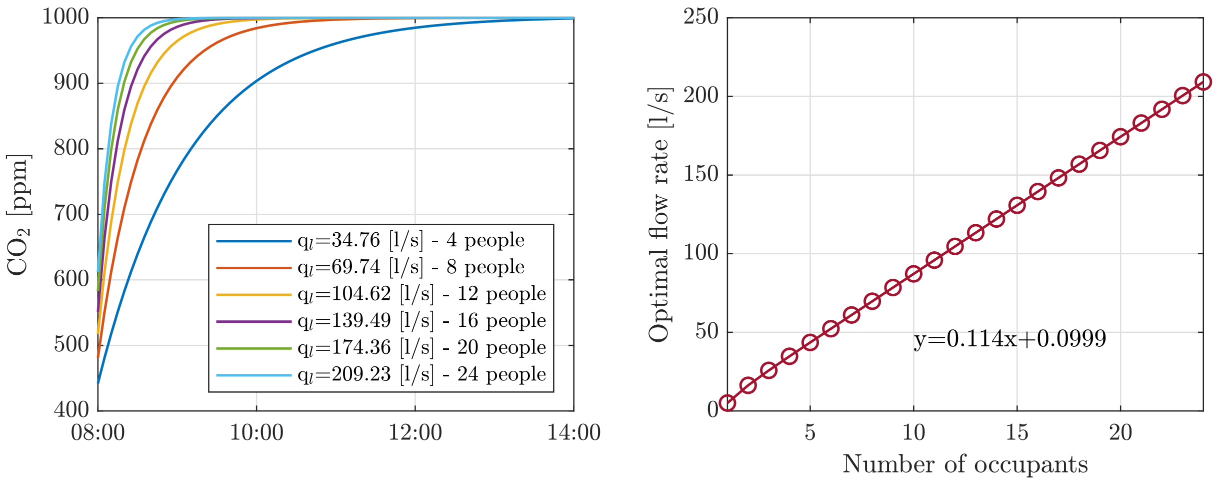

Figure 6.11: Optimal air flow rates for different occupancy and corresponding CO_2 concentration

From the previous figure the optimal air flow rate and the linearity between occupancy and flow rate according to the dilution equation can be seen. This relation is used as a guideline for the experimental air flow rate measurements in Chapter 7. In addition, the time it takes for the CO_2 to stabilize can also be seen. For few amount of people the concentration is bellow 1000 ppm for longer time than for a higher amount of people that 1000 ppm is much faster reached.

6.3.2 Relative Humidity

Humidity results show that none of the two classrooms present problematic level. They are all between 20-52%, which is the reference value recommended by DS/EN 15251 [2007]. Raw plotted data can be seen in Appendix, Figure C.4.

6.3.3 Thermal Comfort

There are four thermal comfort ranges in accordance to the DS 1752 [2001], which are explained in Section 5.1.4. Figure 6.12 presents measured temperatures in the occupied zone only during occupied time.

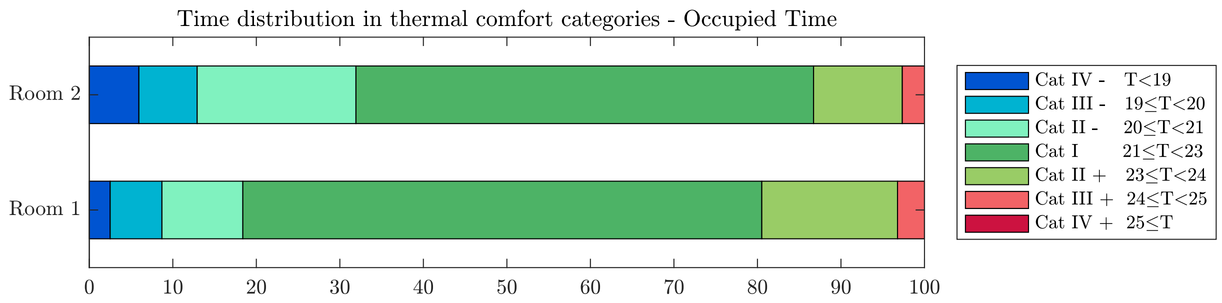

Figure 6.12: Categories according to Room Temperature - data averaged every 10 min.

From the figure above, it is shown that up to 85% of the time, Category I or II is achieved in both rooms, meaning that no problem due to overheating or too cold temperatures have been experienced. Note that colder temperatures have been recorded as the analysis has been performed during the winter season.

Local Thermal Discomfort

Three days are selected (21st, 22nd 23th of January) in order to proceed with the local thermal discomfort measurements, which are vertical gradient temperature and air velocity in the occupied zone. Two poles are located in the room holding 4 anemometers each, as shown in Table 6.3. They measure temperature and velocity at 4 vertical points from 0.2 m to 1.2 m from the floor. A detailed explanation of how anemometers work can be found in Appendix B.4.

Table 6.3 shows the location of the set of anemometers, being P_1 the always next to the window and P_2 in the occupied zone. This one renamed as $P_{2.1}$ the last day due to a change to a position next to the door. This change is made with the intention of reporting if increase in air velocity was occurring when the door is open.

Table 6.3: Location of measurements for Local Thermal Discomfort at the school.

	Monday 21/01	**Tuesday 22/01**	**Wednesday 23/01**
Room	Room 1	Room 2	Room 1
Occ.	Yes	Yes	No
	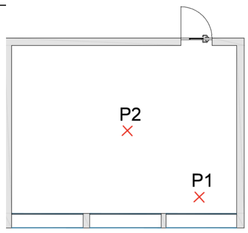	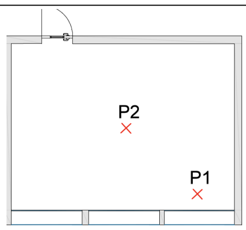	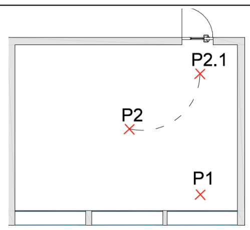

Draught Risk

Draught is calculated from the velocity and temperature measurements using the Equation 5.5 where local turbulence intensity is assumed 40%. In this analysis the aim is to find if velocities of more than 0.2 m/s are experienced. It is also interesting to see if higher air velocities are in the middle of the room P_1 or in front of the window P_2. The last comparison is to see if opening the door influences this parameter.

Figure 6.13 presents the results of the data collected during the occupied days 21st and 22nd (Figure 6.13a), data during the unoccupied day 23rd January with door closed (Figure 6.13b) and data obtained when door is opened and the pole is in $P_{2.1}$ (Figure 6.13c).

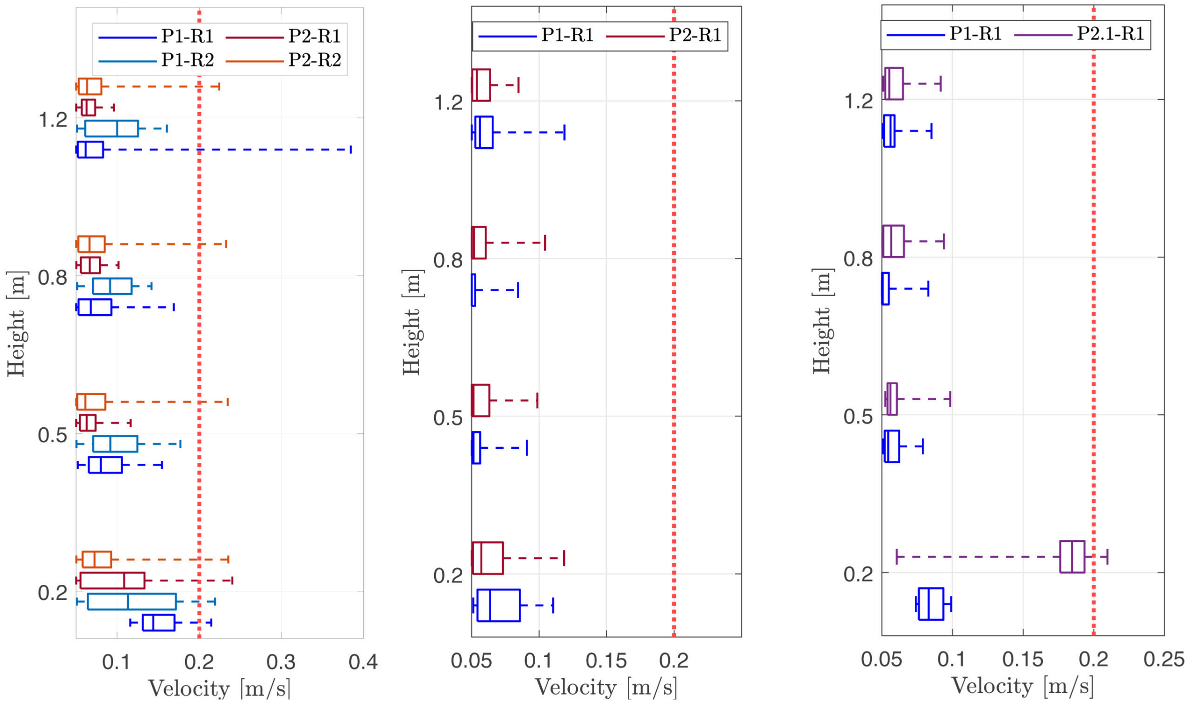

(a) Occupied-Door Closed ***(b)*** Unoccupied-Door Closed ***(c)*** Occupied - Door Open

Figure 6.13: Air velocity measurements from all anemometer in different rooms during different room conditions

From Figure 6.13a results show that the anemometers at the floor level next to the window P_1, reaches values of more than 0.2 m/s and give higher medians. Especially, that is visible on Figure 6.13c, in Room 1 which has less distance from the window to the door, therefore, creates air streams when the door is opened. With regards to the results in the occupied zone, Room 2 is showing higher maximum values although having a similar median value. The reason for this might be because this room is the one having a mechanical exhaust, and consequently, creating and under-pressure that makes more air move though the cavities of the window. In general, the 75% percentile in all of the data stays within the acceptable air velocity range.

Figure 6.14 is a one day representation of the results. Parameters are taken from the anemometer at 1.2 m in position P_2, occupied zone during 22nd January.

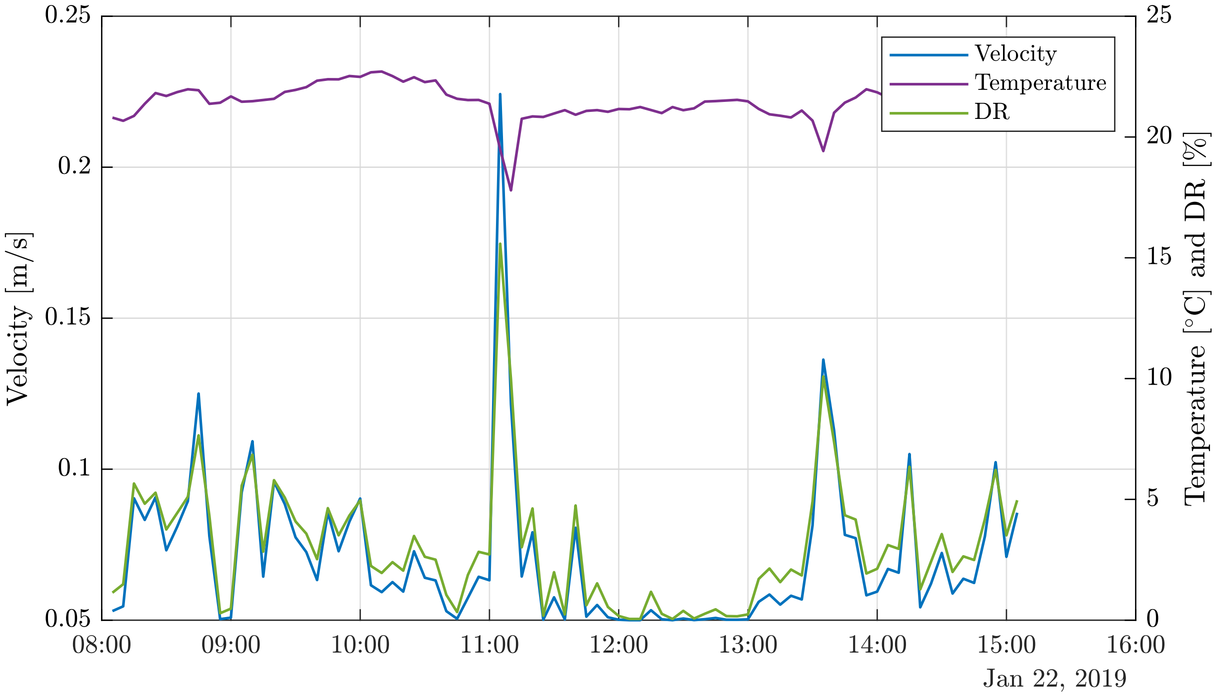

Figure 6.14: Velocity and temperature from an anemometer at 1.2 m in the occupied zone and its corresponding Draught Rate.

Accordingly to the previously mentioned equation, draught rate is strongly depend on the air velocity following the same curve at each time. Also highlight when an increment of air velocity happens a slight decrease of temperature is experienced (11:00 h and 13:30 h). This relation can be extended to all the anemometers.

Afterwards, Figure 6.15 shows a comparison of all the parameters collected by the anemometers at different heights during all the occupied hours. In addition, a vertical line represents the threshold set by the regulations ISO 7730 [2005] in which the draught rate should not be higher than 10 %.

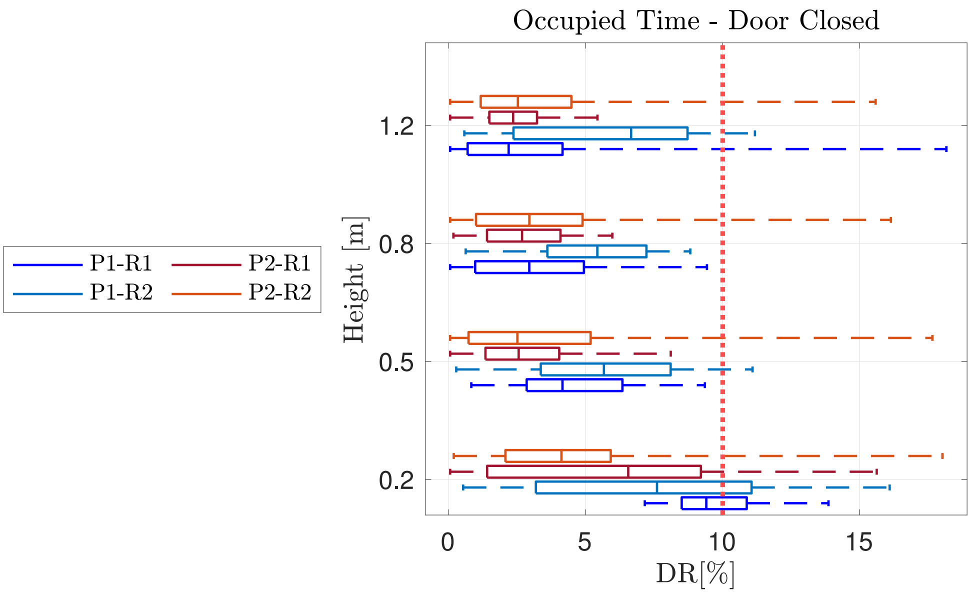

Figure 6.15: Draught Rate from all anemometers during occupied time at position P_1 and P_2.

According to the previous figure, anemometers next to the window P_1-R_1 and P_1-R_2 experience the higher discomfort as the values are greater than in the middle of the room. However, there is a general tendency of the anemometers in the lowest part experiencing higher draught rate than the ones located higher. With regards to the anemometers placed in the occupied zone, P_2-R_1 and P_2-R_2, the values are always smaller, nevertheless, P_2-R_2 experience greater values in all heights. Furthermore, as explained in Figure 6.15 about the close correlation between velocity and draught rate, all anemometer give the same profile as Figure 6.13a.

Vertical Air Temperature Gradient

Vertical temperatures are compared in Figure 6.16 according to the different heights and locations only during the two days with occupancy.

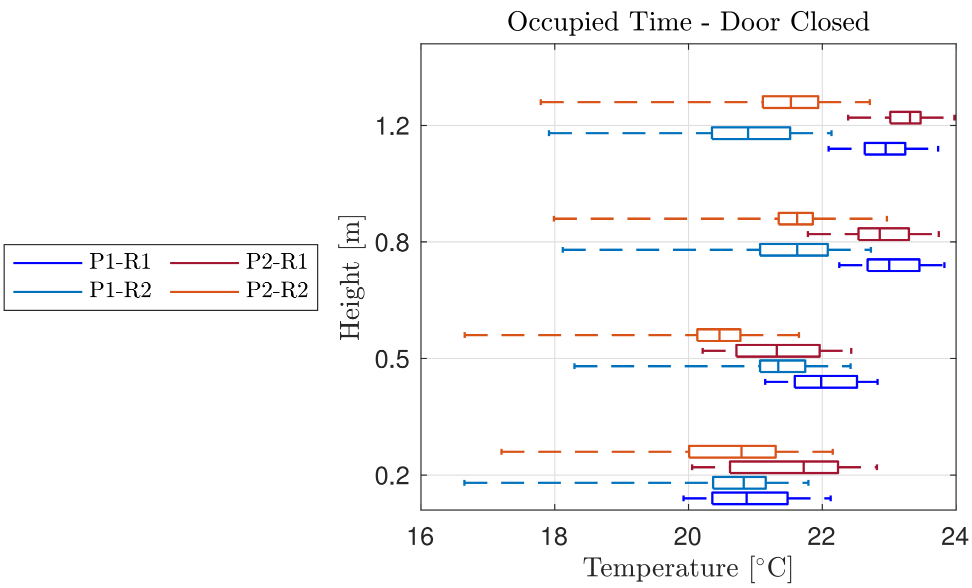

Figure 6.16: Air Temperature measurements from anemometers at different heights.

The results presented in the Figure 6.16 show that the temperature increase with the height. For this reason, the difference (ΔT) between the anemometers placed at 0.2 m and at 1.2 m is further analyzed on the following figure for both rooms. In addition, the actual occupancy profile and the instants when the door is opened are added to see its influence.

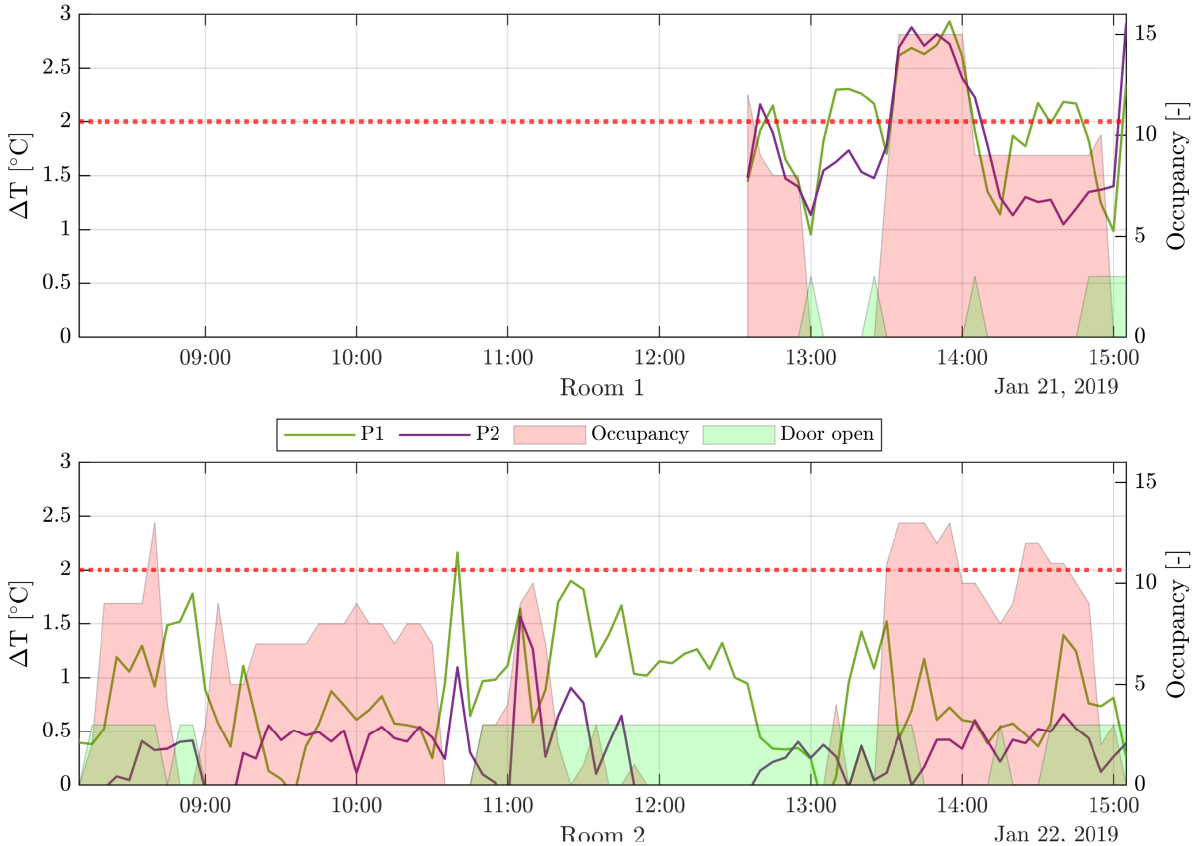

Figure 6.17: Air Temperature Gradient between top and bottom anemometers in position P1 and P2, in each room during occupied hours.

From Figure 6.17 it can be seen that ΔT exceeds the limit of 2 °C set by the regulations specified by ISO 7730 [2005] when higher occupancy. In addition, with regards to Room 1 when the door has been closed during all logging time (only three punctual opening happened at 13:00 h, 13:25 h and 14:05 h), the anemometers in the occupied zone P_2 follow the occupancy pattern. This means that temperature is strongly driven by heat sources, whereas the one next to the window P_1 is not. However, this effect does not occur in Room 2, where the door has been open for long periods of time during the day. Therefore, indicating that the air flow exchanged between the corridor and the room has an influence with regards to the thermal conditions in the rooms.

6.4 Window Performance

When pre-heating mode (PH-mode) is in use temperatures in the upper part of the cavity are above 12 °C and below 30 °C. Cooling mode (C-mode) opens when temperature gets to be 30 °C or more. However, during this winter season no outside temperatures above 15 °C have been recorded, therefore the Bypass valve has remained closed all the time.

Figure 6.18 compares the frequency of each mode during occupied hours and all the time. Outside temperatures are higher during occupied time than during night, this is why preheating is mostly used. Both charts are divided by supply and no supply from the window. Highlight from the left-hand side of the figure that for 44% of the occupied time there is no fresh air supply.

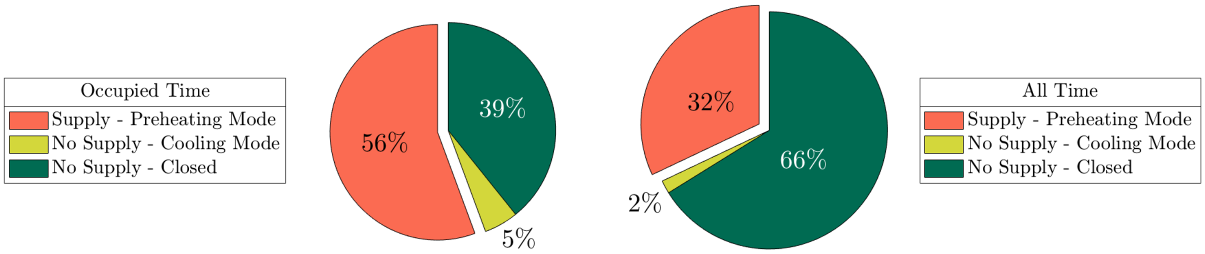

Figure 6.18: Comparison of the frequency in use of each working modes during occupied hours or during all day- data averaged every 10 min.

Figure 6.19 takes the right hand side data from Figure 6.18 and displays its daily distribution. This allows to see every changing mode during the day. Shaded area represent weekends and holidays, meaning no occupancy in the rooms. By different colors the working modes by temperatures with its referred solar radiation are presented.

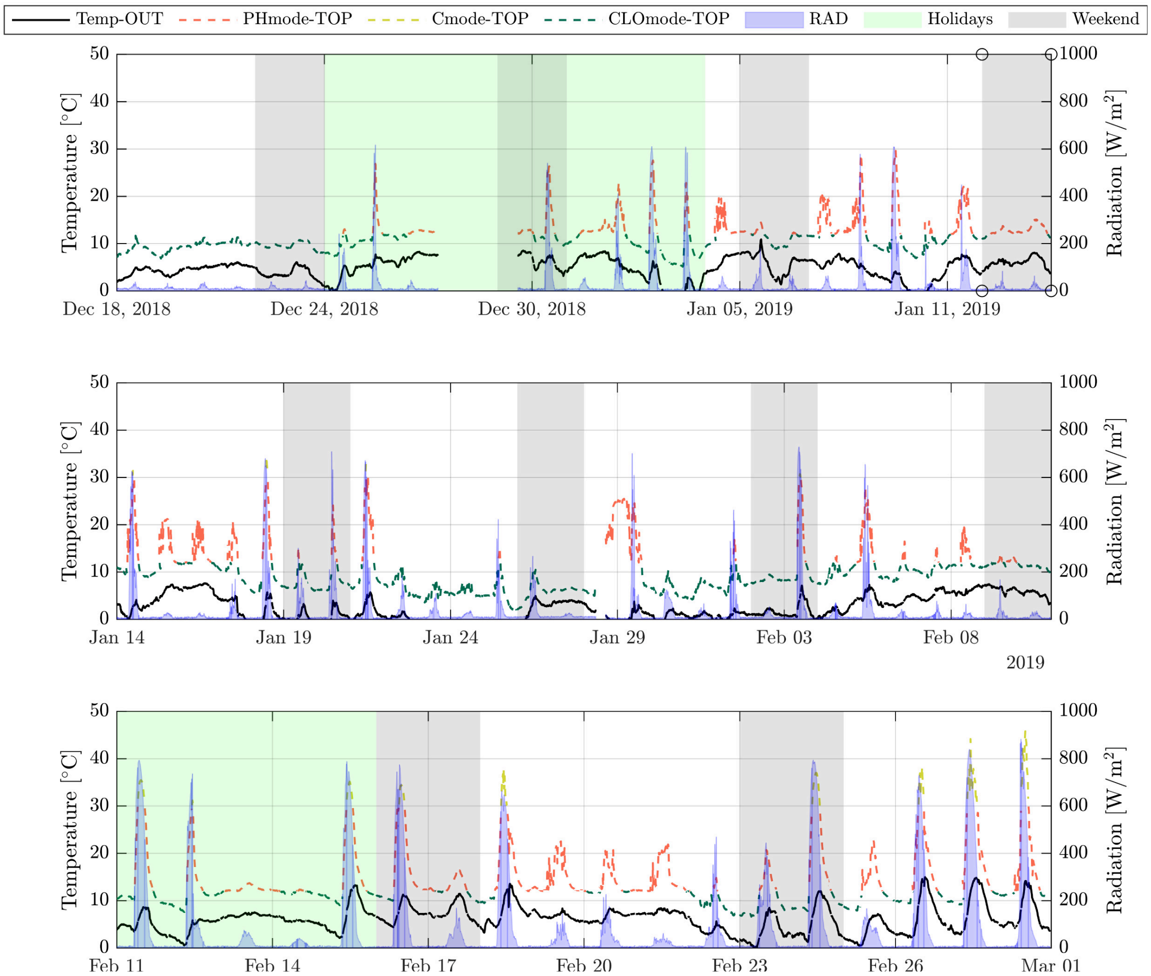

Figure 6.19: Daily variation between working modes of the window - data averaged every 10 min.

In December, less air is supplied due to too low outdoor temperatures ($T_{OUT} < 15$ °C), shown during the week of the 18th Dec.2018. It can be clearly seen that the solar radiation has an influence on the temperatures in the upper part of the cavity (T_{TOP}), as seen during 18th February for example. More solar radiation means a higher increment of the temperatures inside the cavity. However, during 15th and 16th of January, days with low solar radiation and low outdoor temperature, high temperatures at the top of the cavity have been reported. Comparing 15th and 16th of January (occupied days) with 13th - 14th February (unoccupied day) all with low solar radiation, the occupancy might have a big influence on the window performance. This effect could be caused by an influence of the indoor conditions and heat transferred to the window. This specific case is further studied in section 6.4.1, as Case 1.

Window thermal behavior is evaluated zooming in during two representative winter days in Figure 6.20 only during occupied hours: a sunny winter day and an overcast winter day.

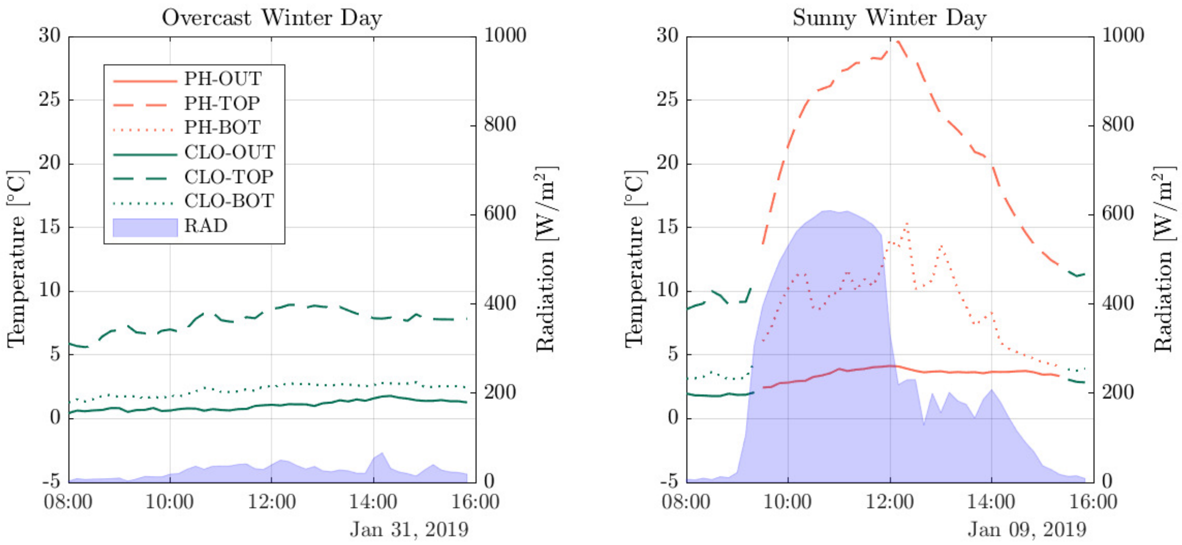

Figure 6.20: Comparison of window performance during winter period in a sunny and overcast sky - data averaged every 10 min.

The supply top temperature is related to outdoor air temperature and strongly related to solar radiation. During the night or in the overcast day, the preheated air temperature is proportional to outdoor air temperature,as seen from the left hand side of Figure 6.20. However, when solar radiation is present, the supply temperature significantly increases and reaches a peak. It is when the solar radiation is strongest, shown in right hand side of the figure. From the sunny day it is also relevant to highlight that even though after 12:00 h the solar radiation decreases, the temperature at the cavity still increases. This might be due to the fact that the thermal mass of the building also helps on releasing heat to the cavity when solar radiation starts to decrease.

In Table 6.4 a synthesis of the mean, standard deviation, maximum, minimum and percentile values of the main thermal measurements with regards to each working mode are reported. During occupied hours, preheating mode represents 56%, cavity closed a 39% and cooling mode a 5% of the time.

Table 6.4: Ranges for temperatures outside and at the window during different working modes during all time - data averaged every 10 min.

Parameter	Mode	$\mu \pm \sigma$	p90	p10	Max	Min	Preheating Mode Cooling Mode Closed Mode
$\mathbf{T}_{TOP}$	Preheating	14.76 ±2.94	22.50	12.19	29.92	12.00	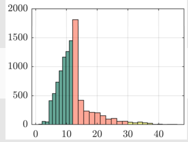
	Cooling	33.75 ± 1.71	37.7	30.55	45.79	30.02	
	Closed	9.01 ± 0.90	11.52	5.74	12.00	1.95	
$\mathbf{T}_{OUT}$	Preheating	6.22 ± 1.06	8.25	2.97	14.97	-3.29	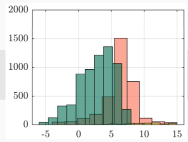
	Cooling	10.05 ± 1.20	14.09	5.34	14.86	2.57	
	Closed	2.74 ± 0.94	5.94	-1.02	7.46	-5.01	
$\mathbf{T}_{BOT}$	Preheating	9.36 ± 2.51	15.08	6.78	33.78	-0.13	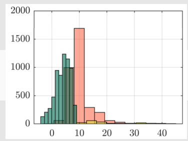
	Cooling	21.03 ± 3.08	36.20	11.86	44.41	9.12	
	Closed	3.90 ± 0.97	7.07	0.079	8.511	-3.99	
$\Delta\mathbf{T}_{TOP-BOT}$	Preheating	5.18 ± 1.94	9.81	3.51	20.82	-8.70	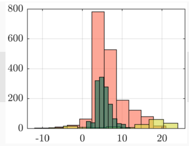
	Cooling	13.37 ± 3.47	21.133	-2.11	23.39	-11.23	
	Closed	5.12 ± 0.56	6.74	3.49	11.69	1.56	
$\Delta\mathbf{T}_{TOP-OUT}$	Preheating	8.54 ± 2.90	17.57	4.86	28.32	3.45	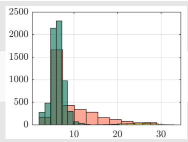
	Cooling	23.70 ± 2.01	28.27	20.08	32.39	15.29	
	Closed	6.27 ± 0.68	7.91	4.49	14.35	2.26	

Upper cavity temperature (T_{TOP}) shows clearly when switching working mode between closed to preheating, meaning that there are no overlaps in the histogram. Most of the measurement are between 11-13 °C, which is the criteria for switching mode. Therefore, it could happen that for a period of time the valve is not fully opened yet towards one mode.

- Percentile 90 from preheating 22.50 °C and percentile 10 from Cooling 30.55 °C do not match. This is because when PH-mode, temperatures are most frequent closer to the lower limit of 12 °C than the upper one 30 °C.
- Percentile 90 from Closed position is 11.5°C and percentile 10 from preheating 12°C match.

Outdoor temperature (T_{OUT}) has the same ranges for all working modes, as seen in the histogram for this parameter. Based only on this parameter it is not accurate to know the working mode of the window because all are between -5°C and 14°C. However, a pattern based on the mean values has been found:

- In Preheating mode outdoor temperature oscillates between 6.22 ± 1.06 °C.
- In Cooling mode outdoor temperature oscillates between 10.05 ± 1.2 °C.
- In Closed position outdoor temperature oscillates between 2.74 ± 0.94 °C.
- As temperatures over 15°C have not been measured, no Bypass mode is reported.

Bottom temperature (T_{BOT}) is only interesting when comparing the gain in the cavity $\Delta T_{TOP-BOT}$ as it shows how much the air is preheated in the cavity. These differences in their gradients are directly related to solar radiation:

- Preheating mode temperature gradient Δ $T_{TOP-BOT}$ gains on average 5.18 °C.
- Cooling mode temperature gradient Δ $T_{TOP-BOT}$ gains on average 13.37 °C.
  * Preheating and cooling mean value is not real due to the possible reverse flow that the window experiences in which the bottom is at a higher temperature than the top one. For this reason some frequency in the histograms can be seen on the negative range. Therefore, minimum values are negative. Taking only the positive temperature gradients, the mean values increase to 5.83 °C, PH-mode and 16.52 °C, C-mode.
- Closed mode temperature gradient Δ T_{TOP-} gains on average 5.12 °C.

Temperature differences between outside and top cavity (Δ $T_{TOP-OUT}$) shows how much the air is pre-heated from outside.

- Preheating mode temperature gradient Δ $T_{TOP-OUT}$ gains on average 8.54 °C.
- Cooling mode temperature gradient Δ $T_{TOP-OUT}$ gains on average 23.7 °C.
- Closed mode temperature gradient Δ $T_{TOP-OUT}$ gains on average 6.27 °C.

The reason why big differences come when comparing the heat gain from outside to the bottom are due to the thermal mass of the building and also, the heat transfer from the sash to the air. When preheating or cooling are running, more intense solar radiation is occurring, however, in closed mode only 1 °C is increased in average. This might be due to the low outdoor conditions or not enough solar radiation during this winter season.

Table 6.5 shows the same synthesis for solar radiation. Only data during occupied time has be taken.

Table 6.5: Solar Radiation on the façade and windows during different working modes only during occupied hours - data averaged every 10 min.

Parameter	Mode	$\mu \pm \sigma$	p90	p10	Max	Min	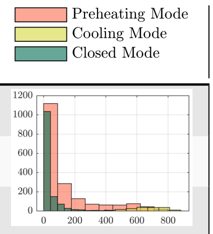
	Preheating	145.85 ± 107.61	467.54	14.14	882.58	2.64	
Radiation	Cooling	624.68 ± 115.55	789.21	470.68	870.87	204.40	
	Closed	41.37 ± 30.99	89.71	8.39	432.23	2.42	

Mean values with the standard deviation show clearly a relation between radiation and working mode. A range of 0-90 W/m^2 would be the range for Closed mode, from 470 W/m^2 it would be when Cooling starts, leaving the middle range for Pre-heating mode. From the data it can be concluded that:

- Percentile 90 from preheating at 467.54 W/m^2 and Percentile 10 from Cooling at 470.68 W/m^2 match.
- Percentile 90 from Closed at 89.71 W/m^2 and Percentile 10 from preheating at 14.14 W/m^2 does not match. This might be due to the relation between top temperature and internal heat gains when there is low solar radiation.

From Figure 6.21 relation between Δ $T_{OUT-TOP}$ and the solar radiation can be seen.

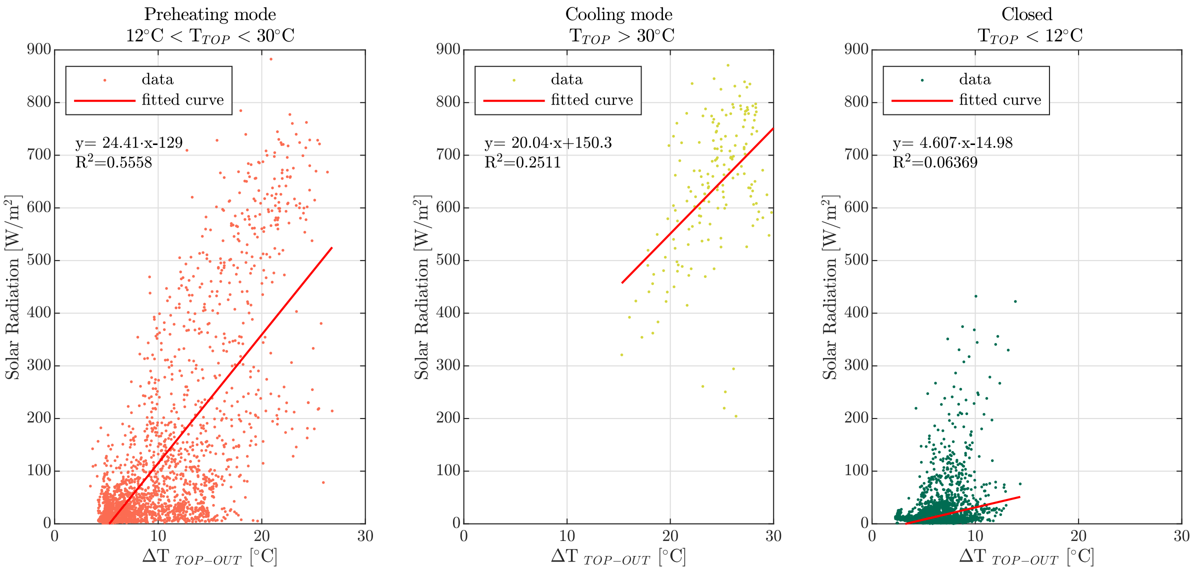

Figure 6.21: Comparison of the relation between $\Delta T_{TOP-OUT}$ and solar radiation for each working mode - data averaged every 10 min.

It differs clearly between cooling mode (300-800 W/m^2) and cavity closed (0-200 W/m^2), while preheating covers all solar radiation range from 0-900 W/m^2 as explained from the previous table. It is also visible that as the temperature at the top of the cavity is heated under the same conditions both for preheating and cooling, a similar linearity can be seen even though the data is spread. The reason for this might be due to the different air flow rates through the window.

6.4.1 Comparative Case Studies

After the previous overview analysis, some specific combination from individual parameters conduct a special behaviour in the window performance. Table 6.6 summarizes which parameters are analyzed by different cases.

Table 6.6: Different Case Analysis for window performance with regards Indoor Environment.

Is it affected? X	**High Value** ↑	**Low Value** ↓	**Event** ✓	**Not applies** -
Parameters	**Case 1**	**Case 2**	**Case 3**	**Case 4**
OUT Temp	-	-	-	-
TOP Temp	X	X	-	↓
BOT Temp	X	-	X	X
Temp OZ	-	-	-	-
CO_2	-	-	↑	-
Solar Radiation	↓	↓	-	✓
Working mode	Pre-heating	Closed	Pre-heating	Cooling
Occupancy	✓	✓	-	-
Door	Opened	Closed	Closed/Opened	-
Crucial Period	12:30-14:30	9:30-10:30 13:30-15:00	9:00-10:15 10:15-12:00	12:00-14:00

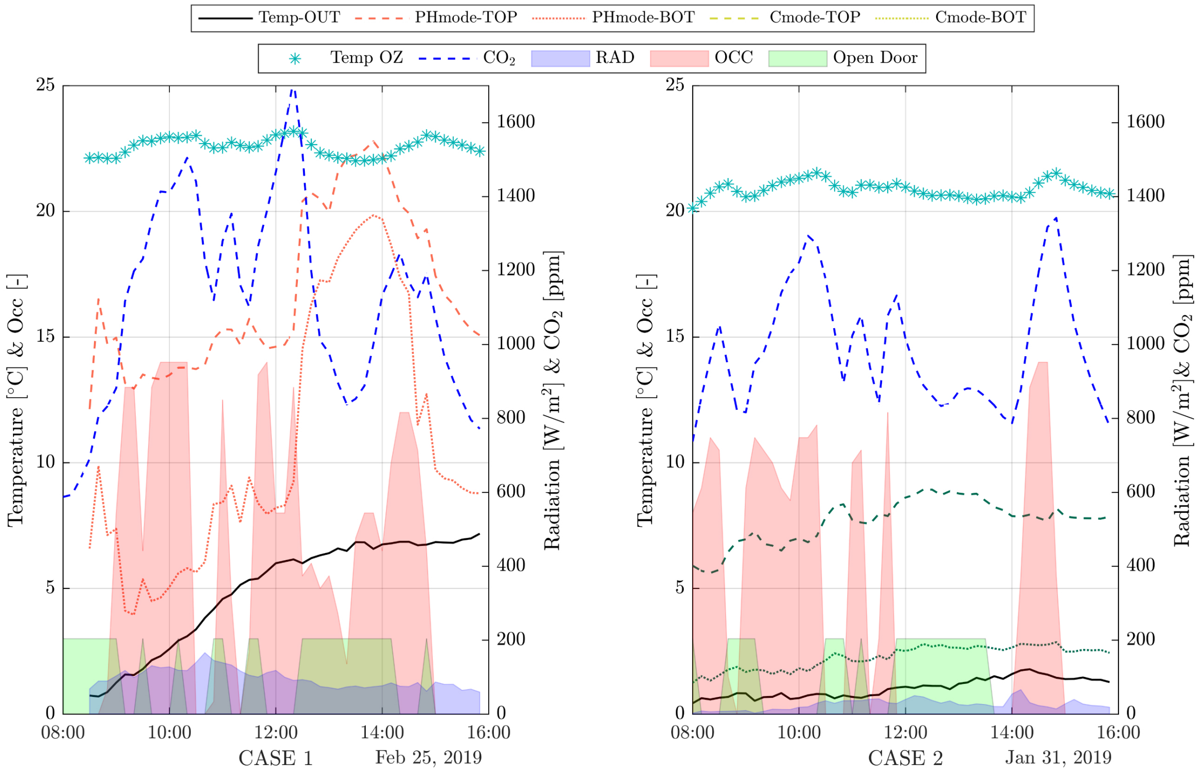

Figure 6.22: Indoor parameters changes together with window performance, Case 1 and Case 2.

Case 1 in Figure 6.22 shows a day when there is no high solar radiation, Pre-heating mode is working because temperature in the cavity (PHmode-TOP) is more than 12 °C. Even though there is a low radiation, at 12:00 h, the bottom temperature (PHmode-BOT) increases. This can be caused by indoor thermal conditions in which the air might be flowing from the room to the window, meaning that the airflow could be reversed. The opening supply to the room is converted to an inlet extracting the air through the cavity to outside. However, it could also be due to the heat contributions of the room to the window. This behaviour can be seen when door is opened from 12:30 to 14:30 h, overlapping the time when this air movement trough the window occurs. However, this event is non representative and happened for only 1.12 % of the total measuring period.

The Case 2 from Figure 6.22 shows that when the air in the cavity is below 12°C the preheating valve does not open and no air is supplied to the room. That is due the low outdoor temperatures. This leads into very high CO_2 concentrations, being more than 1000 ppm during all occupied hours. It is clear that when the door is open the air goes out through the door as visible, from 12:00-13:30 h when the CO_2 concentration has been reduced. However, from 9:30-10:30 h and 13:30-15:00 h when the door is kept closed and there is a typical occupancy around 13-15 people the concentration rises almost until 1400 ppm. It can be concluded that if outdoor temperature is low and no supply air from the windows, together when the door is closed, CO_2 exceeds 1000 ppm.

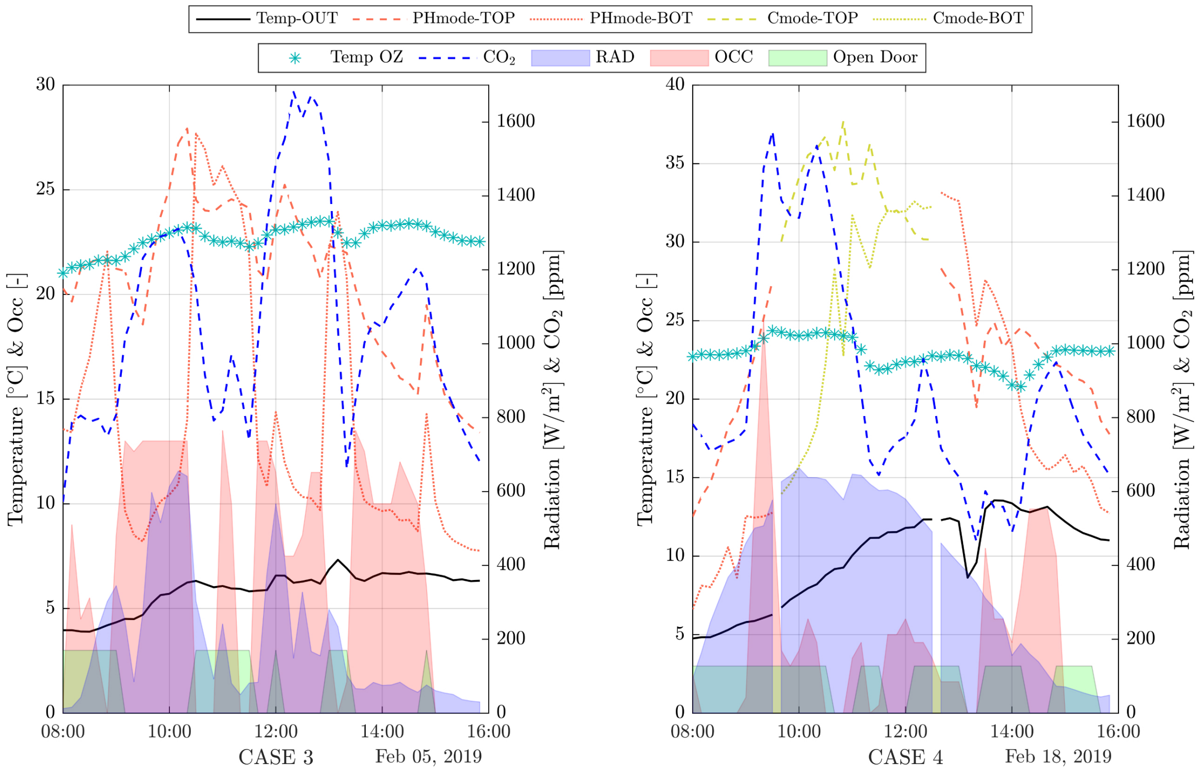

Figure 6.23: Indoor parameters changes together with window performance, Case 3 and Case 4.

Figure 6.23 highlights in Case 3 that when pre-heating mode is in use the air moves in two different directions. From the figure describing indoor environment and window behaviour:

- Door Closed (9:00-10:15 h): at the bottom cavity, the air temperature is closer to the outdoor temperature. The solar radiation warms the air and it seems to move in the classic direction.
- Door Open (10:15-12:00 h): at the bottom cavity, the air temperature is higher than the top temperature. This might be due to the air moving from inside of the room to the outside. In addition, solar radiation values are 150 W/m^2.

Figure 6.23 in Case 4 Cooling mode is analyzed. No air is supplied to the room during this time so high CO_2 concentrations are experienced. Bottom temperature exceeds top temperature. This can mean again a reversed flow direction between 12:00-14:00 h or a malfunctioning of the cooling mode if the valve is not fully opened. This is happening for shorts periods of time, no more than one hour and they represent a 15.56 % of all the C-mode.

6.4.2 Heat Recovery

Under solar radiation effect, thermal gains in the room are achieved by heat recovery through the air from the gap. Deeper analysis of the window heat recovery shall be calculated only using data during preheating mode. HR is only calculated for preheating mode due to the fact that it the only one that actually recovers energy. The performance of the window is evaluated based on the explanation from section 5.2.2. The calculations are divided into Active and Passive, when there is solar radiation and non-solar radiation respectively. No solar radiation is filtered by values below 10 W/m^2.

Passive Heat Recovery

As previously explained, solar radiation is not the only parameter influencing Heat Recovery Rate. Internal heat gains or thermal mass of the building can contribute in heating the cavity also have an impact if the temperature of the room is higher than the supply from the window. Passive Heat Recovery results are presenter in Figure 6.24:

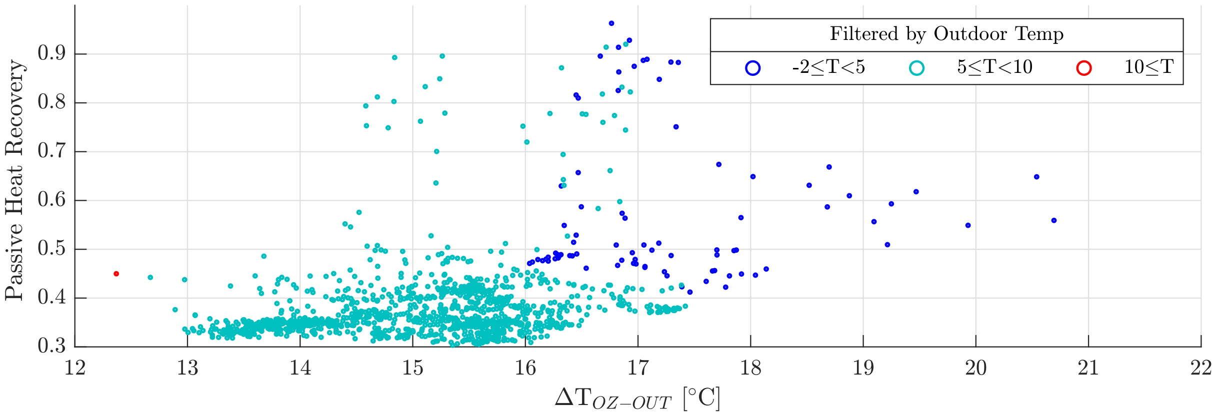

Figure 6.24: Passive Heat Recovery Room 2 - 10 min averaged values.

From the results in Figure 6.24 it can be seen that the higher the temperature difference between indoor and outdoor is, the higher the heat recovery is. This means that the cavity of the window is also heated when the temperature in the room is warm. In addition, it can also be seen that although there is no radiation, there is always some heat recovered. Under no solar radiation, this window still performs better than a conventional window, resulting in low heat recovery. However, as this experiment has been executed without knowing the flow rates through the cavity, the results are spread and do not show a clear linearity.

Active Heat Recovery

Figure 6.25 shows the results from calculation divided by outdoor temperatures in order to find the relation.

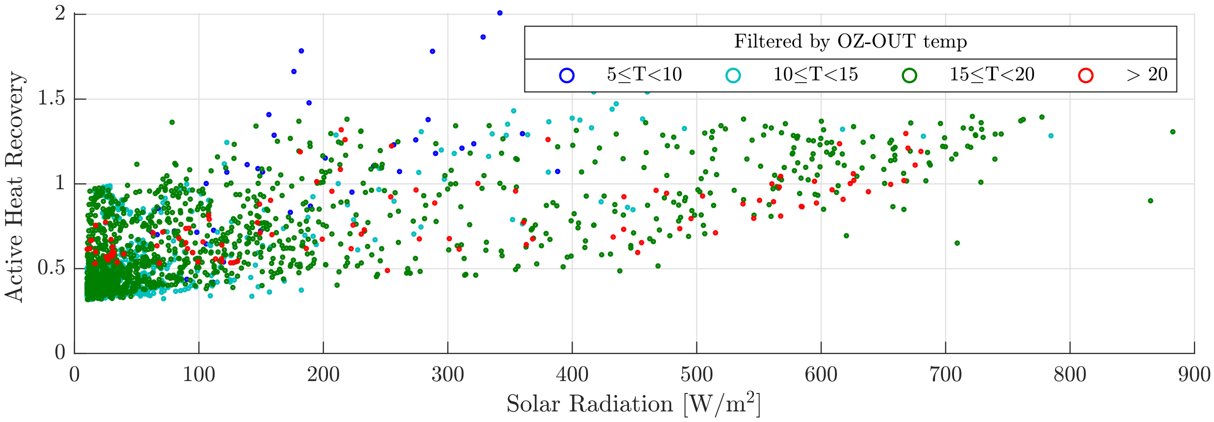

Figure 6.25: Active Heat Recovery Room 2 - 10 min averaged values.

The ventilation heat recovery rate is a function of solar radiation as it heats the air of the cavity and outdoor temperature. Therefore, it has been divided into four outdoor temperatures ranges, as shows previous figure. The ventilation heat recovery performance is proportional to the solar radiation under same flow rate. However, the flow rates through the windows are unknown and therefore, the values obtained are spread giving a wide range of heat recovery values for each solar radiation.

Heat Recovery lower than 1 means that the temperature supplied to the room (T_{TOP}) is lower than the air temperature of the indoor environment, however, it still provides with air higher temperature than the outdoor. Values greater than 1 indicates the good HR performance. That means the air supplied to the room by windows is warmer than the room air.

6.5 Visual Comfort

This section is divided into DF measurements and DF results based on simulations using DIALux. First, data has been acquired in order to make an analysis of the real situation in the school during an overcast day. Then, a model of a classroom has been created where the simulations are compared to the real measurements with the intention of validating the model.

6.5.1 Daylight Factor Calculations

These measurements during 23rd of January have been taken within an overcast sky conditions. The intention is to evaluate if the daylight factor fulfills the requirements of a minimum 2% DF in the working area.

Table 6.7 describes blinds conditions during the process of the experiment and the measured points in each classroom using luxmeters at a height of 0.8 m. Additionally outdoor measurements have been also recorded in order to calculate the Equation 5.8 for DF.

Table 6.7: Blinds conditions when visual comfort has been analyzed in the school, showing the measured points in each classroom.

Room 1	Venetian blinds down tilted horizontally except for the bottom window in from of point 1, whose slats are vertical (totally closed).	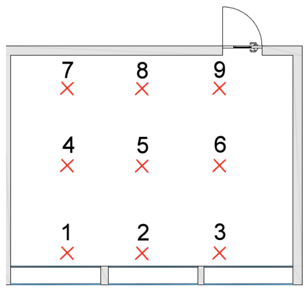
Room 2	Venetian blinds down tilted horizontally and curtains open.	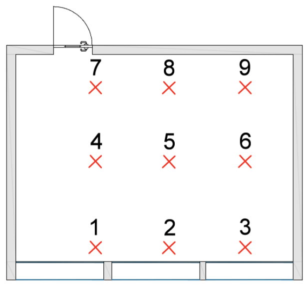

Calculations at the measured points are plotted in Figure 6.26 and Figure 6.27 following the same location shown in Table 6.7 for Room 1 and Room 2, respectively.

0.6522	0.6957	0.6739
1.217	1.087	1.13
0.8261	1.87	1.174

Windows

Figure 6.26: DF distribution from measured data in Room 1

0.3077	0.4231	0.4615
0.6538	0.8077	0.8077
1.423	1.115	0.8077

Windows

Figure 6.27: DF distribution from measured data in Room 2

It can be clearly observed that higher values for DF are next to the window, which is represented by the lowest row. Big differences can be seen in the opposite wall of the windows. Only position 1 in Room1 contradicts with the evidence giving low value. It is because that blind was fully closed, as explained in Table 6.7. In addition, the regulations are not fulfilled as DF barely reaches 2%.

6.5.2 Daylight Factor Simulations

Therewith, rooms, blinds and window characteristics have been modelled using DIALux. They have been designed including original location, room volume, window, blinds and surfaces materials. These characteristics are summarized in Appendix C.1.

Figure 6.28 shows the 3D views from inside of the model in DIALux while Figure 6.29 show the results from the simulations. Figure 6.30 illustrates the model and its distribution of points on the working area. This working area is defined as in the school, at 0.8 above the floor level. Figure 6.31 present the results comparison between DIALux simulation and calculation from the measurements.

Figure 6.28: 3D view from inside of blinds down from DIALux mode.

0.396	0.415	0.406
0.838	0.889	0.854
1.786	2.392	0.926

Windows

Figure 6.29: DF results from DiaLux.

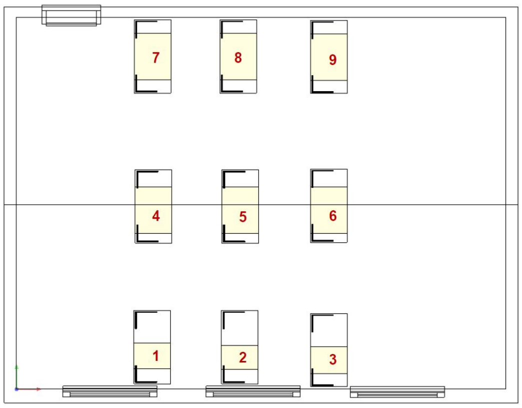

Figure 6.30: Calculation areas for Room 2 in DIALux.

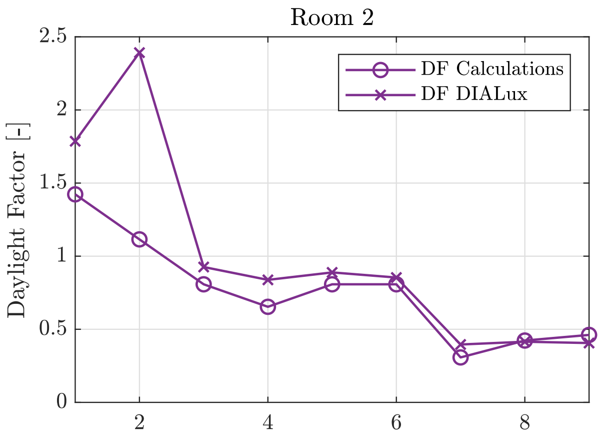

Figure 6.31: Comparison of DIALux and experimental results.

It can be concluded from the results that the model is a fine approximation, following a similar curve in all its distribution. There is an exception close to the window, from point 1 and point 2 where daylight factor distribution is less uniform and giving more deviation in the results. However, as the main concern is to transport daylight to the back side of the classrooms, the model is validated and assumed that the results can be trusted and represent real conditions.

Hereafter, the model is used to calculate DF when the blinds are up, Figure 6.32. The reason is to know the maximum DF capacity and test the influence of the blinds.

Figure 6.32: Inside 3D view blinds up from DIALux model based on classroom in school.

0.684	0.722	0.706
1.491	1.583	1.519
5.77	7.277	3.483

Windows

Figure 6.33: DF distribution from DIALux simulation with blinds up.

The results from Figure 6.33 show that under no sun protection the DF can reach values of 7 % and a maximum value of no more than 0.722 at the back of the room. This means that no matter what type of blinds are used, due to the dimensions of the windows and the room it will be impossible to reach 2 % DF as the regulations state. Therefore, the choice of the shading device is of high importance, as it highly influences on the DF distribution.

7

Experimental Analysis Laboratory - WT2

This chapter explains the experimental analysis conducted for window type 2 in Aalborg University Laboratory, which are performed under controlled conditions. The shading device for the new window in the school has been chosen by a visual comfort test. A deeper analysis of the new window (WT2) has been performed with regards to window performance.

The second version of the ventilated window produced by *VentilationsVinduet* has been tested in the period from May-April. This analysis is divided into two parts. First, measurements for illuminance give visual comfort results. A comparison between five different shading devices is performed to choose the one to be installed in the school. The second part with regards to window performance aims to verify the heat recovery rate for different flow rates and different cavity conditions such as the impact of the cavity height and the effect of the blinds in the cavity.

7.1 Laboratory Conditions

This room has been used exclusively to make the window's analysis. The laboratory dimensions and room location are presented in the Figure 7.1 and Figure A.2.

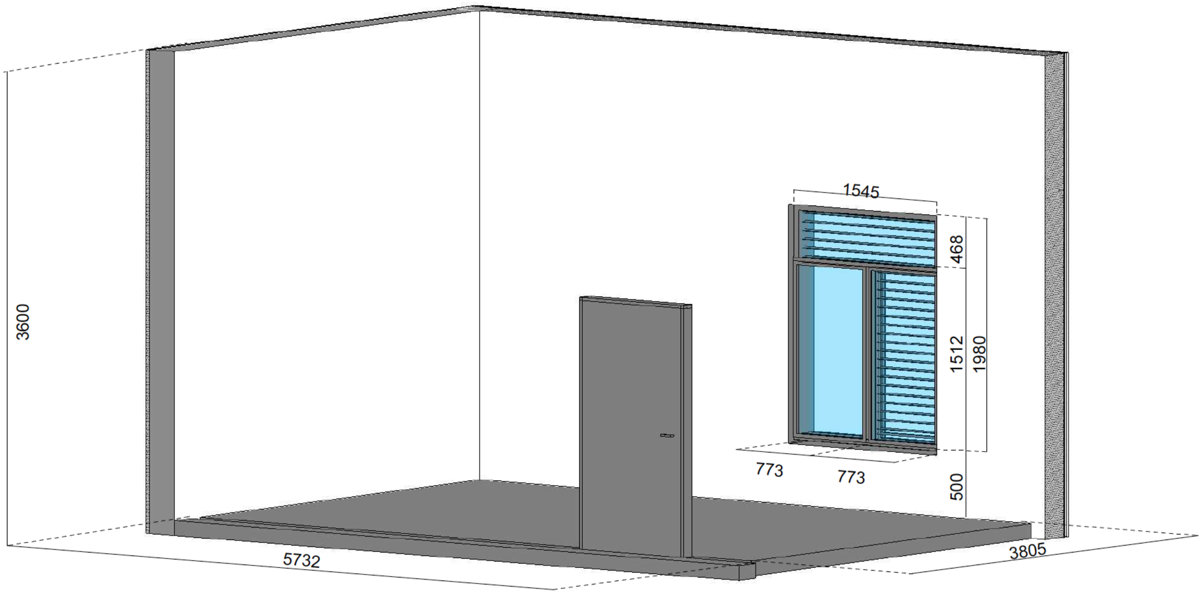

Figure 7.1: 3D laboratory room and window dimensions in AAU [mm].

7.2 Visual Comfort

The aim of this experiment is to find the best solution of the shading device for the new classrooms. During the experiment, five different shadings have been tested in the laboratory. The main concern of this analysis is choose the blinds that provide with a good daylight factor without compromising the view to the outside and at the same time avoiding glare.

7.2.1 Measurement Conditions

The experimental conditions and the measured points are described in the Table 7.1. It can be seen that closer to the window more points have been taken.

Table 7.1: Measuring points in the laboratory and the test conditions.

Experiment conditions	**Measured points**
1. The rest of the windows in the room have been covered, creating a dark room. 2. Four different shading solutions and a venetian blind have been tested on both bottom cavities 1 and 2. 3. Venetian blinds have been tested permanently in cavity 3 for being the best solution to transport light as further as possible in the room. 4. Slats in the venetian blinds have been titled horizontally. 5. Per each experiment, 21 lux points have been measured all over the room surface at 0.8 m from the floor. 6. One outdoor point at 0.8 m has been measured to calculate DF. 7. The experiment has been conducted during an overcast sky.	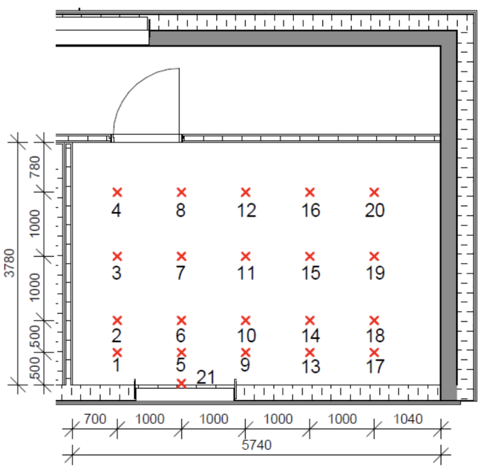

Additionally, the properties of the tested shading solutions are listed in the Table 7.2.

Table 7.2: Properties of the shading solutions.

Sample Nr.	**Sample type**	**Light Transmission [%]**	**Reflection Factor [%]**
1	Venetian blind	-	28
2	Roller screens	11	13
3	Roller screens	29	12
4	Roller screens	15	11
5	Roller screens	5	15

7.2.2 Results

Results verification between the simulation in DIALux and the actual experiment can be seen in Appendix C.5. The experimental test generally follows similar trend as the simulated in DIALux results for all the tested samples. That means that verification of the results is reliable and can be further applied in the school.

Figure 7.2 presents the results for all the tested solutions in front of the window. It represents the transport of DF in the room. The same comparison is shown in Figure 7.3, but highlighting that x-axis have different scale between points in front of the window (point 21, 5, 9, 6, 10 and 11) and the rest of the points, in order to be able to see better the results from all samples and compare them.

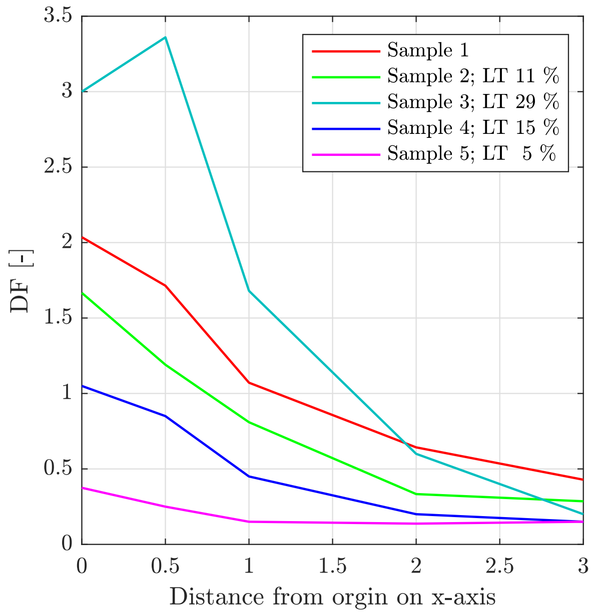

Figure 7.2: Distance from the x-axis origin in front of the window.

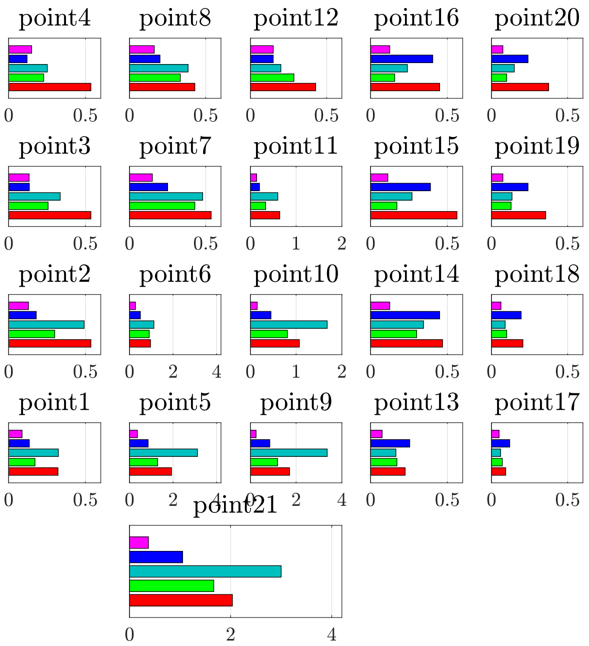

Figure 7.3: DF results for 5 tested samples in the laboratory.

From Figure 7.2 it can be concluded that Sample 5 and 4 do not perform well and they are not recommended for the given case. The DF in both cases is the lowest among all the points in the room. Sample 3 has the highest values, both in its properties and in the measurement. The view to the outside is well-preserved, however risk of glare can occur based on the perception. Therefore, this solution is rejected. The solutions suggested for the classroom conditions are Sample 1 and Sample 2:

- Sample 1 which consists of venetian blinds, represents the most dynamic solution. With regards to the results, it provides with the highest DF on the opposite wall of the windows. Although the measurements are done with the slats in horizontal position, it is the solution that best adapts to the school needs. For example, in a very sunny day with glare or in a situation in which there is a need to have a darker room conditions, the slats can be rotated blocking most of the light to the room. However, in an overcast day, the slats can be in an horizontal position or totally up.

- Sample 2 that consists of roller screens is also a proposal for the school. Because of the lower LT factor, the view to the outside is not fully maintained, but glare problems are avoided. It is a solution that even though does not give the best DF distribution, they do not require much user interaction.

Eventually, supported by the company decision, the venetian blinds are installed in the school as the renovation allows the incorporation of blinds electronically controlled. With regards to this solution, the user interaction plays an important role. The slats can be rotated by almost 180° and moved fully up. It is then crucial that the operation of the blinds is user-friendly and that can take part in the daily needs of the classrooms. The user has the freedom of choosing for instance a full daylight blockage while watching a movie in the classroom or just having the slats positioned horizontally. Like this, light is not totally blocked achieving values of DF as the ones presented above.

7.3 Window Performance

This second part is divided into two analysis. The first objective of the experiment is to analyze the window performance in terms of flow rate capacity and pressure differences. Then a second part with regards heat recovery for different flow rates is explained. Therefore, the experimental analysis is based on answering the following questions:

- What is the influence of the blinds and cavity height on pressure drop?
- Do the blinds interfere on the flow capacity of the window?
- What is the influence of different flow rates on the HR and total heat recovered?
- What is the influence of the blinds on the HR and total heat recovered?
- What is the influence of the cavity height on the HR and total heat recovered?

The test in the laboratory is under controlled conditions. Temperatures and pressures at the window, solar radiation on the façade and outdoor and indoor temperatures have been recorded. Therefore, flow rate capacity under different pressure drops, heat recovery of the window, heat delivered in function of solar radiance and temperature gradients in the cavity are investigated. Then, this section is divided into two experiments: Air Flow and Pressure drop correlation in subsection 7.3.5 and Heat Recovery in subsection 7.3.6. The measurement plan for the experimental analysis of the new window can be found in the Appendix A.2.

7.3.1 Methodology

The equipment used in the following analysis is listed in Table 7.3. Each device has been in use with a sampling time of 10 seconds, 1 min and 5 min. From all data-set, averages from 5 min mean values have been used in the calculations and following analysis. real time-step for the logged data, averaged data. Pressure drop has been taken manually using a Micromanometer when steady state conditions have been reached.

Table 7.3: Logging and averaging of data from all devices used.

Device	Parameter	10 sec	1 min	5 min
Flow meters Lindab x3	Flow rate			
Thermocouples type K x9	Temperature			
Pyranometer x1	Solar Radiation			
IC-meter x3	Temp, RH, CO_2			
Weather Station x1	Temp Outdoors			

7.3.2 Assumptions

During the whole analysis the following listed concepts have been assumed in order to simplify the analysis or due to difficulties to be measured, in order to reach a robust conclusion:

- No consideration of heat losses, no thermal transmittance through the window is analyzed.
- Temperatures at the same height are assumed the same for each cavity.

7.3.3 Measurement Conditions

Valves are positioned in the bypass or preheating mode depending on the experiment. As the window is located in a south façade, no shadows from trees or surrounding buildings are reported. Measurements conditions are described as follows:

Air Flow and Pressure Drop Correlation	**Heat Recovery**

Air Flow and Pressure Drop Correlation

1. Test in preheating and bypass modes.
2. Cavity 1 is tested without blinds to see the influence of the blinds.
3. Cavity 2 is tested with blinds down in the horizontal position.
4. Cavity 3 is tested with the blinds down and horizontal slats, as in the school.
5. Window modes are automatically positioned to the desired working mode during the tests.

Heat Recovery

1. Tested only in preheating mode.
2. Cavity 1 without blinds to see the influence of the blinds.
3. Cavity 2 is tested with blinds down in the horizontal position.
4. Cavity 3 is tested with the blinds down and horizontal slats, as in the school.

7.3.4 Setup

On the Figure 7.4 pressure points in green dots at the window are visible, while on Figure 7.5 red indications are referred to temperatures. Furthermore, in Table 7.4 a more detail explanation of the points can be seen.

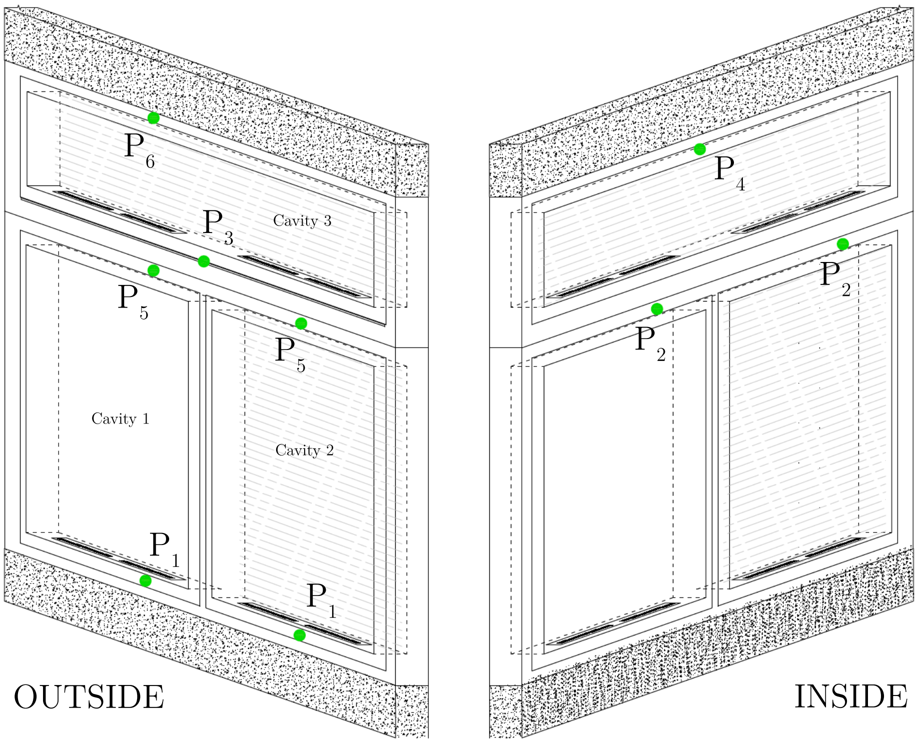

Figure 7.4: Pressure points WT2.

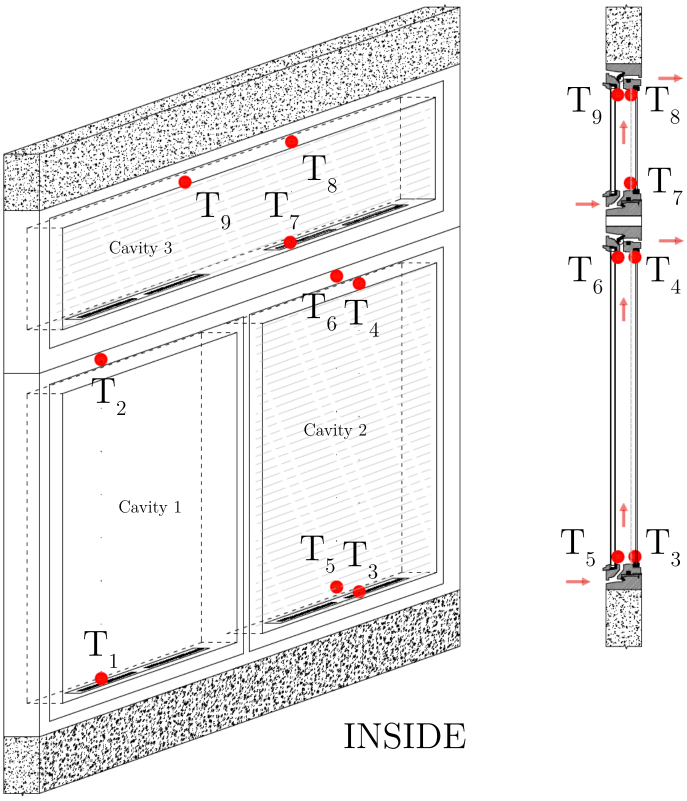

Figure 7.5: Temperature points WT2.

Table 7.4: Pressure and Temperature differences calculated from the points measured.

	Pressure Drop		**Temperatures**
	Preheating Mode	Bypass Mode	Preheating Mode
Cavity 1	ΔP_{1-2_b} $\Delta P_{1-2_{nb}}$	ΔP_{5-2}	T_1 T_2 *no blinds*
Cavity 2	ΔP_{1-2_b} $\Delta P_{1-2_{nb}}$	ΔP_{5-2}	T_3 T_4 T_5 T_6 *blinds*
Cavity 3	ΔP_{3-4_b} $\Delta P_{3-4_{nb}}$	ΔP_{6-4}	T_7 T_8 T_9 *blinds*

For pressure drop test in the preheating mode, at the points ΔP_{1-2_b}, $\Delta P_{1-2_{nb}}$, ΔP_{3-4_b} and $\Delta P_{3-4_{nb}}$ with blinds and without blinds the test is performed. The existence of the blinds does not affect the bypass mode, therefore, measurements are taken only at the points ΔP_{5-2} and ΔP_{6-4}. For temperature measurements, cavity 1 has no blinds whereas cavity 2 and cavity 3 have the blinds down and horizontally tilted.

Figure 7.6 and Figure 7.7 present the setup for the experiments before the blinds have been installed. It can be seen that the exhaust of each cavity is supplied to the room by a duct where a flow meter and a fan are installed. By manual voltage regulation, the fan power can be changed providing different and controllable flow rates. The flow meters are connected to a computer where a LabVIEW script stores the flow rates and temperatures from each duct. In order to avoid any of the air leakage, the outlet is securely constructed, by covering the total window cavity width.

Figure 7.6: Front view to the laboratory setup for the experimental analysis.

Figure 7.7: Side view to the laboratory setup for the experimental analysis.

7.3.5 Air Flow and Pressure Drop Correlation

The air supplied by the ventilated window is driven by the combination of natural forces and a mechanical exhaust. The aim of the test is to find how much air can be supplied through each cavity and to know the pressure drop. Therefore, the procedure consists on adjusting manually the fan to each air flow stated in Table 7.5 for each cavity. Pictures from the test can be found in the Appendix A.4. The flow rates chosen to be tested are based on the Numerical Analysis from subsection 5.1.2.

Table 7.5: Air Flow Rate values in l/s per cavity tested in the Laboratory for WT2.

Air Flow Rate [l/s per cavity]				
10	14	18	22	27

Results

Overall, the correlation between the air flow capacity and the pressure drop is presented in Figure 7.9. Each of the cavities have been tested individually, however assuring the similar external conditions. The fitting curve is a second order polynomial applied to the results. With increasing the air flow rate, the pressure drop increases proportionally. The points in the Figure 7.8 represents the measurement situation.

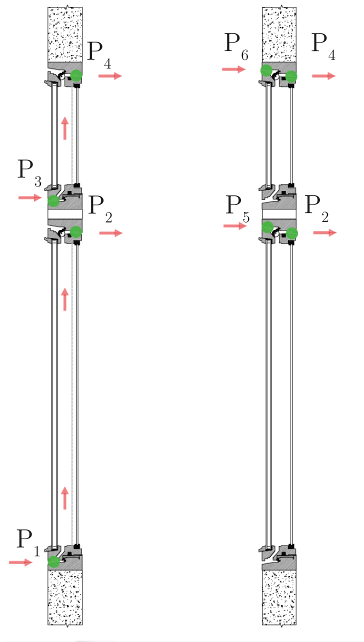

Figure 7.8: Window section pressure test.

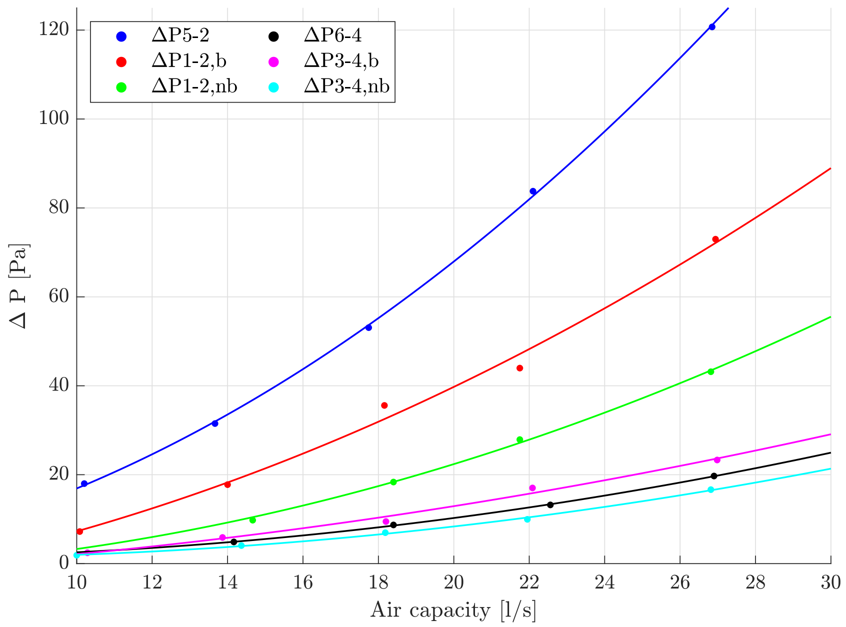

Figure 7.9: Relation between pressure drop and air flow.

By comparing ΔP_{1-2} to ΔP_{3-4}, both preheating mode, it is observed that the height of the window impacts on the investigated relation. The larger the height is, the bigger pressure difference in the window is observed ($\Delta P_{1-2} > \Delta P_{3-4}$). The bottom cavity is almost three times as high as the top. That is however, a confirmation of an expected result.

By comparing ΔP_b to ΔP_{nb}, the existence of blinds in the preheating mode also increases the pressure drop. That is also an expected behaviour, adding i.e filters in the ventilation system increase the pressure drop, while the pressure drop should be kept as low as possible to avoid unnecessary energy consumption.

With regards to the bypass mode, it is expected that both cavities would give similar results since neither the height nor the blinds have any influence. However, ΔP_{5-2} gives a higher pressure drop than ΔP_{6-4}. This might be due to installation of the valves not being in the optimal position at the window. Therefore, the air for the bottom window had a smaller inlet from the outside as the frame of the window is interfering. That is caused by the lack of precision in the design phase of the window. In addition, the quality of the valves might differ from window to window and have some air leakages. In general, the window has a considerable pressure drop that could be improved by a better design of the window.

7.3.6 Heat Recovery Analysis

The performance of the window is tested by calculating the heat recovery under different air flow capacities listed in the Table 7.6. Each test is performed for the same outdoor conditions. The chosen flow rates are calculated from the maximum and minimum requirements at the classrooms, based on the numerical analysis in subsection 5.1.2. As cavity 3 has smaller area, the air flow is adjusted to the same l/s per m^2 as the larger cavities.

Air Flow Rate ranges per cavity						
	Test 1		**Test 2**		**Test 3**	
	[l/s per m^2]	[l/s]	[l/s per m^2]	[l/s]	[l/s per m^2]	[l/s]
Cavity 1	8.56	10	14.52	17	23.1	27
Cavity 2	8.56	10	14.52	17	23.1	27
Cavity 3	8.56	6.19	14.52	10.5	23.1	16.7

Table 7.6: Flow rate step size for heat recovery test.

The experimental analysis of the heat recovery is divided into passive and active analysis, which are described in the following subsections.

Passive Heat Recovery Results

Passive Heat Recovery (PHR) is defined as the heat recovered when there is no solar radiation. It shows the impact of the heat losses from the building as long as the supply air (T_{TOP}) is lower than the room temperature (T_{IN}). To assure no solar radiation, measurements have been filtered by no more than 10 W/m^2. The intention is to obtain the regression between the difference in-outside temperature and top-outside air temperature.

The Figure 7.10 shows the regression from the results for the three cavities for all the flow rates stated in the Table 7.6. In the Appendix C.6, the scatter plots from where the fitting curve has been taken can be seen.

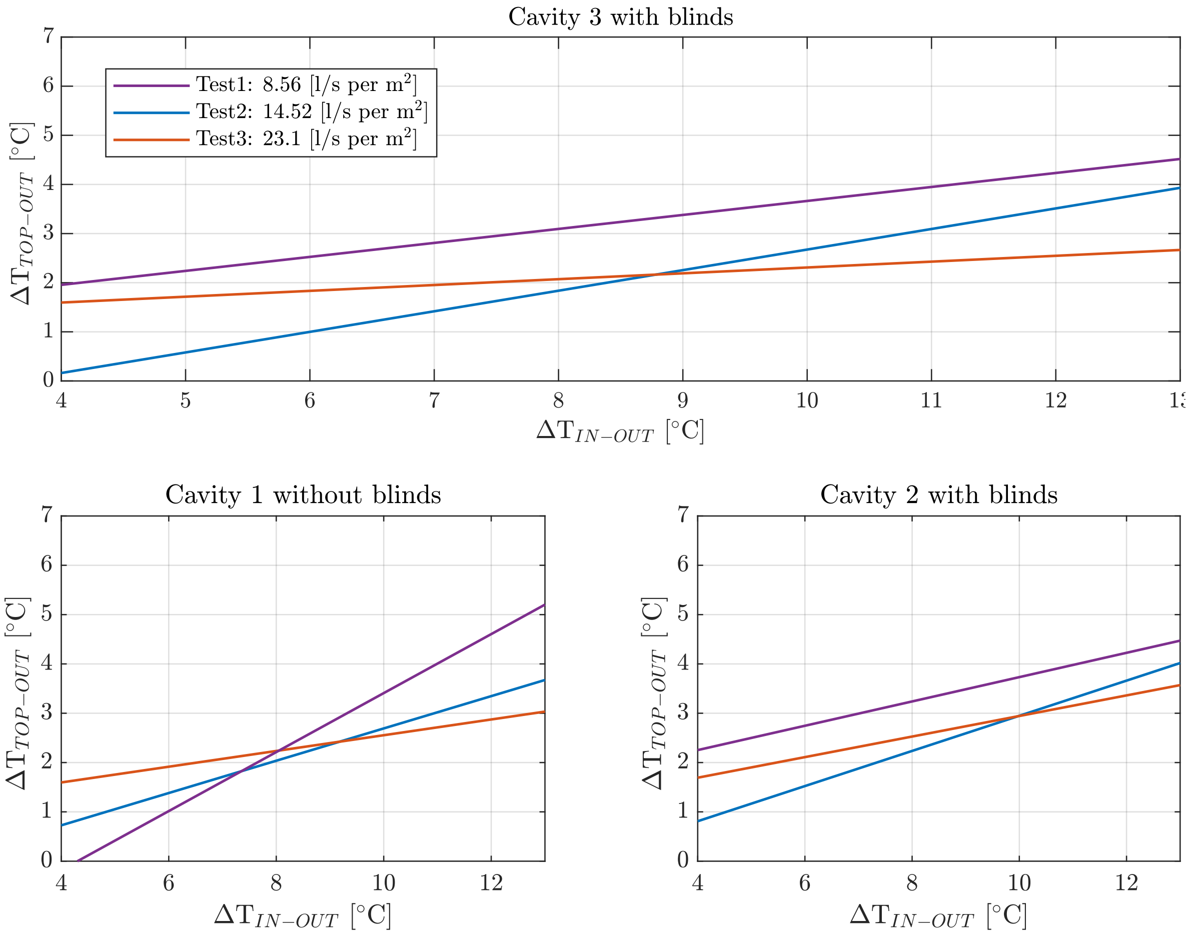

Figure 7.10: $\Delta T_{TOP-OUT}$ - ΔT_{IN-OUT} correlation

The results show a linear positive correlation meaning that the air is preheated the most when the room temperature increases. By comparing flow rates from all cavities, cavity 1 preheats the air the most. It has the steepest slope after $\Delta T_{IN-OUT} > 8$°C for the lowest flow rate. However, when this difference is low, meaning that the room is cold, the air in that cavity is not very heated up, even with the lowest flow rate.

The influence of blinds is noticeable by comparing cavity 1 and cavity 2 results. The blinds do not seem to increase $\Delta T_{TOP-OUT}$ but they seem to isolate the window and prevent the air to be cooled down due to the night sky radiation.

In terms of height difference, it is of interest to compare the cavity 2 and 3 together. It can be noticed that the pattern in the results is similar. In both cases, the highest flow rate does not show notorious increase in the preheated air when ΔT_{IN-OUT} is high, specially in cavity 3.

In addition, before ΔT_{IN-OUT} of 8 °C, in cavity 1, the highest flow rate performs the best. After, this effect is reversed when higher temperature gradient.

With regards to cavity 2 and 3, before ΔT_{IN-OUT} of 10 and 9 °C respectively, the highest flow rate performs better than the middle one, whereas for higher gradient the middle one performs better than the highest one.

Figure 7.11 shows the heat recovery recorded during the measurements.

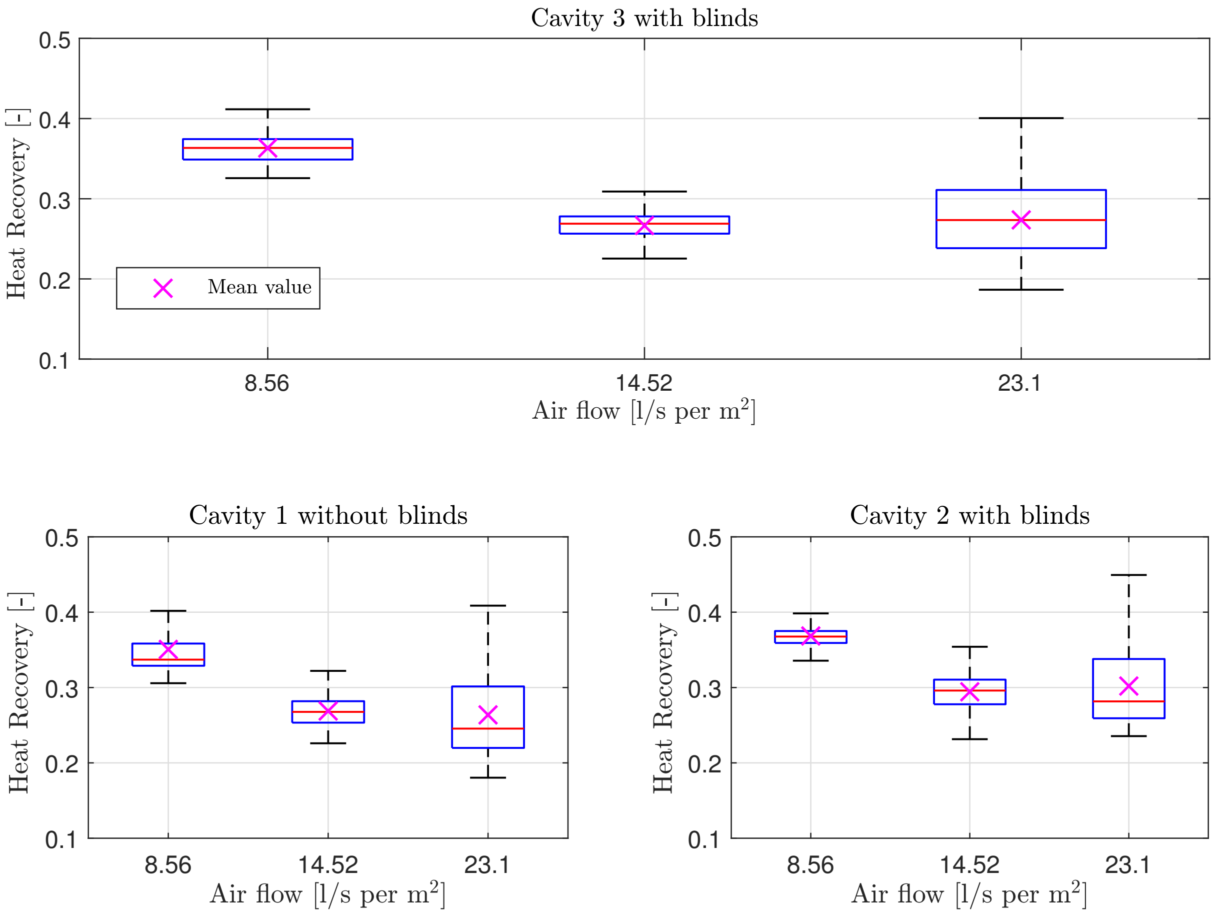

Figure 7.11: Passive Heat Recovery Results

The results show that the lowest air flow supplied through the window provides with the highest heat recovery. For the lowest flow rate the heat recovery is better because it has more time to preheat the air. However, there is not a significant change when increasing the flow from 14.52 to 23.1 l/s per m^2, as seen from the mean values in Table 7.7.

	Test 1	**Test 2**	**Test 3**
μ_{HR} Cavity 1	0.351	0.269	0.264
μ_{HR} Cavity 2	0.369	0.295	0.302
μ_{HR} Cavity 3	0.363	0.267	0.274

Table 7.7: Passive Heat Recovery mean values.

Active Heat Recovery Results

Active Heat Recovery (AHR) is defined as the heat recovered when there is solar radiation. It shows the impact due to both, the heat losses from the building to the window and the effect of solar radiation. To calculate the active heat recovery the same measurements as for the passive heat recovery are used. In this case the data is filtered when the radiation is higher than 10 W/m^2.

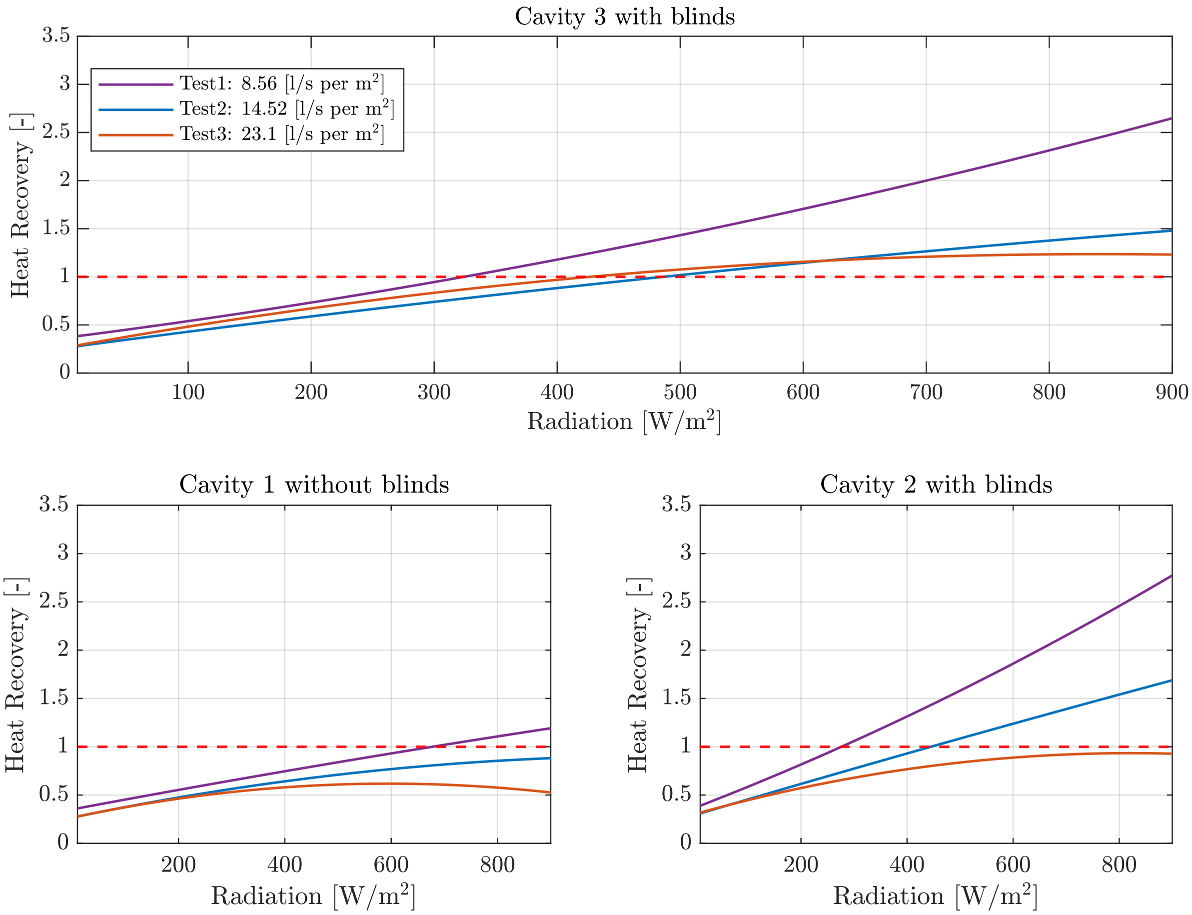

Figure 7.12: Active Heat Recovery Results

The results from the Figure 7.12 show the tendency obtained by the bisquare curve fitting. Raw data can be seen seen in the Appendix subsection C.6.1. The horizontal red line represents the HR equal to one. This means that the air is preheated to the same temperature as the room, therefore risk of draught is avoided due to low temperatures. However, a heat recovery of lower than one still preheats the air to a higher temperature than the ambient.

Cavity 1 and 2 give the evidence that the less flow rate, the higher heat recovery is. The air takes more time inside the cavity and therefore, have more time to be influenced by the solar radiation. Nevertheless, cavity 3 does not show a considerable decrease in the heat recovery when the flow is changed from 14.52 to 23.1 l/s per m^2. This might be due to the effect of the cavity height. However, mention that the heat recovery might have a limit depending on the configuration of the window. From the cavity 3 it can be seen that even though the flow rate has been increased by 59%, the tendency of the lines gets closer and flattened. This concludes that, no matter how much the flow is increased, the heat recovery would remain constant.

In terms of the shading devices, it can be seen that the blinds help in preheating the air more. This is due to the greenhouse effect enhanced in the cavity. When the solar radiation strikes the external glass, it is partially reflected, absorbed and transmitted. The part of the solar radiation which crosses the glazing is then absorbed and reflected by the interior glass and the blinds which warm up. This ones re-emits in all the directions a long wave radiation. Part of the radiation is thus trapped, involving the increase of the interior temperature.

Comparing cavity 1 without blinds and cavity 2 with blinds, cavity 2 reaches a heat recovery of 1 at a much lower radiation and a maximum heat recovery of 3. Nevertheless, cavity 1 without blinds even with the lowest flow rate barely passes a HR of 1 at a very high radiation. In addition, comparing cavity 3 (blinds but smaller glazing area) and cavity 1 (no blinds but larger glazing area), cavity 3 (3 times smaller) reports better preheating capacity due to the effect of the blinds.

Figure 7.13 represents T_{TOP} of the three cavities for a day with high solar radiation at a constant flow of 14.52 l/s per m^2.

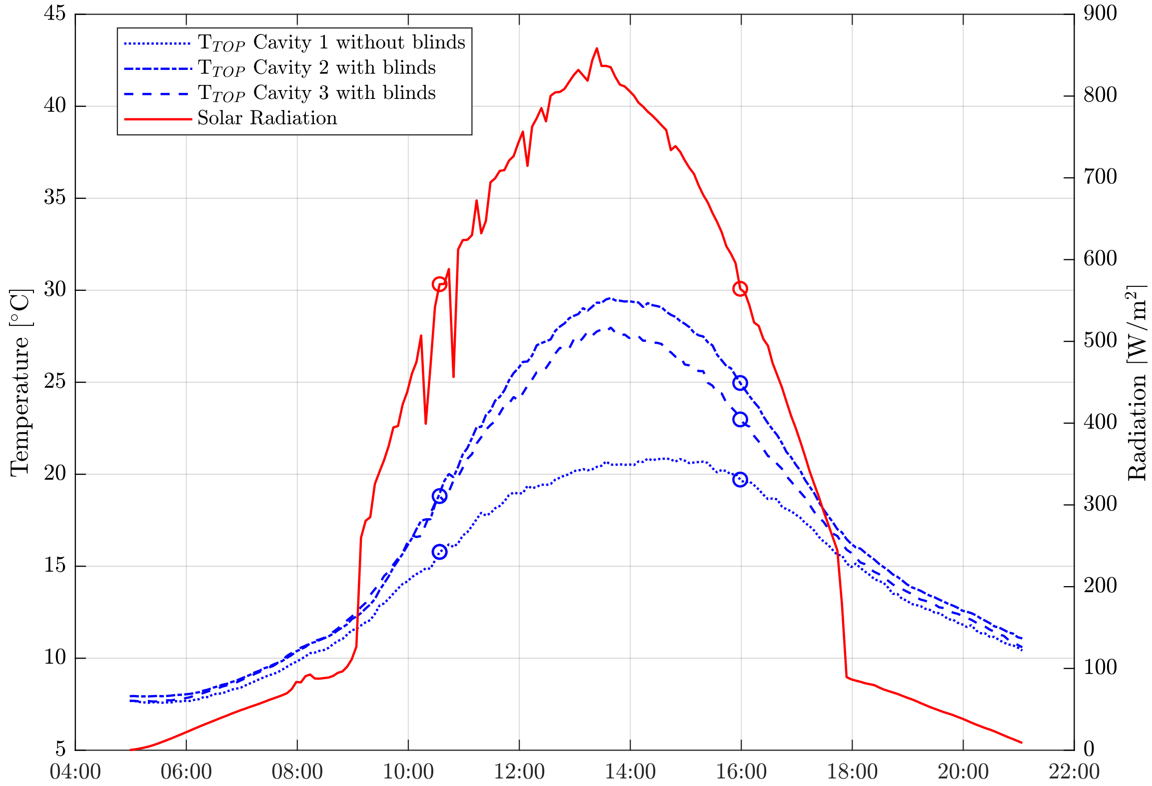

Figure 7.13: Preheated temperature at the cavities for 14.52 l/s per m^2

Following what it was stated in Figure 6.20 about the dynamic behaviour of the supply temperature, it can be concluded that the thermal mass of the building has an impact on air cavity. During the rise period of the sun (4:00 h-13:00 h), not only the air is heated up but also the building starts to store heat. For this reason, when the sun starts to go down, it can be seen that for the same amount of radiation, higher temperatures of air at the cavities are observed. By analyzing the circled values, for a radiation of around 560 W/m^2, different temperatures depending on the time of the day are given. More in detail is shown in the Table 7.8.

	Temperature [°C]		
	Cavity 1	**Cavity 2**	**Cavity 3**
During rise up at 569.9 W/m^2	15.87	18.81	18.81
During sun set at 564.3 W/m^2	19.71	24.96	22.95

Table 7.8: Temperatures for same solar radiation during rise up and rise down period of the sun

7.3.7 Total Heat Recovered

The heat recovery is a coefficient that depends only on temperature difference. However, it is also interesting to study the heat recovered in terms of different flow rates as explained in Section 5.2.2. Figure 7.14 presents the results form the calculations.

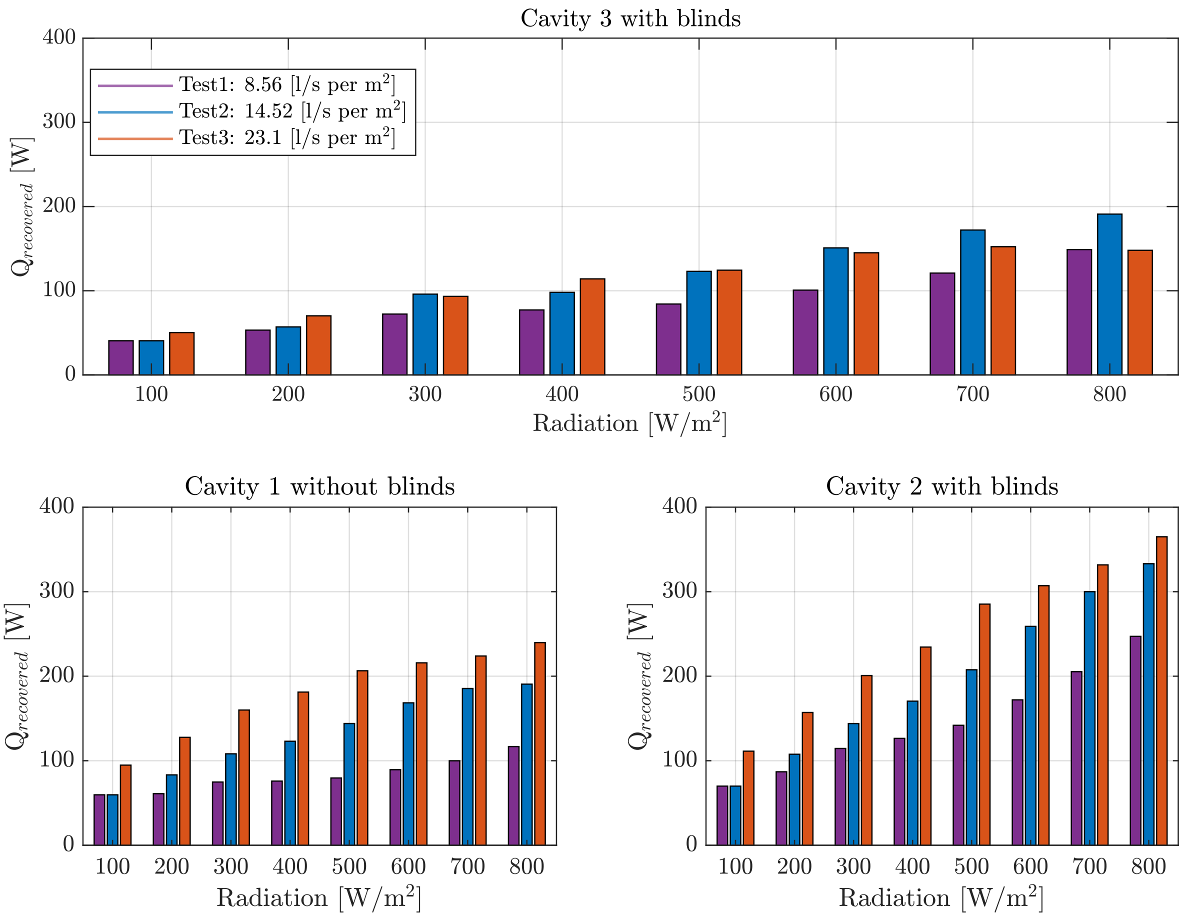

Figure 7.14: Total Heat Recovered

Results show that even though for higher AHR a flow rate of 8.56 l/s per m^2 (as seen in Figure 7.12), the heat recovered is higher when the flow is 23.1 l/s per m^2 (cavity 1 and 2). However, in cavity 3, the heat recovered is similar for low radiation and higher for the middle flow rate of 14.52 l/s per m^2 when radiation is above 500 W/m^2. This is because the HR does not significantly change when the flow rate is increased from 14.52 to 23.1 l/s per m^2.

With regards to the blinds influence, comparing cavity 1 and 2, both show similar values of heat recovered for very low radiation. Nevertheless, for the middle flow rate and high solar radiation the blinds show a clear improvement in the amount of heat recovered.

In addition, regarding to cavity 1 and 3, although the AHR is in general higher for the cavity 3, in terms of the heat recovered, cavity 1 with the highest flow performs better. It can be concluded that this ventilated window performs better than a conventional window which would provide with no heat recovered.

Further Analysis WT2

In this new chapter, further explanation and analysis of new window improvements is proceeded. First, the validated model from the school is used to asses the visual comfort for the WT2. Later on, as this window requires a control strategy unifying windows openings as a whole ventilation system, the new electronic elements, such as sensors, and their response and accuracy are investigated. Eventually, a suggestion for a control strategy in the room is proposed, not without first attempting to decide which input value impacts the most to the system, by calculating a sensitivity analysis.

8.1 Daylight Factor Simulations

The following simulations in DIALux have been conducted in order to get an estimation of the daylight factor distribution in the classroom after renovation of the windows. The new blinds are described in the results from the laboratory experiment (see subsection 7.2.2). Even though the window design has changed, the blinds used in the model are the default venetian blinds from DIALux. The simulation has been conducted with blinds down tilted horizontally in all three cavities. The reason for this is because before the renovation, the blinds were most of the time static in down position tilted horizontally. This was attributed to the difficulties for the users to control them. Especially in Room 1, where they had to be manually changed.

Figure 8.1: Inside 3D view of the classroom after windows renovation (blinds down).

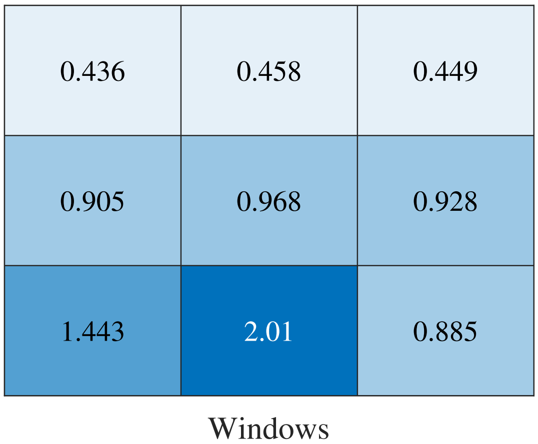

Figure 8.2: DF distribution from DIALux simulation (blinds down).

The results from Figure 8.2 compared to the simulation with WT1 in Room 2 (see Figure 6.29), show that the daylight factor has decreased in the points 1 2 3 and slightly improved in the rest of the room. However, it is important to highlight, as already stated, that the dimensions of the room and location of all the windows on the same wall, do not allow the DF to fulfill the regulations even without any shading (as seen in Figure 6.33).

Figure 8.3: Inside 3D view of the classroom after windows renovation (blinds up).

0.511	0.537	0.528
1.068	1.138	1.094
3.594	4.955	2.061

Windows

Figure 8.4: DF distribution from DIALux simulation (blinds up).

A second simulation is created expecting that users interact with the blinds control. During the simulations cavity 1 and cavity 2 have the blinds half up, as it can be seen in Figure 8.3. This renovation has permitted to incorporate a mechanical control of the blinds in both rooms which is still 100% user dependent, but more user friendly. Like this, it is expected that the users could actively change position and orientation of the blinds according to their needs.

The results from the second simulation can be seen in the Figure 8.4. Points 7, 8 and 9 at the back of the rooms show a DF around 0.5%. Nevertheless, the major effect can be seen next to the windows in points 1 2 3 with a DF of nearly 5%.

8.2 Control Design Investigation

Automation has become more common in the nowadays building operation. As explained in Section 4.4.2, WT2 is an electronically controlled window. Figure 8.5 is used to explain the room sensor position and the sensors in the cavity and how they communicate with the processor. Figure 8.6 shows a flow chart of the communication.

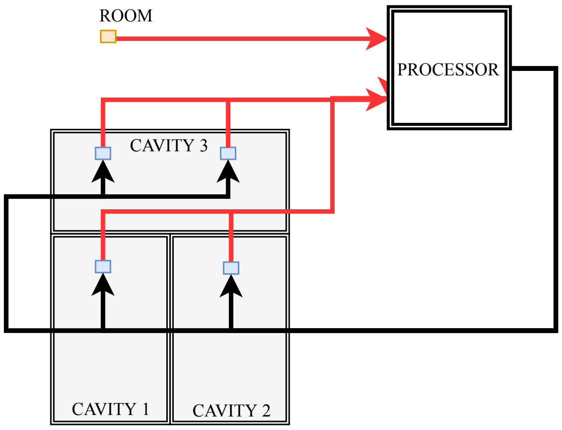

Figure 8.5: Sketch presenting the control communication for windows automation

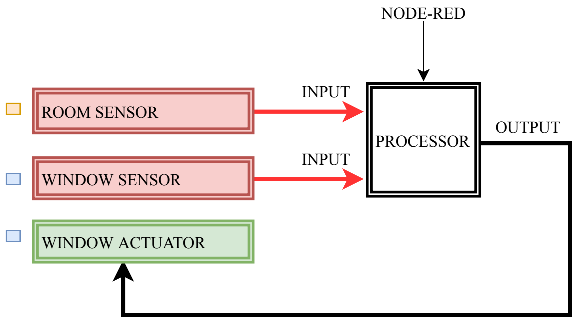

Figure 8.6: Flowchart presenting the control communication for windows automation

The valves are connected with an actuator and a sensor that takes measurements at the top of each window cavity. This data is sent to a processor. This processor decides the position of the valves with regards to the indoor environment measured by another sensor located in the classroom. The control strategy is implemented by Node-Red which is a programming tool for wiring together hardware devices, APIs and online services [JS Foundation , 2019]. The communication between the different electronics is presented in the Figure 8.6.

In Section 8.2.1 an analysis of the sensors used for WT2 is executed in order to know their accuracy and response time when measuring. In addition, a sensitivity analysis from Section 8.3.1 is conducted with the intention of knowing which parameters analyzed during the heating season at the school are the most influential in terms of indoor environment by the correlation between the inputs to the outputs. Consequently, a control design strategy is developed in which the most influential parameters from the SA are prioritized. This final control strategy is presented in Section 8.3.

8.2.1 Sensors Analysis

Before explaining the analysis, an introduction of a sensor behaviour is introduced. There are explained with examples the possible different response from a sensor and the information which results in the answer to know if it is a good or a bad sensor. Afterwards, an explanations of the devices used in the experiment explained after.

Sensors Behaviour

WT2 allows to automatically switch in between the working modes, as previously explained in section 4.4.2. The working modes change depending on the demands set by the indoor environment and conditions at the top of the window cavities. The measurements are done by the use of sensors. A sensor is a device that provides an output signal with respect to a specific physical quantity which is intended to be measured [Johra, 2019]. Therefore, in order to obtain a desired building automation, the properly working sensors and its location is crucial. In order to verify if the sensor performs correctly and can be trusted, the output response of the sensor has to be compared to a reference sensor [Johra, 2019]. Ensuring that the reference sensor give fully trusted output results. By subjecting both of the sensors to various environmental conditions, the measurement variations and response can be observed.

Several assumption about the sensor behaviour can be made based on the results from the experiment. On the Figure 8.7 the possible sensor outcome is presented. It is just an example to understand the basis of sensors behaviour. The red line shows the reference sensor.

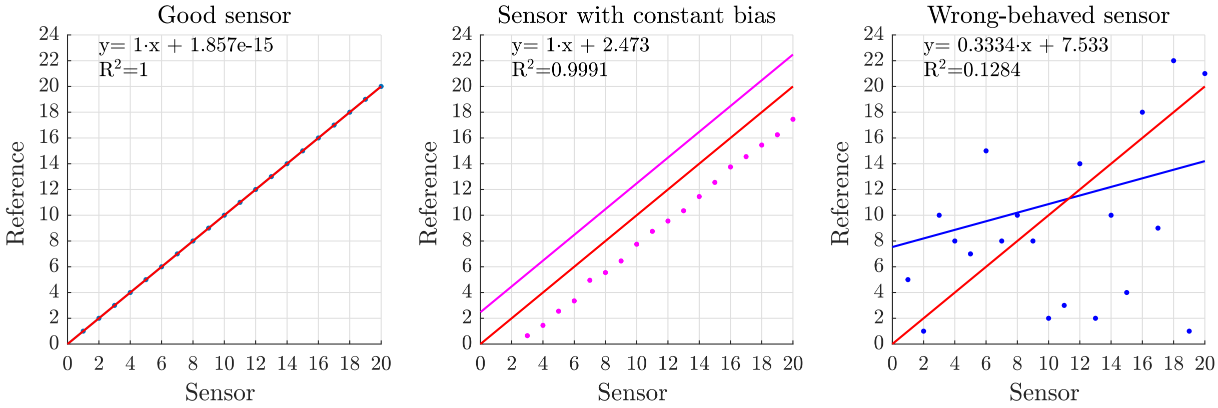

Figure 8.7: Behaviour of the good and bad sensors, red line is the reference value.

Based on the results, three general assumptions can be made. The perfect sensor gives the same outcome as the reference sensor. In that case, the senors can be fully trusted and ready to use. If there is a constant bias between the reference sensor and the tested sensor, the device requires a calibration. By adjusting the bias with the results, the sensor can be used. However, if the sensors shows random and very spread results, not correlating to the reference values, the response of the sensor is wrong. Therefore, the device can not be used and change is required.

Sensors Testing

The sensor chosen for the automation of the WT2 is the Bosch BME680 sensor. It is described as an integrated environmental sensor whose main feature is to measure temperature, barometric pressure, volatile organic compounds (VOC), relative humidity and detect altitude [Bosch, 2019]. The sensor is integrated in a case named as Climawintech sensor, as show Pictures 8.8 and 8.9.

Figure 8.8: Climawintech Sensor.

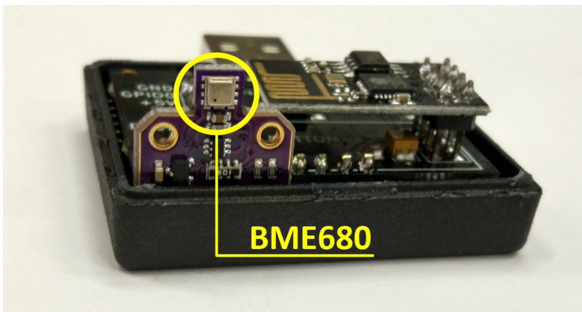

Figure 8.9: Location of Bosch BME680.

The sensors used in WT2 have not been calibrated, nor checked for their accuracy and response behaviour. For that reasons, experimental testing of the sensors is conducted in the following experiment. The principle is to check how precise the sensors are, compared to reference sensors and obtain a calibration formula if possible. Not only the accuracy of the sensors, but also the response to change of the environment has been tested for the following parameters: temperature, CO_2, pressure and relative humidity. Special attention to pollution concentration because the sensor measures VOC for CO_2 concentration purposes.

8.2.2 Methodology

During this test, all sensors and the reference measurements have been exposed to changes in the environment under controlled conditions. Three Climawintech sensors have been used for these experiments. Different reference sensor are used for the parameters. The equipment is listed in the Table 8.1. Depending on the device, the sampling time is 1 microsecond, 1 second, 5 seconds and/or 5 min. From all data-sets, average of 5 min has been used in the calculations and the following analysis.

real time-step for the logged data, averaged data.

Table 8.1: Logging and averaging of data from all devices used during sensor testing.

Device	**Parameter**	1 μs	1 sec	5 sec	5 min
Pt-100 x 4	Temperature				
IC-meter x 4	Temp, RH, CO_2				
Barometer x 1	Pressure				
Bosch Sensors x 3	Temp, RH, CO_2, P				

8.2.3 Setup

During the experimental sensors analysis five different test has been performed. The Test 1 has been performed with the intention of testing temperature, relative humidity and pressure. The environment has been triggered to change with the radiator located in the room. Test 2 has been placed outside . During Test 3, Test 4, Test 5 the variable occupancy load has been applied. To check the influence of the Climawintech box where Bosch sensor is located, the case has been removed during the test 4 and test 5. The test period and conditions are listed in the Table 8.2.

Table 8.2: Different testing conditions.

	Test 1.	**Test 2**	**Test 3**	**Test 4**	**Test 5**
Date	18 April	25 April	25 April	14 May	16 May
Conditions	Radiator ON	Outdoor	Indoor	Indoor	Indoor
Focus	Temp RH P	Temp RH CO_2	Occ - CO_2	Occ - CO_2	Occ - CO_2

An example of the placing the sensor is presented in the Figure 8.10 performed in the laboratory room. The CO_2 analysis is performed in a smaller room varying occupancy during the logging period.

Figure 8.10: Setup for the sensor test. Black boxes - BOSCH sensor, white - IC meters, grey cables - Pt-100.

8.2.4 Sensors Results

Tested parameters are described and analyzed separately with an exception for pressure. Description about conditions of adaptation to different environmental conditions are presented below each section thoroughly.

Temperature

Temperature is one of the most important parameter in the analysis, as the Ventilationsvinduet company focuses mainly on thermal comfort and indoor environment of the classroom. Also the set points for the control strategy are based on this temperature ranges.

For this analysis, the IC-meters have been used as a reference of ambient temperature for a range of temperature from 10° C to 30° C. In addition, inside the box of each sensor three Pt-100 have been placed to identify if the air is preheated inside, as it may result in an influence on the final sensors temperature. Also, to work properly, the sensor for measuring the gases requires heating up [Bosch, 2019,p.17], which might influence on the final temperature result.

Figure 8.11 present the overall temperature reaction to different environmental conditions and the relation between the temperature reference (IC-meters and PT-100 during test 1 are averaged) and the sensor. During the test 1, radiator is used.

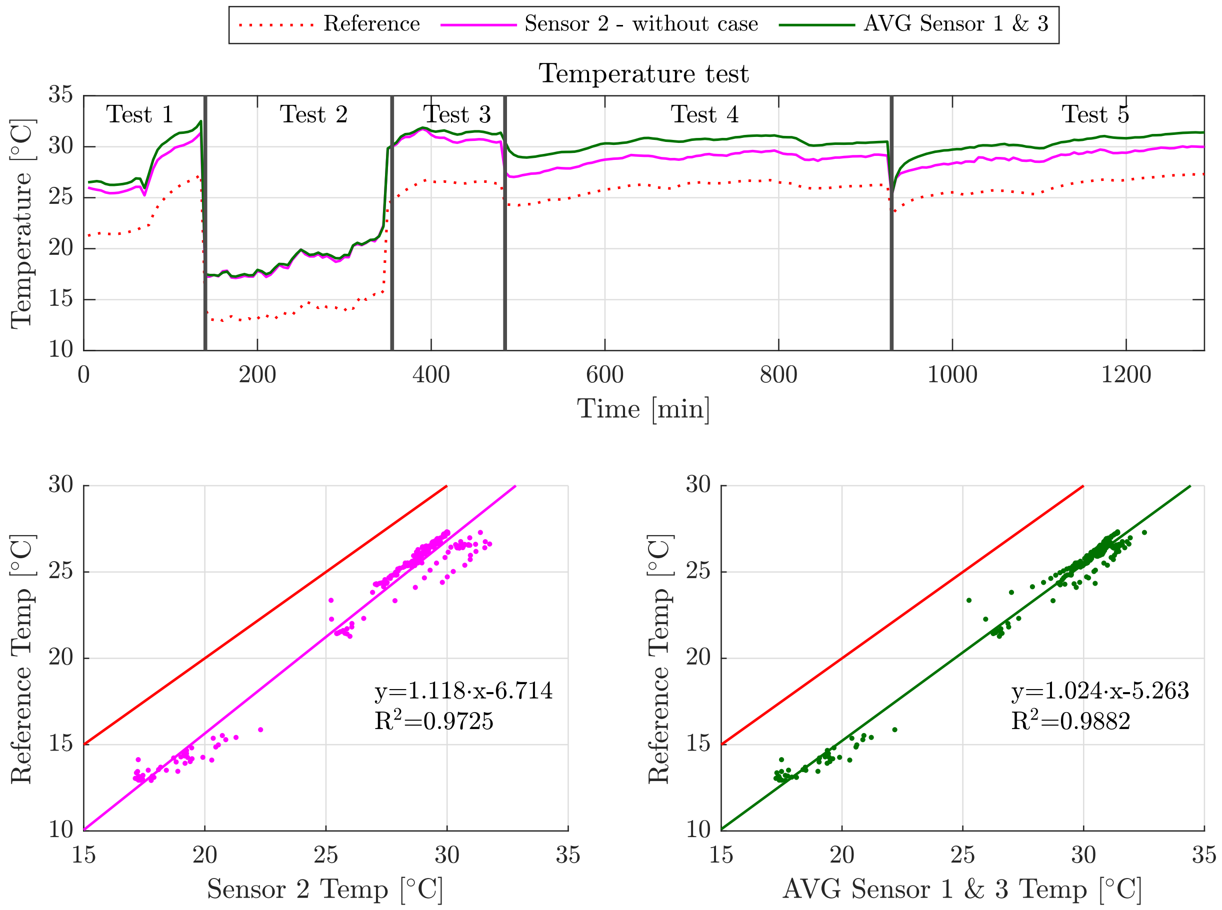

Figure 8.11: Results for the temperature behaviour test, red line represents the ideal linearity.

The measurement time is plotted against the temperature during the full test, as presented on the Temperature test, Figure 8.11. Based on the obtained results, it can be concluded that when the sensors adapt to the environmental change, they react in similar time, having a low time constant. It is observed that both increase and decrease of temperature has been noticed. The relation between the sensor and reference is fairly linear, obtaining the R^2 for all of the three sensors, close to 1. It can be stated that the bias between the sensor and reference results is within an acceptable range.

From the results of test 1, the Pt-100 that measures the temperature inside the box shows to be closer to the sensor results than to the IC-meter ambient temperature. Meaning that the air in the box is heated up, disturbing the final sensor measurements. The relative error between these two parameters is biased up to 14.68%. In terms of measurement without case during the test 4 and 5, the relative error equals 11.13%. For this reason, it is suggested to assure that the box has a better ventilation and the heat is removed faster or that the case should have a different design that can avoid this problem.

Overall, the relation presented on the bottom Figures 8.11 is the final result for the temperature correlation. The polynomial equation that is presented on the Figure, should be applied in order to obtain the real temperature results, while using the sensors. Two separate equations are applied, for case with and without the case. The sensor for temperature can be trusted and only requires a simple calibration.

Barometric Pressure

The experimental conditions for pressure test has been the same as the ones for temperature test. In case of pressure, it is of interest to observe its relation with the temperature. The experimental results from the sensor testing are presented in the Figure 8.12.

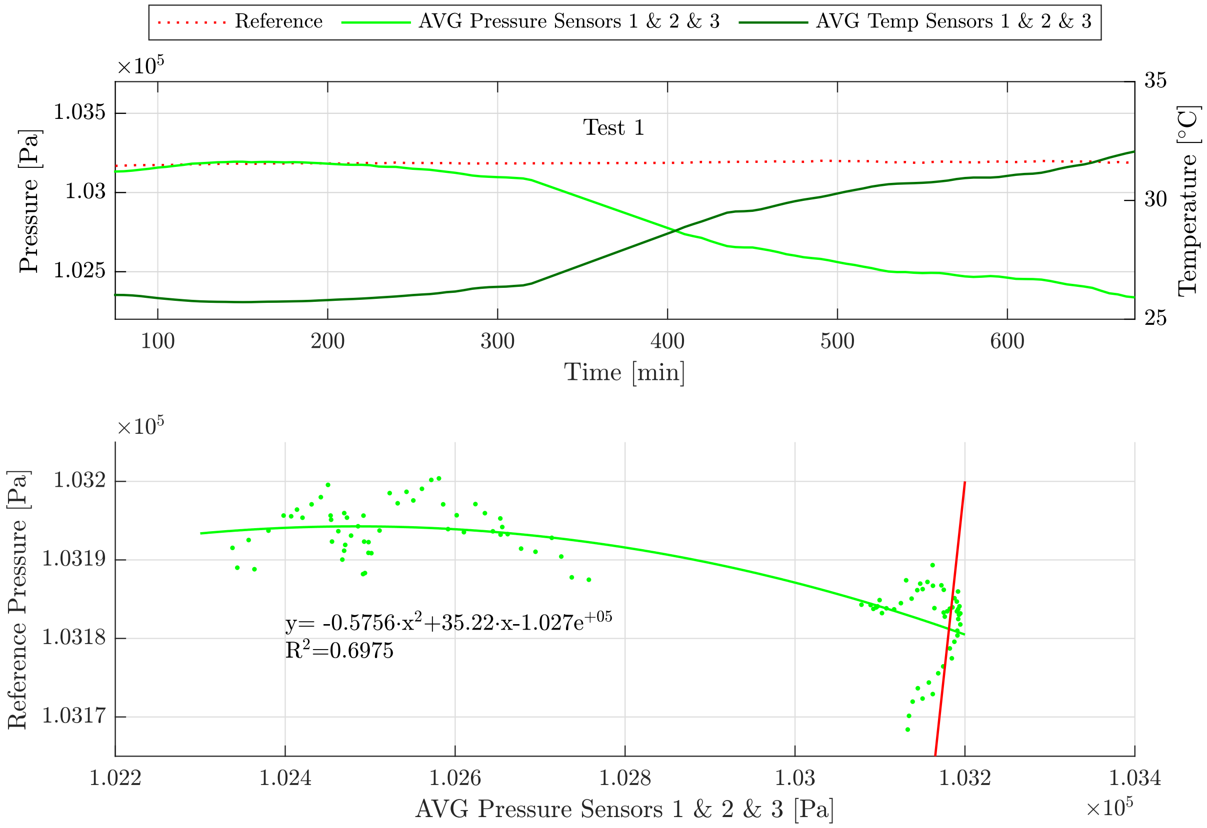

Figure 8.12: Pressure calibration test

The reference pressure measurement recorded from the barometer, as visible in the Figure 8.12 on top, almost did not change. This is because barometric pressure inside a room is not easily subjected to change. For this reason, the barometric pressure is stable while the results from the sensor varies. Moreover, it can be noticed that the sensors results and the temperature react against each other. Therefore, it seems that Bosch internal algorithms overcompensate pressure readings depending on temperature.

As observed in the Figure 8.12 there is no relation between the actual measurement and the sensors. However, a compensation for temperature changes could be applied and test the sensor again. That could result in a good sensor response.

CO_2 concentration

This parameter is another reference used for the control strategy of the window. For the comfort of the occupants is it very important that the sensors measures precisely, so that the correct working modes of the window are activated. It has to be noticed that the Bosch sensor does not measure the CO_2 concentration, but the Volatile Organic Compound.

Supported by the Melgaard and Mikalainis [2018] experiment, this type of sensors do not perform well and are not recommended as a reference measure for the CO_2 concentration. They are defined as a function of the occupancy. For this reason, during the experiment variation of occupancy is tested for the verification of the sensors accuracy. The experimental analysis results are presented in Figure 8.13.

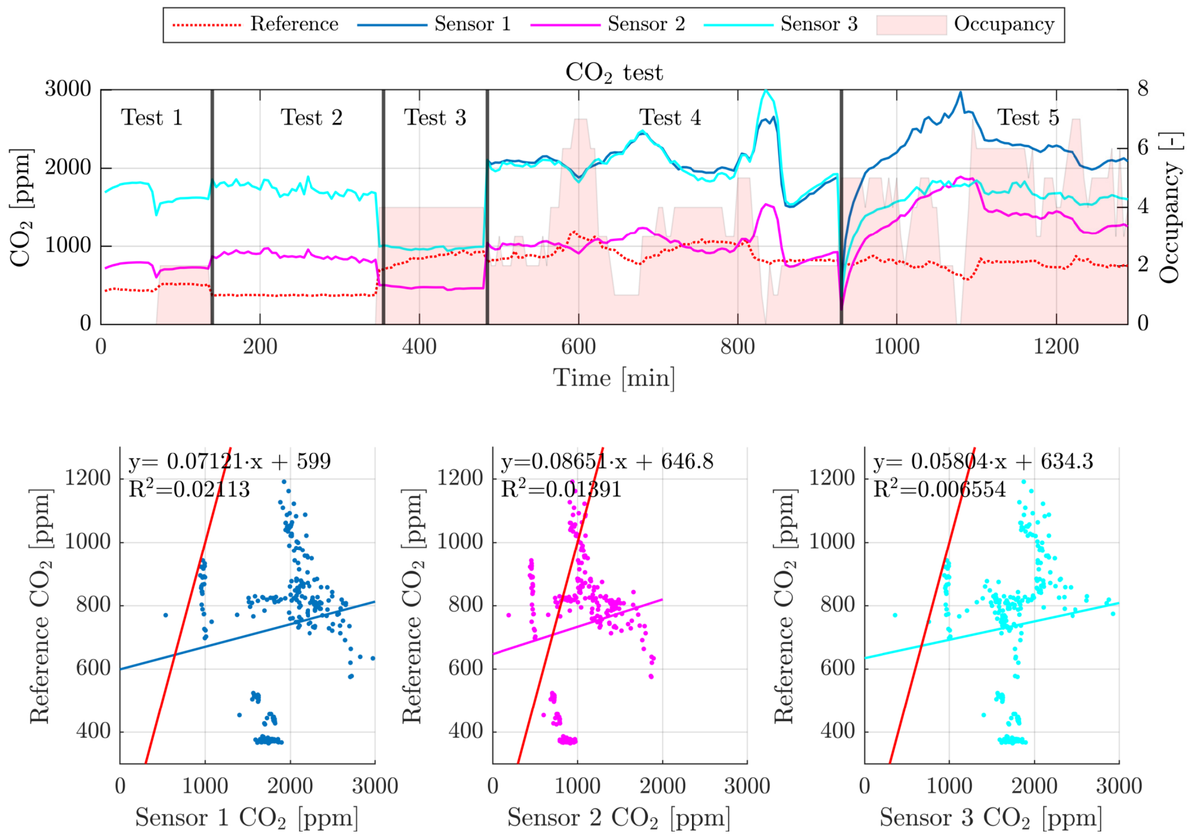

Figure 8.13: CO_2 calibration test

As presented in the figure above, it can be seen that the reference measurements and the sensors behave differently when changing conditions. It can be noticed that reaction to the environmental change is observed for all of the sensors. The highest occupancy load is during test 4 and test 5. However, it cannot be concluded that the sensors are correlated with the reference measure. Additionally, the sensor 1, 2 and 3 are not even correlated between each other. For instance, during tests 1,2 and 3 the results from the sensors 1 and 3 are the same, while sensor 2 shows lower values, more related to the reference results. However, during the test 5, when exposed to higher occupancy load, the three of them give different results.

The relationship between the sensors and the reference measurements is presented on the CO_2 test, Figure 8.13 at the bottom. No linearity in the results is visible, obtaining the R^2 close to 0. It is a wrong-behaved sensor, which should not be used for the measurement. The sensor behaviour cannot be trusted and an actual CO_2 sensor is recommended.

Relative Humidity

In terms of relative humidity, the test conditions are the same as for the other tests. In that case, the sensor behaviour is fairly linear, the response and the sensor adaptation to different conditions has been observed satisfactory. On the Figure 8.14 data treatment for the relative humidity is presented.

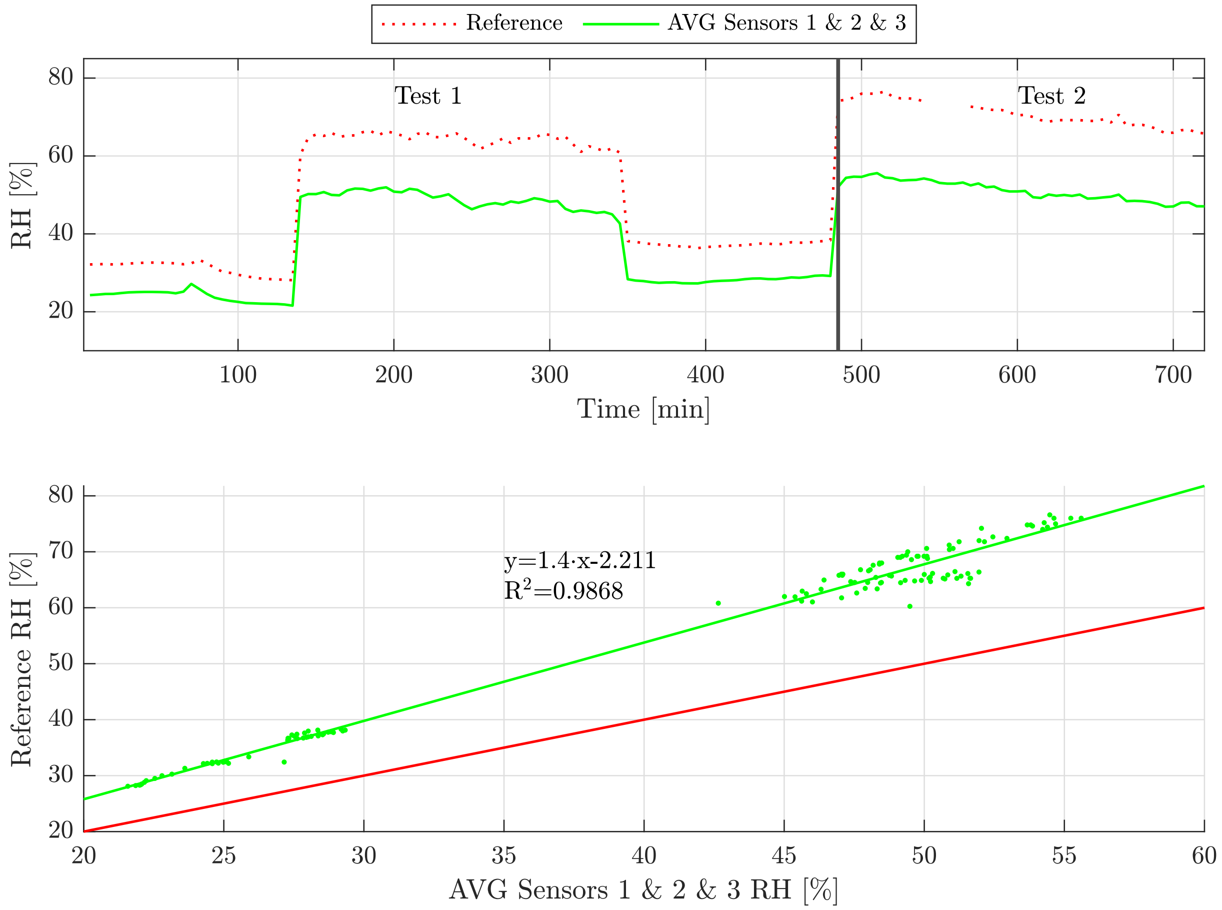

Figure 8.14: Results for the Relative Humidity behaviour test.

The sensor and the reference has shown a similar tendency. There is a constant bias between the reference results and the results from Bosch sensor. In order to obtain the real relative humidity results, the equation presented in the figure above should be applied for the calibration.

The Relative Humidity sensor is a well-behaved sensor. By applying the simple calibration the sensors can be trusted and used as a measurand of indoor conditions.

8.3 Control Design Proposal

This section focuses on the evaluation of the most influential parameters with regards to the indoor comfort. By the results obtained, a proper control strategy is developed for the classrooms. For this reason this section purpose is to answer the last question presented in aim of the study:

> *What is the optimal control strategy design to provide comfortable indoor environment in the classrooms?*

8.3.1 Sensitivity Analysis

The aim of the sensitivity analysis is to resolve the first part of the control investigation, find which inputs influences the output the most. This helps to rank the most influential parameters in order to prioritize them for the design control. That means that the main inputs will create greater disturbances even with small variation to the studied outputs. This calculation is conducted based on data taken every 5 min during the occupied hours from Room 2, as it is the room where the thermocouples have been installed at the window.

Pearson Coefficient

Pearson coefficient is a measure of the linear correlation between two variables X and Y. Results represent a monotonic association between these two variables. It means that when one parameter increases the other one increases, resulting in correlation of 1. However it can also be that when one increases the other decreases, giving a correlation of -1. Any of these results represent the most correlated values. The closer it is to 0, the less correlated [Schober et al., 2018].

$$Correl(X,Y) = \frac{\sum(x-\overline{x})\cdot(y-\overline{y})}{\sqrt{\sum(x-\overline{x})^2\cdot\sum(y-\overline{y})^2}} \tag{8.1}$$

X	Each of the inputs used for the study
Y	Each of the outputs used for this study

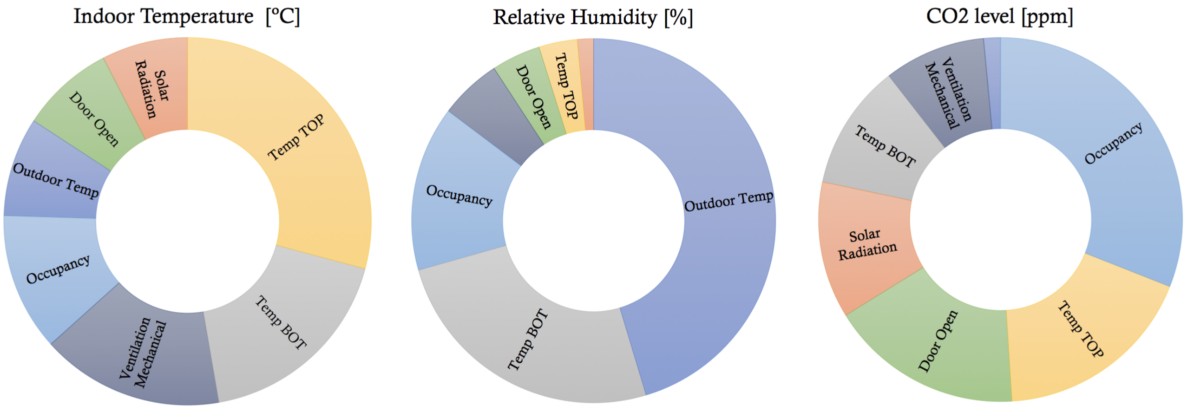

Figure 8.15: Results from Sensitivity Analysis using Pearson Coefficient.

ANOVA

To support the decision about which parameter should be the setpoint for the control strategy, ANOVA simulation is performed. It is an analysis of variance (ANOVA), which gives a ranking of the parameters that are the most significant towards its output.

Table 8.3: ANOVA Solution for the studied outputs.

	Indoor Temperature	**Relative Humidity**	**CO_2 concentration**
Rank	Input	Input	Input
1	T_{TOP}	T_{OUT}	Occupancy
2	T_{BOT}	T_{TOP}	T_{TOP}
3	Ventilation	Solar Radiation	Solar Radiation
5	Occupancy	Door Open	T_{BOT}
6	Solar Radiation	T_{BOT}	Ventilation
7	Door Open	Ventilation	T_{OUT}

Sensitivity Analysis Results

With regards to indoor temperature, T_{TOP} is the most sensitive parameter which involves the impact of the supply air by the window. The second parameter is T_{BOT}, which might be due to the correlation between T_{BOT} and T_{TOP}. The following influential parameter is the mechanical ventilation because forces to supply more fresh air by the windows. Occupancy is the next parameter in the ranking, therefore having an impact in the indoor temperature for being a heat source. Outdoor temperature, door and solar radiation are the least influential parameters. They only impact indirectly the indoor temperature.

Based on relative humidity results, it can be observed that the outdoor temperature has the highest and very significant impact. That means relative humidity is mostly affected by changes in T_{OUT}. As the T_{BOT} is a parameter highly correlated with the outdoor temperature, it is the following in the list continued by occupancy. As the relative humidity is defined by the amount of vapour in the air, it is obvious that occupancy and its impact is a sensitive parameter in the analysis. The influence of the subsequent parameters is not of that high importance as presented on the previously presented figure. That means that even a big change in, for instance, solar radiation, will not affect on the result of the relative humidity significantly. For this reason, these last parameters do not match between Pearson and ANOVA study.

In terms of the CO_2 concentration, the most influential parameter is occupancy. It is an expected result as occupants are the only source of CO_2. The next parameter in the raking is T_{TOP}. It is the setpoint to change the working mode in the window. That means either fresh air is supplied or the cavity remains closed. With regards to the door, as demonstrated before, it helps in reducing the amount of CO_2 concentration when opened. Mention that in terms of the mechanical ventilation, although it contributes to remove the contaminants, it is a variable that has remains fairly constant.

8.3.2 Control Strategy Proposal

As already stated in Section 6.3.1, the control strategy of the WT1 is not efficient and does not adjust to the indoor conditions. During time periods of high CO_2 concentration, the valves remained closed because of outdoor temperatures. For this reason, the incorporation of electronics that measure both the indoor and window conditions is a great improvement.

The main elements that can be found in control design are the controller, sensors and actuators. As previously explained in Section 8.2.1, sensors are the key to give an accurate signal for a specific response of the actuators. However, even the most precise sensor would not be effective if the control strategy is not designed properly. It is then crucial to specify the main goal of the control strategy.

In the design phase, it is of high importance to include all the parameters and possible scenarios. The design of the control strategy for the ventilated window has become a challenge, as explained in the section 2.1.1, due to the lack of research in that area. Therefore, the suggested proposal is based on the results from the experimental analysis in the school. The key of the design is to identify the main problems that have occurred in the school and propose a operation of the window working modes.

For a better understanding of the design for the control strategy, this section is divided into the following questions:

1. Which indoor parameter should be prioritized in the control strategy?
2. Which parameters participate in the control strategy?
3. What is the order of the valves opening?
4. How many valves should be opened?

Which indoor parameter should be prioritized in the control strategy?

In order to come up with an optimal design, it is crucial to prioritize some of the parameters over the others. When designing the control strategy in schools, the health and well-being of the occupants becomes a first concern. Therefore, the indoor environment is considered as a main priority over the thermal comfort. This decision is supported by the WT1 results. Too high CO_2 concentration has been constantly reported, while indoor temperatures and relative humidity in the room remained in a comfortable range for most of the time. An acceptable range defined by the [BR 18, 2018] should not exceed 1000 ppm. Therefore, the control strategy is defined by the following parameters:

- CO_2 concentration: parameter that defines the amount of valves to opened in the windows. Therefore, indirectly controls the air flow rate.
- Indoor temperature and window temperature: parameters that define the working mode of the valves.

This decision is supported by the results from the SA, showing that the temperature at the window supply T_{TOP} is the most sensitive parameter to the thermal comfort. The setpoints are defined by the regulations (Section 3.3) and the acceptable range for the heating season is obtained between 21-23 °C. Lastly, when the CO_2 level and the indoor temperature are satisfactory, the relative humidity is verified based on the setpoints defined by the regulations, which should be between 30-70%.

Which parameters participate in the control strategy?

CO_2 $_{OZ}$	T_{OZ}	T_1	T_2	RH $_{OZ}$	RH_W

CO_2 $_{OZ}$, T_{OZ} and RH_{OZ} are the values measured in the occupied zone. The rest T_1, T_2 and RH_W are explained as follows.

Figure 8.16 presents the three windows located in each room with each of the sensors highlighted in blue. For the control strategy the cavities are divided into two groups: upper and bottom cavities. The division is based on their height and blinds operation. The control of the blinds for the bottom cavities move together. This means that the cavities 1 and 2 always have the same position of the blinds. In addition, as the windows are exposed to the same outdoor conditions, it is very likely that each group of cavities have the same temperature. For this reason the temperatures of the sensors are averaged. This explanation also concerns the top cavities in which the blinds are moved together.

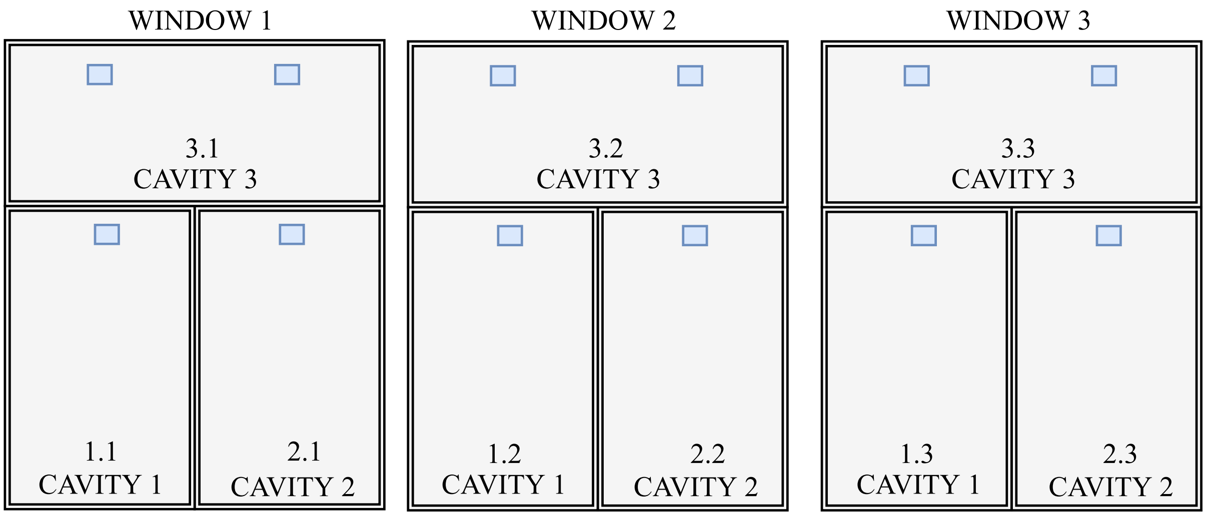

Figure 8.16: Set points for the control strategy based on room and window temperatures from Climawintech sensors.

Temperatures and relative humidity are averaged as shown below:

$$T_1 = \frac{T_{1.1} + T_{1.2} + T_{1.3} + T_{2.1} + T_{2.2} + T_{2.3}}{6}$$

$$T_2 = \frac{T_{3.1} + T_{3.2} + T_{3.3}}{3}$$

$$RH_w = \frac{R_{1.1} + R_{1.2} + R_{1.3} + R_{2.1} + R_{2.2} + R_{2.3} + R_{3.1} + R_{3.2} + R_{3.3}}{9}$$

What is the order of the valves opening?

There are two options to open the valves. Either the valves start to open from the bottom cavities or from the top cavities. This criteria is based on the indoor and window conditions, for instance:

- If the temperature in the cavity is warmer than the room, the bottom cavities are opened first in order to avoid the warm air staying close to the ceiling (from valve 1.1 to 3.3).
- If cold air has to be supplied to the room, the top cavities are arranged first in order to avoid draught by low temperatures to the occupants (from valve 3.3 to 1.1).

How many valves should be opened?

The control strategy is always prioritized by the CO_2 concentration level (see Figure 8.17). This figure represents the order of opening and amount of valves. When the CO_2 concentration is adequate, temperature in the room is prioritized (see Figure 8.18).

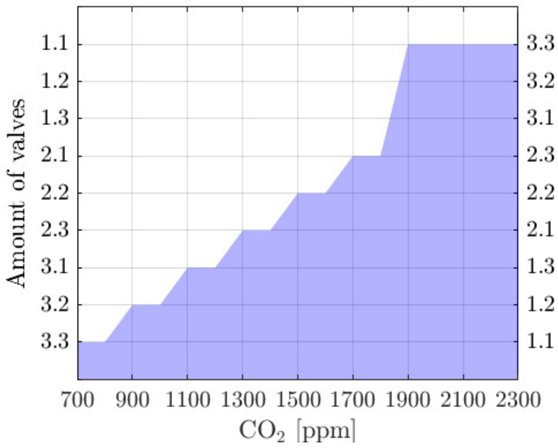

Figure 8.17: Cascade curve defining the amount and order of valves to open for CO_2

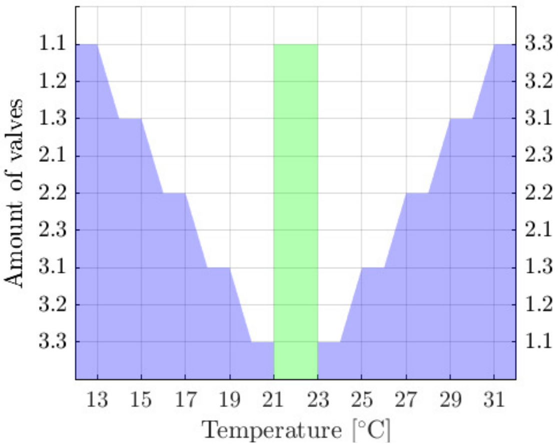

Figure 8.18: Cascade curve defining the amount and order of valves to open for temp.

As an example, when the CO_2 concentration in the room equals to 1700 ppm six valves are opened. In the situation above 1900 ppm, all valves open. In addition, as can be seen even though the CO_2 is less than 900 ppm there is always one cavity open to assure a minimum supply to the room. In case of good CO_2 but a temperature in the room of 27° C five valves are opened. In addition, when bypass/cooling used, one of the valves in each cavity work in cooling and the other two in bypass in order to supply with fresh air but recirculate air through the cavity.

Figure 8.19 presents the proposal for the control strategy.

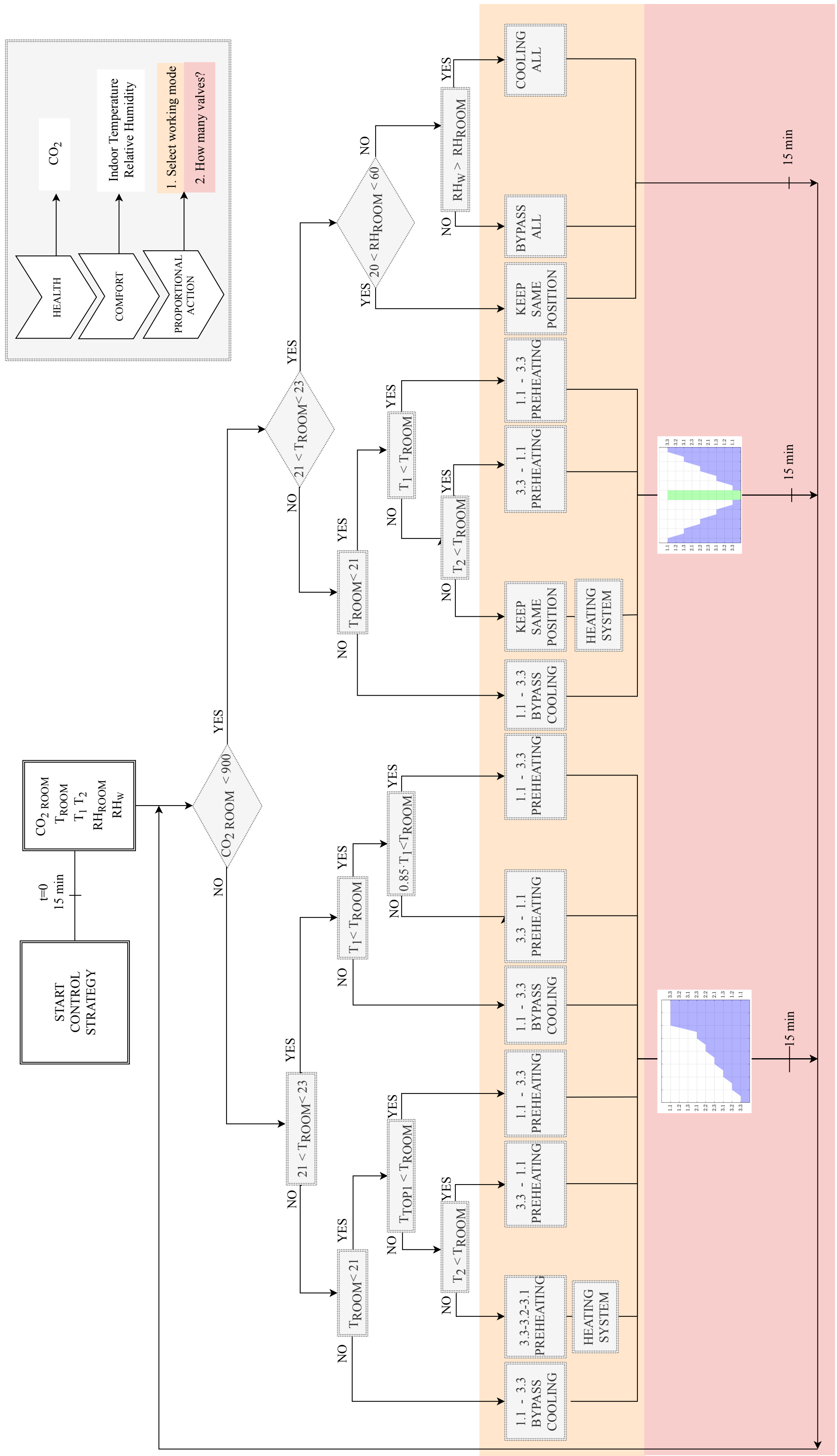

Figure 8.19: Diagram for the control strategy.

9

Summary of Results

9.1 Indoor Environment

The studied rooms did not report temperature or humidity problems. However, it is important to consider that this results only concern the heating season. In terms of local thermal discomfort, no problems were reported, except for the temperature gradient exceeding ΔT of 2 °C in some instances. Nevertheless, as the windows were replaced for a larger airflow capacity windows, this test is recommended to be executed again.

It is known that the occupancy is a very sensitive and important parameter while making energy calculations and dimension of the building services. However, this parameter is often assumed by profiles such as a school schedule. From the results, schedules and real occupancy profiles have large differences without a traceable pattern. The schedule overestimates 59% of occupancy while 60% of the time there are occupants not expected by the schedule. Consequently, it is suggested not to use fixed schedules for building simulation or system operations, as they would not give realistic results.

Based on the ventilation effectiveness results, the airflow follows a mixing ventilation strategy. Nevertheless, as the IC meters were placed above the occupied zone, the results show that the air is well mixed close to the ceiling. The reason for the IC location was not to disturb the occupants.

With regards to the CO_2 measurements, both classrooms have reported severe problems not fulfilling the regulations. During the occupied hours, Room 1 with naturally driven exhaust reported 54% of the time CO_2 concentrations higher than 1000 ppm, whereas Room 2 with mechanical exhaust reported 38%. The main reason is due to the low air flow supplied by the windows. The opening of the door has proven to have a significant influence on decreasing the CO_2 concentration. Therefore, to conclude, it is fundamental that the ventilated windows are supported by a mechanical exhaust, not only to force more air through the windows but also to have a control strategy that depends on the CO_2 concentration in the rooms.

Before and after the renovation of the windows, visual comfort results did not achieve a DF of 2% in the working area of the classroom. However, the DF distribution slightly increased at the opposite side of the windows for the new design. This is due to the fact that the location and dimensions of the windows for the room do not allow for a proper distribution of the DF. Nonetheless, due to the new electronically controlled blinds, it is expected that the users would interact much more with the blinds position adapting them to their needs. Consequently, avoiding the reported glare problems without compromising the view to the outside and light transmittance to the inside.

9.2 Window Performance

Regarding the functioning of WT1 a bad quality control strategy of the valves has been reported. The results show that during occupied hours, the CO_2 level exceeds 1000 ppm during 16% when there is no supply and 22% of the time that air is supplied. 44% of the occupied time the valves have remained closed. Consequently, for a considerable amount of time no fresh air is supplied to the classroom. Both preheating and cooling mode reported temperatures higher at T_{BOT} than T_{TOP}. This shows that either the flow was reversed going from the outlet to the inlet or a malfunctioning of the valve position. During heating season, cooling mode is in use for only 5% of the time and due to the low outdoor temperatures, bypass mode has never been in use. Based on these results, the thermal expansion valve has shown to be inefficient and obsolete.

The height and the blinds influence on the pressure drop results. Tests have shown that the inclusion of blinds and higher cavities report higher pressure drop between the inlet and outlet of the cavities. However, it has also been observed how differences in the construction and positioning of the valves, have given higher pressure drops than expected. This might be due to the fact that the WT2 was a first prototype whose construction could be improved.

The results from the window performance in the school have reported an increasing tendency of the AHR with the solar radiation. However, as the flow rate through the window was unknown, the conclusions are focused on the results from the experiments in the laboratory under controlled conditions of temperatures and flow rates.

With regards to the PHR, as long as T_{TOP} is lower than T_{IN}, the contribution of heat from the interior of the room to the window seems to increase with higher T_{IN} temperatures. In addition, the lowest air flow rate of 8.56 l/s per m^2 shows higher PHR results, whereas the other flow rate tests of 14.52 and 23.1 l/s per m^2 show no changes in the mean values. In terms of the blinds, they report a positive effect during the night as they avoid heat transferred by night sky radiation.

The results from the AHR have shown a clear tendency of higher AHR with higher radiation. A general conclusion between the three cavities report that the higher the flow rate, the lower the AHR. This is due to the fact that the air moves faster and stays less time in the cavity, therefore, it has less time to be heated. In addition, it is interesting to highlight that the cavity 3, which is shorter than the others, seems to give similar HR for high flow rates. This effect represents a physical limit in the HR, concluding that after certain flow rate, the HR will remain constant. In terms of the blinds due to their reflective material, the greenhouse effect in the cavity is enhanced. In addition, the thermal mass of the building considerably contribute to preheating the air.

With regards to the heat recovered of a ventilated window, cavity 1 and 2 have shown that even for high flow rates, with low HR values there is always an amount of heat recovered. However, for cavity 3, the middle flow of 14.52 l/s per m^2 rate reported more heat recovered. The reason for this might be due to the limitation of the HR caused by the height of the cavity.

As a conclusion, it can be stated that the height of the cavity and the inclusion of blinds with reflective visual properties between the panes definitively enhance the effect of the thermal performance of the window. In terms of the heat recovered, a ventilated window reports energy savings over a convectional window.

9.3 Control Design

The sensor tests has been executed for 3 Climawintech sensors and a general calibration curve has been suggested if possible. However, for the future use of the sensors, it is recommended that each of them is individually calibrated.

In general terms, pressure measurements by Bosch sensor do not correlate with the reference barometric pressure. Nevertheless, it is recommended that a compensation parameter is applied and the sensor is tested again in order to correct the decompensation by the temperature.

With regards to temperature, a redesign of the case in which the sensor is more ventilated would be beneficial. However, temperature results have given a constant offset, therefore, by applying the proposed calibration equation the new temperature measurements will be more accurate. This conclusion can also be applied to humidity in which the calibration equation could be used.

With regards to CO_2 measurements, the results have shown obvious deviation from the reference sensors. Therefore, an actual CO_2 instead of a VOC sensor is strongly suggested, especially, when CO_2 together with temperature, are the most crucial parameters if a control strategy is going to be implemented at the school.

Based on the window performance study of the WT1, a dynamic control strategy is required. Consequently, a strategy whose flow rate in the room is defined by the amount of valves opened is suggested. By the indoor and window conditions the proper working mode of the valves is defined. In addition, humidity levels are also considered.

The suggested control strategy aims to improve the indoor environment in school. The operation of the window is adjusted to the indoor environment and window conditions, resulting in a holistic approach.

10 Conclusion

A ventilated window is a recommend solution to be implemented in naturally ventilated buildings (see Chapter 2). As this system has not been previously tested in schools, this report pursues to contribute to the lack of research in this topic.

Subsequently, by testing the window in the school, thermal comfort and relative humidity levels reported stable and satisfactory results. However, poor indoor air quality led to a constant discomfort of the students. The most noticeable problem was too high CO_2 concentration. It has been observed that the mechanical extraction provided 16% more time with CO_2 level below 1000 ppm than the natural extraction. In addition, the window working modes, did not respond to the indoor conditions due to the poor control strategy of the thermal expansion valve.

The solution to solve the previously reported problems in the classrooms is to replace the natural for a mechanical extraction, which is controlled according to the CO_2 levels. In addition, it is important to highlight that the replacement of the windows could provide with a larger air capacity and whose working modes also adapt to the indoor conditions was a considerable improvement. Results from window performance test have shown that the effect of blinds and higher cavity windows report in higher supply temperatures. Consequently, in terms of design it is important to make sure that the window is able to recover heat with the lowest pressure drop as possible.

In terms of visual comfort, glare and low DF was the main problem at the classrooms. In addition, the blinds were always down for not being easily accessible to manipulate. For this reason, the solution is to have a user friendly mechanical control of the blinds and that depends on the user needs.

Not only the redesign for a higher capacity windows with electronic control (WT2) is a good idea but also the future implementation of a control strategy. Its interaction with indoor and window conditions allows to keep the CO_2 levels stable, therefore, fulfilling the regulations while supplying sufficient air flow at a comfortable temperature.

10.1 Further Improvements

After this thorough study of the inclusion of ventilated windows in school classrooms and laboratory investigations, the following suggestions for further work are proposed:

- It is suggested to add a mechanical extraction to the room with natural to improve the window operation. Air quality levels will be positively affected.
- Including a valve at the window inlet will help to avoid air circulating when the valves are closed. It is for the situation of cold temperatures outside and too low in the cavity, unable to supply comfortable temperatures. It is then interesting to close the cavity trying to use heat gains from indoors. Consequently, when the cavity is closed it would work as a conventional window.
- Better quality design of the valves and window itself with the intention of decreasing the pressure drop is recommended.
- Change the position of the sensor measuring the indoor environment to the occupied zone is crucial for the accuracy of the results.
- Replacement of the VOC sensors for CO_2 sensors.
- The addition of a sensor that measures outdoor conditions in the control strategy.
- Implementation of the heating system in the control strategy.
- The incorporation of a fan control at the exhaust to decide the supply flow rate depending on the indoor conditions.
- The addition of a shading control based on solar radiation in the control strategy would enhance both heat recovery and visual comfort provided by the windows.
- The suggested control strategy describes the criteria, however there is a need to implement it in a programming language.
- Further experiments to test heat recovery in which the effect of different blinds position. For instance, blinds down and vertical slats during the night in which the effect of blinds isolation would be more obvious in the PHR.
- Further studies on the effect of the building thermal mass on the preheating model of the window.
- Creation of a model in which the energy balance and the control strategy is incorporated. This allows to simulate window performance and energy studies in order to test other outdoor scenarios or support the experimental results. In addition, the variation of boundary conditions or occupancy profiles could be tested. It would be a beneficial tool to use in order to improve the design and control strategy.
- The creation of a CFD model of the window would help in understanding the behaviour of the flow inside the cavity and therefore, if the design could be improved.

Bibliography

Almeida and Ferreira, 2017. Manuela Almeida and Marco Ferreira. *Cost effective energy and carbon emissions optimization in building renovation (Annex 56).* Energy and Buildings, 152, 718 – 738, 2017. ISSN 0378-7788. doi: 10.1016/j.enbuild.2017.07.050.

Almeida et al., 2015. Ricardo M.S.F. Almeida, Vasco Peixoto de Freitas and João M.P.Q. Delgado. *School Buildings Rehabilitation.* Cham Springer, 2015. ISBN 978-3-319-15358-2. doi: 10.1007/978-3-319-15359-9.

Appelfeld and Svendsen, 2011. David Appelfeld and Svend Svendsen. *Experimental analysis of energy performance f a ventilated window for heat recovery under controlled conditions.* Energy and Buildings, 43(11), 3200–3207, 2011. ISSN 03787788. doi: 10.1016/j.enbuild.2011.08.018.

Bosch, 2019. Bosch. *BME680-Datasheet*, 2019. URL `https://ae-bst.resource.bosch.com/media/_tech/media/datasheets/BST-BME680-DS001.pdf`.

BR 15, 2015. BR 15. *The Danish Building Regulations 2015 (BR15).* Danish Transport and Construction Agency, 2015.

BR 18, 2018. BR 18. *Executive order on Building Regulations 2018.* Ministry of Transport, Building and Housing, 2018.

Carlos et al., 2010. Jorge S. Carlos, Helena Corvacho, Pedro D. Silva and J. P. Castro-Gomes. *Real climate experimental study of two double window systems with preheating of ventilation air.* Energy and Buildings, 42(6), 928–934, 2010. ISSN 03787788. doi: 10.1016/j.enbuild.2010.01.003.

Carlos et al., 2011. Jorge S. Carlos, Helena Corvacho, Pedro D. Silva and J. P. Castro-Gomes. *Modelling and simulation of a ventilated double window.* Applied Thermal Engineering, 31 (1), 93–102, 2011. ISSN 13594311. doi: 10.1016/j.applthermaleng.2010.08.021.

Carrer et al., 2002. P. Carrer, Y. Bruinen de Bruin, M. Franchi and E. Valovirta. *The EFA project: indoor air quality in European schools*, volume 77. 2002.

DS 1752, 2001. DS 1752. *DS1752: Ventilation for Buildings- Design criteria for the indoor environment.* Danish Standard Association, 2001.

DS/EN 15251, 2007. DS/EN 15251. *DSEN15251: Indoor environmental input parameters for design and assessment of energy performance of buildings addressing indoor air quality, thermal environment, lighting and acoustics*. Danish Standard Association, 2007.

European Commission, 2019. European Commission. *Energy Performance of buildings*, 2019. URL `https://ec.europa.eu/energy/en/topics/energy-efficiency/energy-performance-of-buildings`.

Hamid et al., 2018. Abdul Akram Hamid, Karin Farsäter, Åsa Wahlström and Petter Wallentén. *Literature review on renovation of multifamily buildings in temperate climate conditions*. Energy and Buildings, 172, 414 – 431, 2018. ISSN 0378-7788. doi: 10.1016/j.enbuild.2018.04.032.

Hannoudi et al., 2016. L Hannoudi, M Lauring and J. E Christensen. *Architectural qualities of Danish office buildings built between 1960 and 1980, seen in a contemporary sustainable perspective*. WIT Press, 2016. ISBN 978-1-78466-111-3.

Heiselberg et al., 2013. Kalayanova Olena Heiselberg, Per, Mingzhe Liu, Chen Zhang, Hicham Johra, Lars Herold, Jose Mendez, Jorge Cabral, Nuno Brito, Andreas Zegowitz and Ingo Heusler. *ClimaWin - Technical Summary Report*. 160. 2013.

Heiselberg, 2002. Per Heiselberg. *Principles of Hybrid Ventilation. IEA Energy Conservation in Buildings and Community Systems Programme Annex 35: Hybrid Ventilation in New and Retrofitted Office Buildings*. IEA-ECBCS Annex 35, Aalborg, 2002.

Heiselberg, 1999. Per Heiselberg. *Hybrid Ventilation in New and Retrofitted Office Buildings*, volume R9922 of *46*. Aalborg: Dept. of Building Technology and Structural Engineering, 1999.

Horn Group, 2019. Horn Group. *Ventilated Window working principles*, 2019. URL `http://ventilationsvinduet.dk/`.

Hou et al., 2015. Yuefei Hou, Junjie Liu and Jiayu Li. *Investigation of Indoor Air Quality in Primary School Classrooms*. Procedia Engineering, 121, 830–837, 2015. ISSN 18777058. doi: 10.1016/j.proeng.2015.09.037.

ICIEE-DTU, 2019. ICIEE-DTU. *International Centre for Indoor Environment and Energy*. DTU Technical University of Denmark, 2019.

ISO 7730, 2005. ISO 7730. *Ergonomics of the thermal Environment. Analytical determination and interpretation of thermal comfort using calculation of the PMV and PPD indices and local thermal comfort criteria*. International Organization for Standardization, 2005.

Jensen et al., 2018. Per Anker Jensen, Esmir Maslesa, Jakob Berg Brinkø and Christian Thuesen. *10 questions concerning sustainable building renovation*. Building and Environment, 143, 130 – 137, 2018. ISSN 0360-1323. doi: 10.1016/j.buildenv.2018.06.051.

Johnson et al., 2018. David L. Johnson, Robert A. Lynch, Evan L. Floyd, Jun Wang and Jacob N. Bartels. *Indoor air quality in classrooms: Environmental measures and effective ventilation rate modeling in urban elementary schools*. Building and Environment, 136 (March), 185–197, 2018. ISSN 03601323. doi: 10.1016/j.buildenv.2018.03.040.

Johra, 2019. Hicham Johra. *Testing Sensors for Building Application*, volume 216. not-published, 2019.

JS Foundation , 2019. JS Foundation . *Node-RED*, 2019. URL `https://nodered.org/`.

Kalimeri et al., 2016. Krystallia K. Kalimeri, Dikaia E. Saraga, Vasileios D. Lazaridis, Nikolaos A. Legkas, Dafni A. Missia, Evangelos I. Tolis and John G. Bartzis. *Indoor air quality investigation of the school environment and estimated health risks: Two-season measurements in primary schools in Kozani, Greece*. Atmospheric Pollution Research, 7(6), 1128–1142, 2016. ISSN 13091042. doi: 10.1016/j.apr.2016.07.002.

Kamendere et al., 2015. Edite Kamendere, Gatis Zogla, Agris Kamenders, Janis Ikaunieks and Claudio Rochas. *Analysis of Mechanical Ventilation System with Heat Recovery in Renovated Apartment Buildings*. Energy Procedia, 72, 27 – 33, 2015. ISSN 1876-6102. doi: 10.1016/j.egypro.2015.06.005. International Scientific Conference Environmental and Climate Technologies, CONECT 2014.

Kolding Kommune, 2019. Kolding Kommune. *Steppingvej 14*, 2019. URL `https://bbr.dk/pls/wwwdata/get_ois_pck.show_bbr_meddelelse_pdf?i_municipalitycode=0621&i_realpropertyidentifier=255561`.

Liu et al., 2017. Mingzhe Liu, Per Kvols Heiselberg, Olena K. Larsen, Lone Mortensen and Jørgen Rose. *Investigation of Different Configurations of a Ventilated Window to Optimize Both Energy Efficiency and Thermal Comfort*. Energy Procedia, 132, 478–483, 2017. ISSN 18766102. doi: 10.1016/j.egypro.2017.09.660.

Markussen, 2007. Lau Markussen. *Thermal Performance of Air Flow Windows*, 2007.

Mathworks online, 2018. Mathworks online. *MATLAB Optimization Toolbox*, 2018. URL `https://se.mathworks.com/help/stats/box-plots.html`. The MathWorks, Natick, MA, USA.

Melgaard and Mikalainis, 2018. Simon Pommerencke Melgaard and Mindaugas Mikalainis. *Test and evaluation of indoor climate sensors in Gigantium with focusto accuracy of CO2 measurements*. not published, 2018.

Menå and Larsen, 2010. Henriette Ryssing Menå and Eva Maria Larsen. *Indoor Environment in Schools*. Master thesis, -(February), 127, 2010.

Schober et al., 2018. Patrick Schober, Christa Boer and Lothar A. Schwarte. *Correlation Coefficients: Appropriate Use and Interpretation*. correlation coefficients, 126, 2018. doi: 10.1213/ANE.0000000000002864.

Singh et al., 2019. Manoj Singh, Ryozo Ooka, Hom Rijal, Sanjay Kumar, Anuj Kumar and Sadhan Mahapatra. *Progress in thermal comfort studies in classrooms over last 50 years and way forward*. Energy and Buildings, 2019. doi: 10.1016/j.enbuild.2019.01.051.

Skistad, 2004. Håkon Skistad. *Displacement ventilation in non-industrial premises*. Rehva guidebook. Rehva, Brussels, 2. ed. edition, 2004.

Trompetter et al., 2018. W. J. Trompetter, M. Boulic, T. Ancelet, J. C. Garcia-Ramirez, P. K. Davy, Y. Wang and R. Phipps. *The effect of ventilation on air particulate matter in school classrooms*. Journal of Building Engineering, 18(September 2017), 164–171, 2018. ISSN 23527102. doi: 10.1016/j.jobe.2018.03.009.

Vorre et al., 2017. Mette Havgaard Vorre, Mads Hulmose Wagner, Steffen E. Maagaard, Peter Noyé, Nadja Lynge Lyng and Lone Mortensen. *Branchevejledning for indeklimaberegninger*. 1. edition, 2. printing. Statens byggeforsnkingsinsitut, 2017.

A

Measurement Plan

A.1 Experimental Analysis School - WT1

In this section based on the structure of the Numerical Analysis in Chapter 5 each parameter recorded in the school is categorized and located in the classroom. It is explained first that measurements have been collected during different duration of time. This is because the school is in use and impede the placement of some meters in the middle of the room for a long time. For this reason divides each parameter in these categories:

- Constant, const.: corresponds to time dependent variables whose location do not disturb the normal activity in the room.
- Temporary, tempo.: corresponds to time dependent variables whose location could disturb the normal activity in the room. Therefore, this measurements which are placed in the occupied zone, have been installed only during a period of time of 3 days.
- Instantaneous, inst.: correspond to non-time dependent variables, meaning that there is no need to keep any device receiving data in the room.

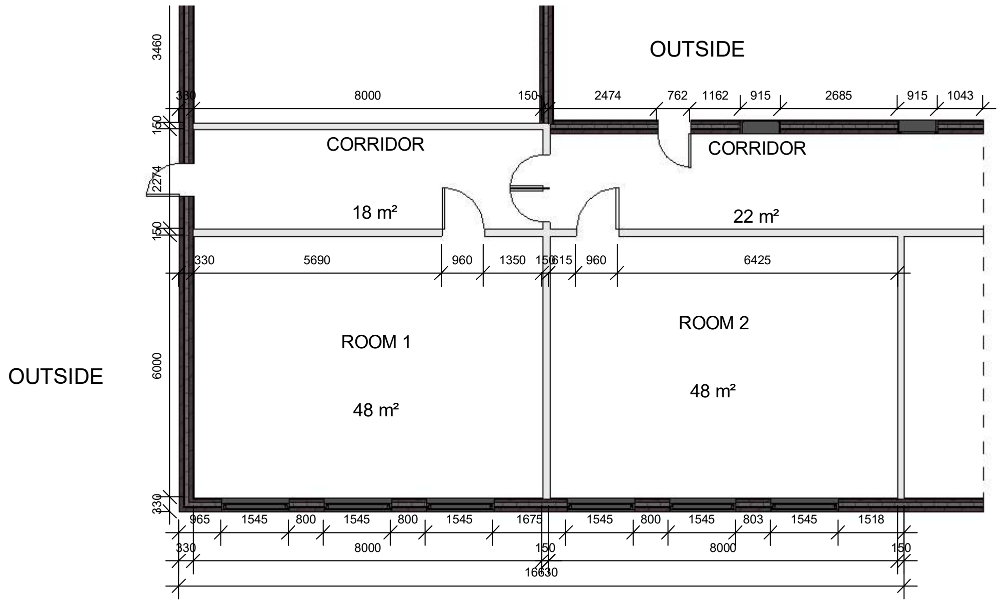

Figure A.1: Floor plan of the classrooms.

A.1.1 Indoor Air Quality

In Table A.1all the parameters involved in terms of indoor air quality that have been measured in the classrooms can be found.

Table A.1: Measurements related to indoor air quality conditions

	Units	Definition	Instrument	Time	Point
C_{e_1}	[ppm]	CO_2 exhaust Room 1	IC-meter	const.	e1
C_{e_2}	[ppm]	CO_2 exhaust Room 2	IC-meter	const.	e2
C_{out}	[ppm]	CO_2 concentration exterior	Thermocouple	const.	out
C_{oz_1}	[ppm]	CO_2 occupied zone Room 1	IC-meter	const.	oz1
C_{oz_2}	[ppm]	CO_2 occupied zone Room 2	IC-meter	const.	oz2
Occ_1	[-]	People in Room 1	Camera	const.	cam1
Occ_2	[-]	People in Room 2	Camera	const.	cam2

A.1.2 Relative Humidity

In Table A.2 all the parameters involved in terms of relative humidity that have been measured in the classrooms can be found.

Table A.2: Measurements related to relative humidity conditions

	Units	Definition	Instrument	Time	Point
RH_{oz_1}	[%]	Relative humidity occupied zone Room 1	IC-meter	const.	oz1
RH_{oz_2}	[%]	Relative humidity occupied zone Room 2	IC-meter	const.	oz2

A.1.3 Thermal Comfort

Table A.3 details all the parameters involved in thermal comfort measurements, including local thermal discomfort.

Table A.3: Measurements related to thermal comfort conditions

	Units	Definition	Instrument	Time	Point
θ_{oz_1}	[°C]	Temp. occupied zone Room 1	IC-meter	const.	oz1
θ_{oz_2}	[°C]	Temp. occupied zone Room 2	IC-meter	const.	oz2
v_{p1}	[m/s]	Air velocity in oz Room1/Room2	Anemometers	tempo.	p1(x2)
v_{p2}	[m/s]	Air velocity near window Room1/Room2	Anemometers	tempo.	p2(x2)
ΔT_{p1}	[°C]	Temp. grad. in oz Room1/Room2	Anemometers	tempo.	p1(x2)
ΔT_{p2}	[°C]	Temp. grad. near window Room1/Room2	Anemometers	tempo.	p2(x2)

A.1.4 Visual Comfort

Table A.3 details all the parameters involved in visual comfort.

Table A.4: Measurements related to visual comfort conditions

	Units	Definition	Instrument	Time	Point
I_i	[lux]	Illuminance inside Room1/Room2	Lux meter	inst.	Table 6.7
I_e	[lux]	Illuminance outside Room1/Room2	Lux meter	inst.	Table 6.7

A.1.5 Window Performance

The air temperature is measured in every opening, inlet and outlets of the window to know precisely the vertical temperature gradient through the ventilation air gap and the frequency in time of each working mode. The thermocouples used are temperature sensors made by silver coated type K. For the Thermocouples at T$_{BOT}$ a silver tube with a fan to have a constant air flow around it and protect the device from solar radiations. Based on the following, the variables in Table A.5 are measured.

Heat Recovery

Table A.5: Measurements related to Heat Recovery of the window performance WT1 and WT2.

	Units	Definition	Instrument	Time	Point
T_{TOP}	[°C]	Temp. upper part of the cavity	Thermocouples	const.	top
T_{OUT}	[°C]	Temp. outside	Thermocouples	const.	out
T_{BOT}	[°C]	Temp. bottom part of the cavity	Thermocouples	const.	bot

Air Flow Calculations

Table A.6: Measurements related to Ventilation of the window performance WT1.

	Units	Definition	Instrument	Time	Point
q_{e1}	[l/s]	Flow rate exhaust at Room 1	Flow meter	const.	e1
q_{e2}	[l/s]	Flow rate exhaust at Room 2	Flow meter	const.	e2
D_1	[-]	Open/close of the door Room 1	Camera	const.	cam1
D_2	[-]	Open/close of the door Room 2	Camera	const.	cam2

A.2 Experimental Analysis Laboratory - WT2

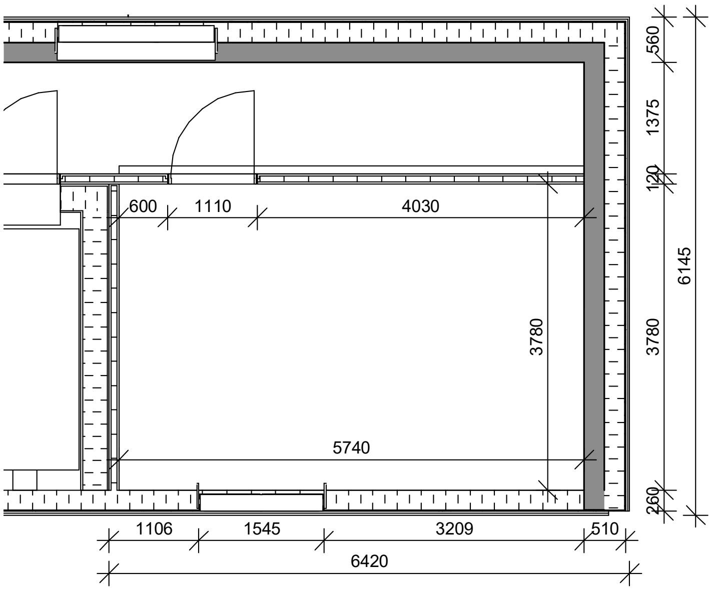

Figure A.2: Floor plan of the laboratory room dimensions [mm].

A.2.1 Visual Comfort

Table A.7: Measurements related to visual comfort conditions

	Units	Definition	Instrument	Time	Point
I_i	[lux]	Illuminance inside room/lab	Lux meter	inst.	Table 7.1
I_e	[lux]	Illuminance outside room/lab	Lux meter	inst.	Table 7.1

A.2.2 Window Performance

Air Flow and Pressure Drop Correlation

Table A.8: Measurements related to Pressure differences through the window WT2.

	Units	Definition	Instrument	Time	Point
P_1	[Pa]	Pressure inlet bottom in ph	Micromanometer	const.	P_1
P_2	[Pa]	Pressure supply bottom ph/bypass	Micromanometer	const.	P_2
P_3	[Pa]	Pressure inlet top ph	Micromanometer	const.	P_3
P_4	[Pa]	Pressure supply top ph/bypass	Micromanometer	const.	P_4
P_5	[Pa]	Pressure inlet bottom in bypass	Micromanometer	const.	P_5
P_6	[Pa]	Pressure inlet top in bypass	Micromanometer	const.	P_6

Heat Recovery

Table A.9 shows measured temperature points to calculate HR in preheating mode based on Figure 7.5. Type K thin thermocouple

Table A.9: Measurements related to Temperature differences through the window WT2.

	Units	Definition	Instrument	Time	Point
T_1	[°C]	Bottom temperature cavity 1	Thermocouples	const.	T_1
T_2	[°C]	Top temperature cavity 1	Thermocouples	const.	T_2
T_3	[°C]	Bottom temperature cavity 2 inside	Thermocouples	const.	T_3
T_4	[°C]	Top temperature cavity 2 inside	Thermocouples	const.	T_4
T_5	[°C]	Bottom temperature cavity 2 outside	Thermocouples	const.	T_5
T_6	[°C]	Top temperature cavity 2 outside	Thermocouples	const.	T_6
T_7	[°C]	Bottom temperature cavity 3 inside	Thermocouples	const.	T_7
T_8	[°C]	Top temperature cavity 3 inside	Thermocouples	const.	T_8
T_9	[°C]	Top temperature cavity 3 outside	Thermocouples	const.	T_9

A.3 Devices used for Measurements in the school

Pictures for an overview of the classrooms are shown in Figure A.3 and Figure A.4.

Figure A.3: Room 1 distribution and main elements involved in this analysis.

Figure A.4: Room 2 distribution and main elements involved in this analysis.

Figure A.5: Lindab and IC-meter - Room 1.

Figure A.6: Lindab and IC-meter - Room 2.

Figure A.7: IC-meter & cameras - Room 1.

Figure A.8: IC-meter & cameras - Room 2.

(a) Pyranometer - Thermocouple. ***(b)*** Thermocouples window. ***(c)*** Data logger Grant.

Figure A.9: Real position of the Grant logging data from pyranometer and thermocouples in the school.

Figure A.10: Anemometers connection.

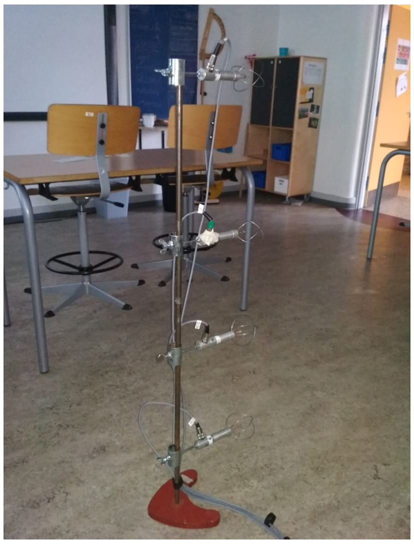

Figure A.11: Pole with anemometers.

Figure A.12: School façade window type 1.

Figure A.13: School façade window type 2.

Figure A.14: Pictures from the electronics in WT2.

Figure A.15: Bottom inlet grill of WT1.

Figure A.16: Top inlet grill of WT1.

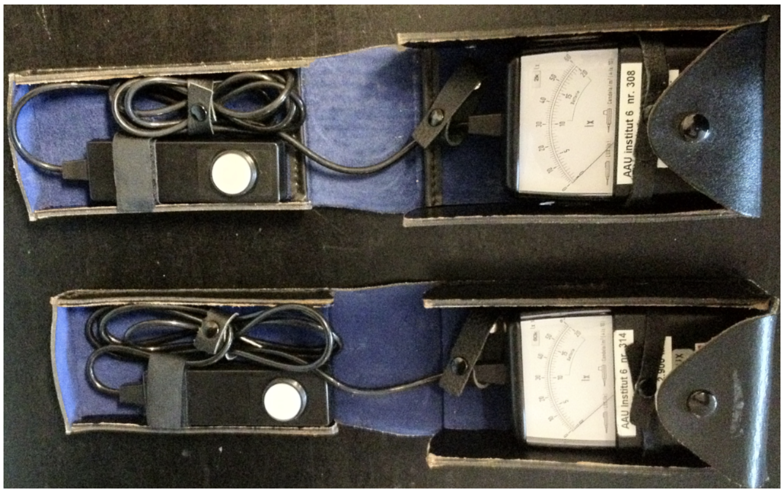

Figure A.17: Luxmeters used indoors and outdoors in the classrooms and laboratory

A.4 Devices used for Measurements in the laboratory

A.4.1 Visual Comfort

Table A.10: Blinds chosen for the visual test in the laboratory.

Sample 1 - RF28	**Sample 2 - LT11 RF13**	**Sample 3 - LT29 RF12**
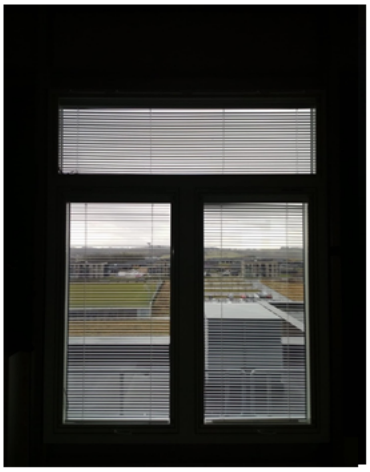		
Sample 4 - LT15 RF11	**Sample 5 - LT5 RF15**	
		

A.4.2 Air Flow and Pressure Drop Correlation

Figure A.18: Tube position in the window for pressure drop experiment in the laboratory.

A.4.3 Heat Recovery

Figure A.19: Thermocouple in the window to measure solar radiation in the laboratory.

Figure A.20: Pyranometer on the façade to measure solar radiation in the laboratory.

Figure A.21: Pyranometer on the façade to measure solar radiation in the laboratory.

B

Calibration

Calibration has been performed in AAU Laboratory. Devices have been tested and the delivered data has been compared to reference devices or more accurate devices to check their accuracy.

B.1 Flow Meters

Figure B.1 presents the Lindab used in the school. They are Lindab ultralink FTMU diameter 160 mm, 141 l/s maximum flow ± 1.6 l/s. In order to store the data they have been connected to a national instrument, shown in Figure B.2, which using the software LABView a .txt has been save with temperatures and flow rates.

The same procedure has been ran for ultralink FTMU diameter 100 mm, 55 l/s maximum flow ± l/s located in the laboratory. Guaranteed measurements uncertainty 0.2-15.0 m/s. Labview has been used as logging software provided by Hicham Johra.

Figure B.1: Lindab at the school.

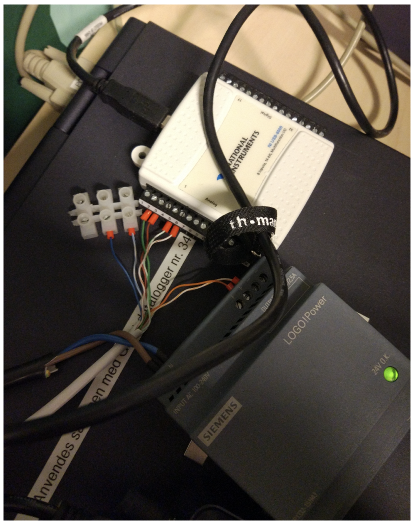

Figure B.2: National Instrument and power supply at the school.

B.2 Thermocouples

The main idea behind calibrating the thermocouples is to find which offset do they have from real value. For this, Isotech 6 VENUS^{PLUS} 2140 shown in Figure B.4 has been the device in charge to control and to set a constant temperature, creating an isothermal environment for the comparison calibration of temperature sensors. It only gives uncertainties of no more then 0.001 °C. A F200 sensor precision thermometer is used shown in Figure B.3. This temperature is compared to the one given by the thermocouples and generate an adjusted curve to give an accurate result.

Figure B.3: F200 precision thermometer.

Figure B.4: Isocal .

Figure B.5 presents the grant - Squirel SQ1600 which is a data logger for the thermocouples. This device is connected to a computer that will generate a file with all the data. The thermocouple itself is presented in Figure B.6.

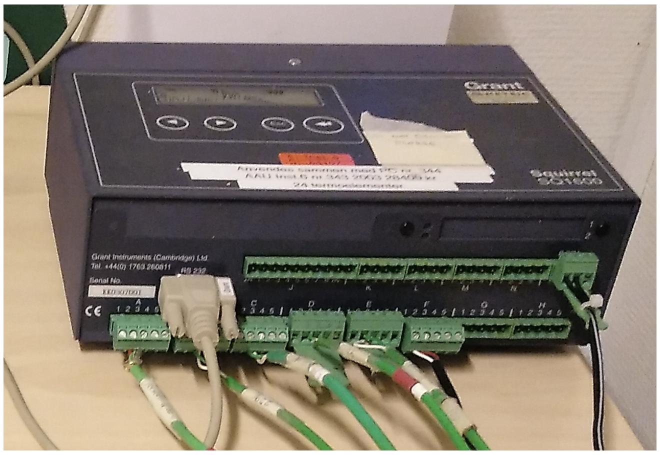

Figure B.5: Grant.

Figure B.6: Thermocoulpes.

Figure B.7 shows the calibration equation extracted as a result from the measurements, shown in red for each thermocouples. Data in blue to the right-hand side of the figure shows how much the results differ.

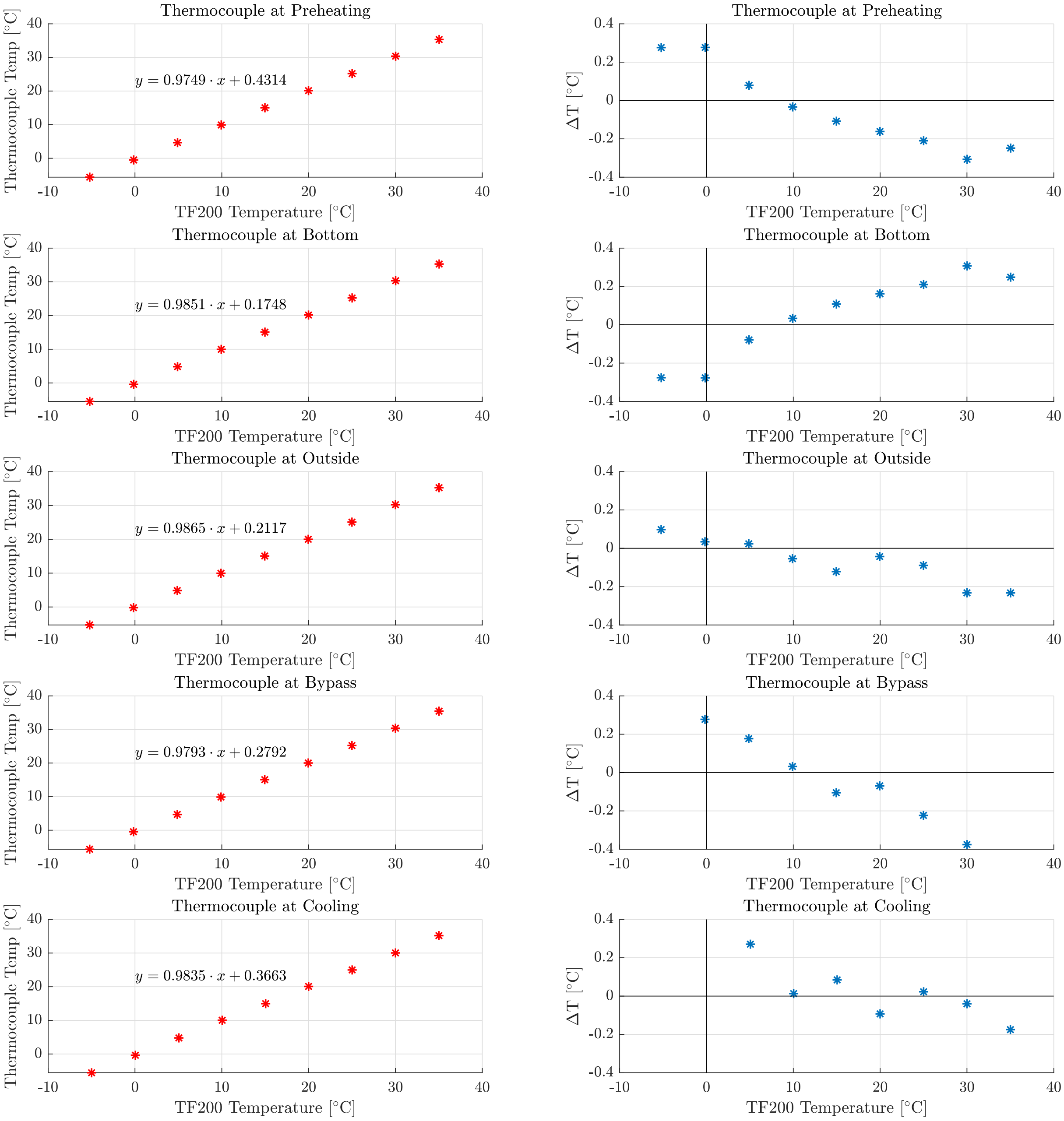

Figure B.7: Thermocouples calibration curves.

All data collected in the school has been afterwards calibrated using MATLab. Calibration correlation coefficients exceeded the analytic threshold of R2 >= 0.999.

B.3 Pyranometer

One of the main influential parameters is the solar radiation in order to investigate the solar heat gains in the ventilated air gap. One pyranometer Kipp & Zonen Pyranometer, model CMP21 has been used on the façade of the building. Vertical position has been chosen to know the radiation reached at the glazing surface of the windows with the same orientation with regards the sun. All measurements from the pyranometers are registered by the Grant - Squirel SQ1600 data logger every 1 minute having a response time of 5 seconds. Sensitivity is $5.75\cdot 10^{-6}$ V/W$\cdot$ m^2, maximum solar irradiance 4000 W/m^2.

B.4 Anemometers

Figure B.8 shows a hot-sphere of the anemometers that are used for air velocity and temperature measurements. To calibrate them it has been used a jet wind tunnel which can supply constant air velocity. It provides a control which the user can rotate to supply the desired air velocity. The jet is generated using a fan and different orifices plates for different ranges of m/s. The used jet tunnel is presented in Figure B.9.

Figure B.8: anemometers.

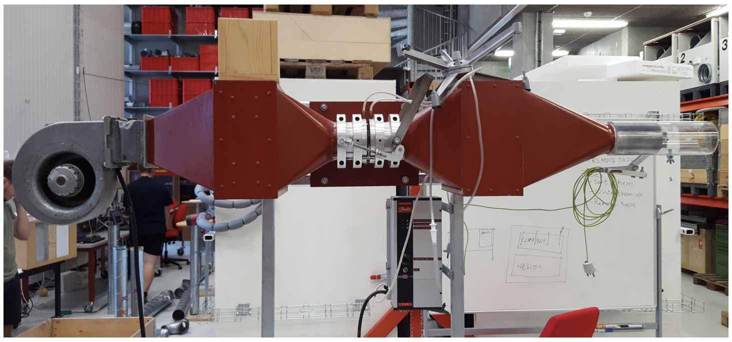

Figure B.9: Wind tunnel.

Eight anemometers have been calibrated, which have been divided onsite in two poles to evaluate air in different positions. 16 samples for each anemometer orifice plates of 10 mm, 23 mm, 46 mm to generate a curve for each separately, presented in Figure B.10.

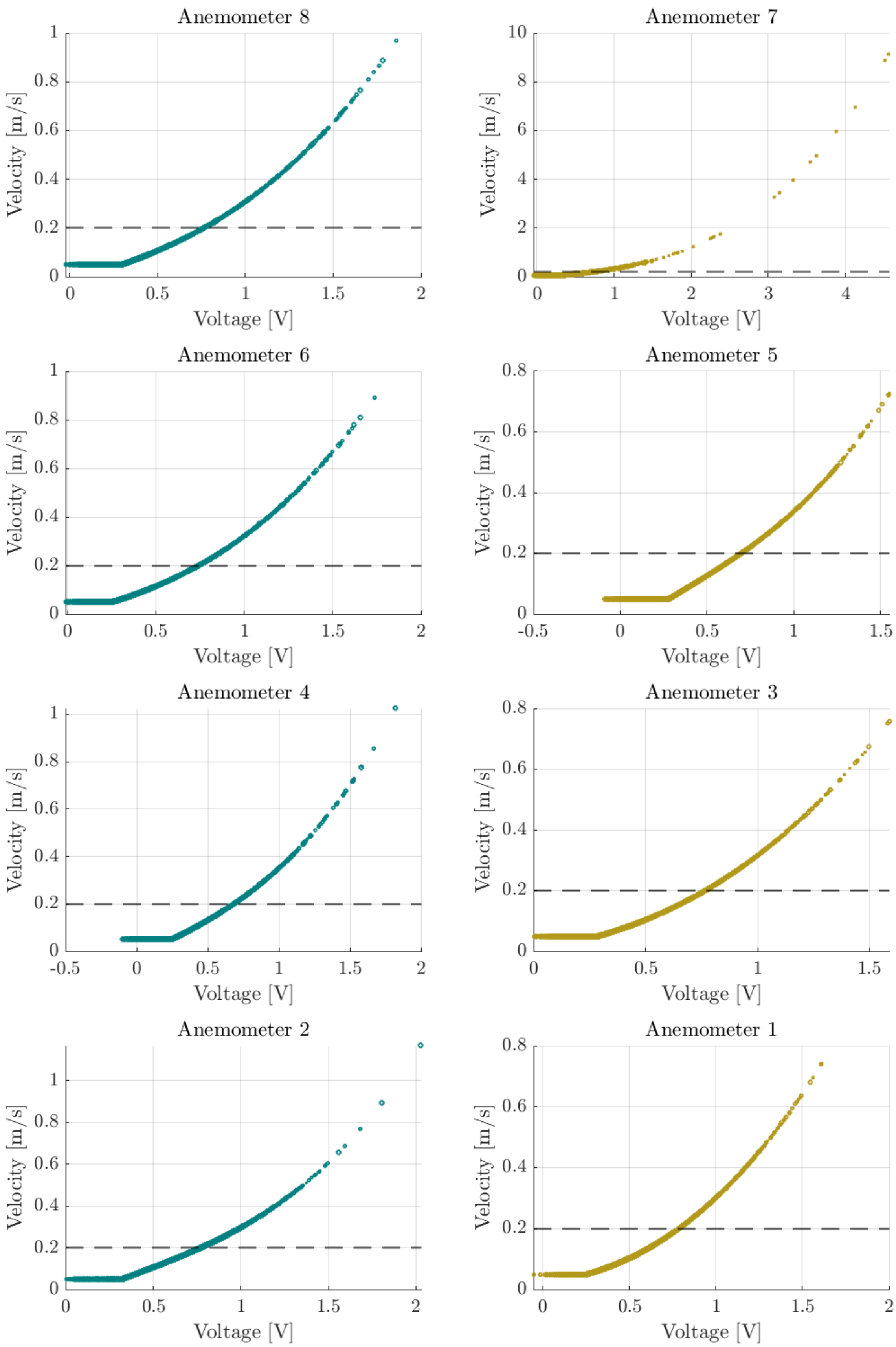

Figure B.10: Calibration curve for each of the anemometers.

C

Data Treatment

C.1 Boxplot Representation

During the report several boxplots are used to represent data. These ones are created using Mathworks online [2018] boxplot function. A boxplot is a standardized way of displaying the distribution of data based on:

- The internal horizontal line shows the median of the data.
- Top and bottom of the box display the 25th and 75th fractile. The distance between the top and bottom is the interquartile range.
- The whiskers are lines extending above and below each box. Whiskers are drawn from the ends of the interquartile ranges to the furthest observations within the whisker length.
- Observations beyond the whisker length are marked as outliers. By default, an outlier is a value that is more than 1.5 times the interquartile range away from the top or bottom of the box.
- If a cross is observed in the boxplot, this one represents the mean value of the dataset.

C.2 Results Indoor Environment

C.2.1 Indoor Air Quality

As explained in the section 6.3.1, the correlation between the occupancy and the CO_2 shows similarities in the results. The results obtained for Room 1 are presented in the figure below. The results conclude that Monday and Fridays are the days with the highest CO_2 concentration level. These days seems to overpass the limit of 1000 ppm the most. However, Tuesday and Thursday show the same tendency in the results. The average value of the CO_2 concentration is below the limit. On Wednesday, the average value does not exceed 900 ppm, which is caused by the smallest occupancy. However, the highest peak of the CO_2 can be observed on Monday, where the level increases up to 2500 ppm, resulting in the highest value of CO_2. It can be observed, that when the CO_2 level increases, it is mostly caused by the occupants. Generally, the profiles follow each other.

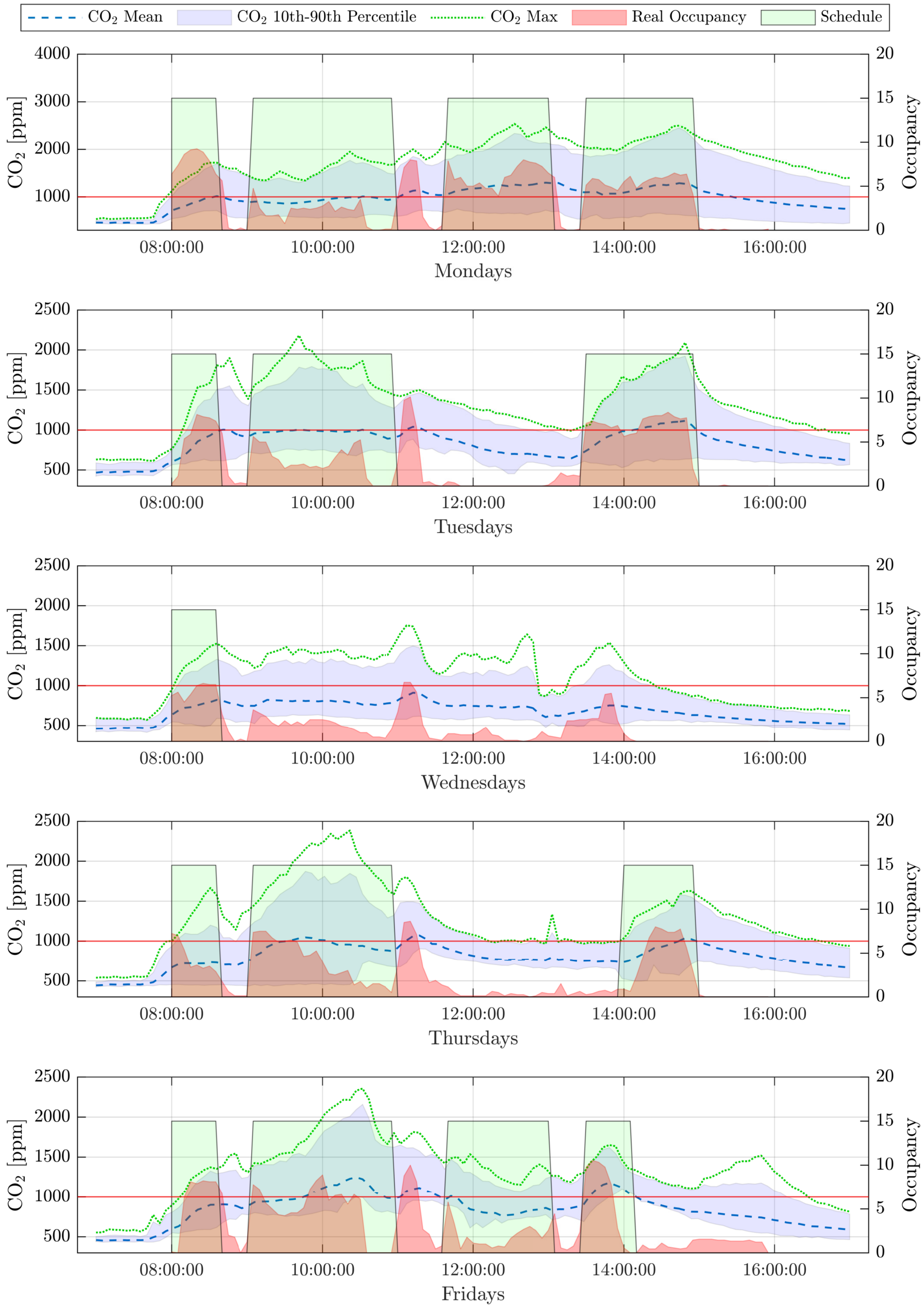

Figure C.1: Occupancy data and CO_2 concentration in Room 1.

The variation between the occupancy and the design schedule is presented in the figure below.

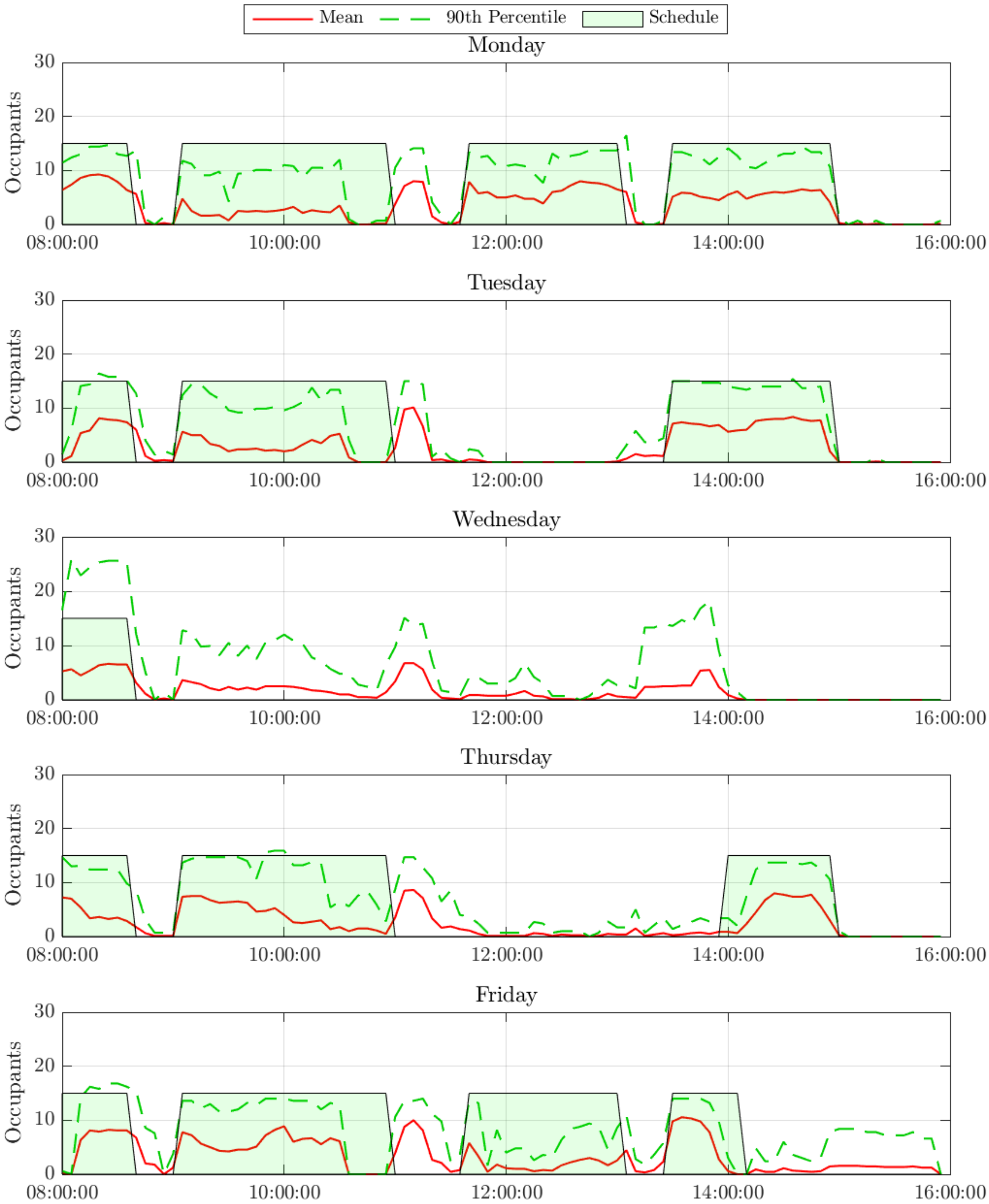

Figure C.2: Occupancy profile in Room 1.

Based in the figure above, it can be concluded that for 68% of the time, there are people in the room when not expected. That is just a confirmation that users interaction with the building, is different than expected. The highest occupancy outside the scheduled time, is visible on Fridays, resulting in 92% of the time. On Wednesday and Thursday, it is around 70%. On average, during the breaks, there is 1 occupant in the classroom. In terms of the designed and real occupancy, there are only 32% of the kids present during the classes. That means, on Mondays 15 people is expected in the classroom, but only 5 are present.

It is of interest to look into the 90th and 10th percentile of the occupancy. School are the institutions with a highly variable occupancy loads. As visible, on the example of Wednesday, 25 people is present in the room for at least 1h. While designing the indoor environment of the room, it is important to consider that such extreme situation can happen. In the Figure C.3 the analysis of the occupancy profile is presented.

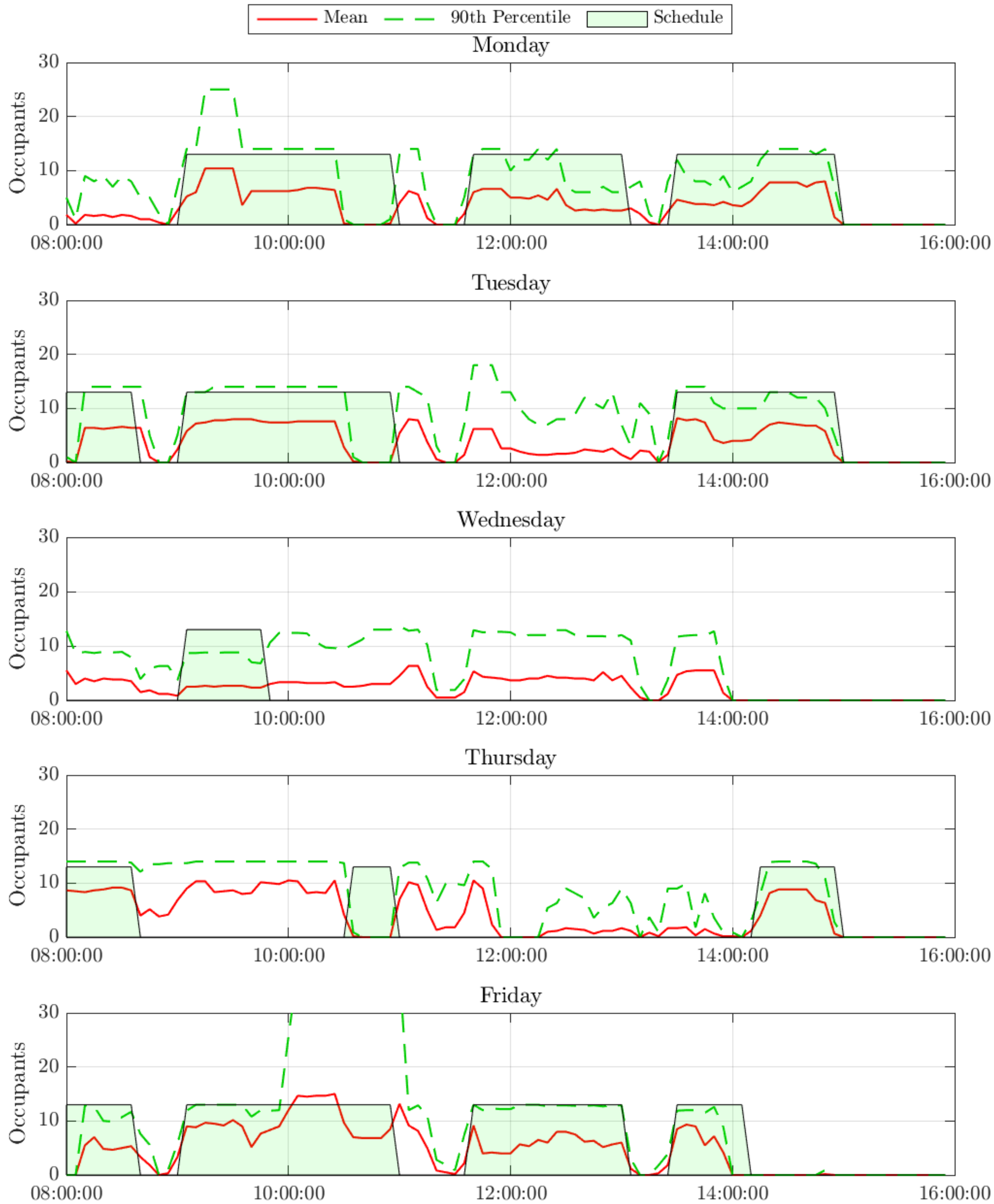

Figure C.3: Occupancy profile in Room 2.

As presented in the figure, there is a big variation in the mean value and the 90th percentile. The most noticeable difference occurs on Friday with 30 people and Mondays 25 people in the same time in the room. On Thursdays and Wednesdays for 91% and 86% of the time, there are people in the room, when not expected. Overall, on average 60% of the time, there are people in the room when not expected. It is also related to the breaks. Generally, it is assumed that children leaves the room for the break. However, on the average, there are 2 occupants present in the room. In terms of number of people designed for the room and the real value, there is a difference of 41%. Everyday, during the school day, 15 people should be located in the room, however there are only 5 on average.

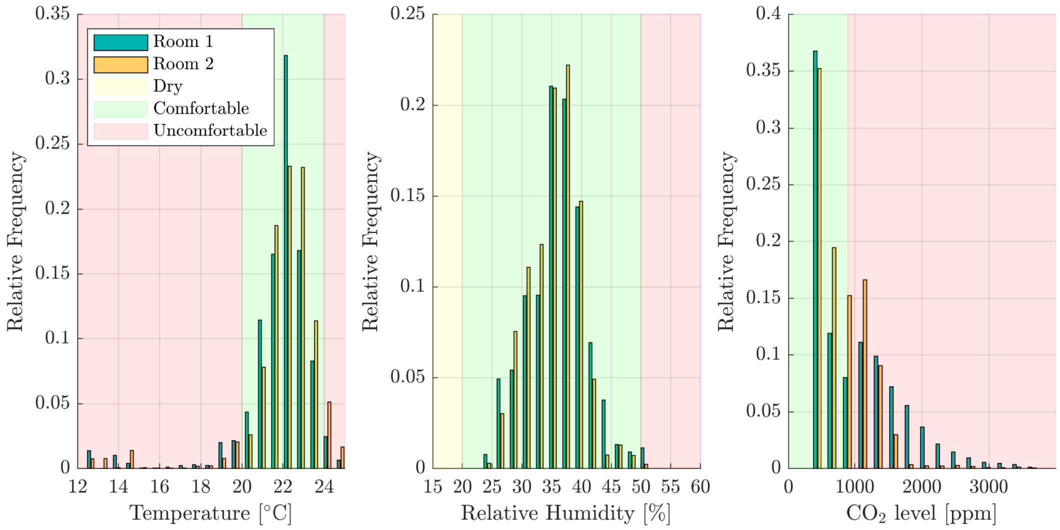

Figure C.4: Relative Frequency of all values extracted from IC-meters logged every 5min only during occupied hours.

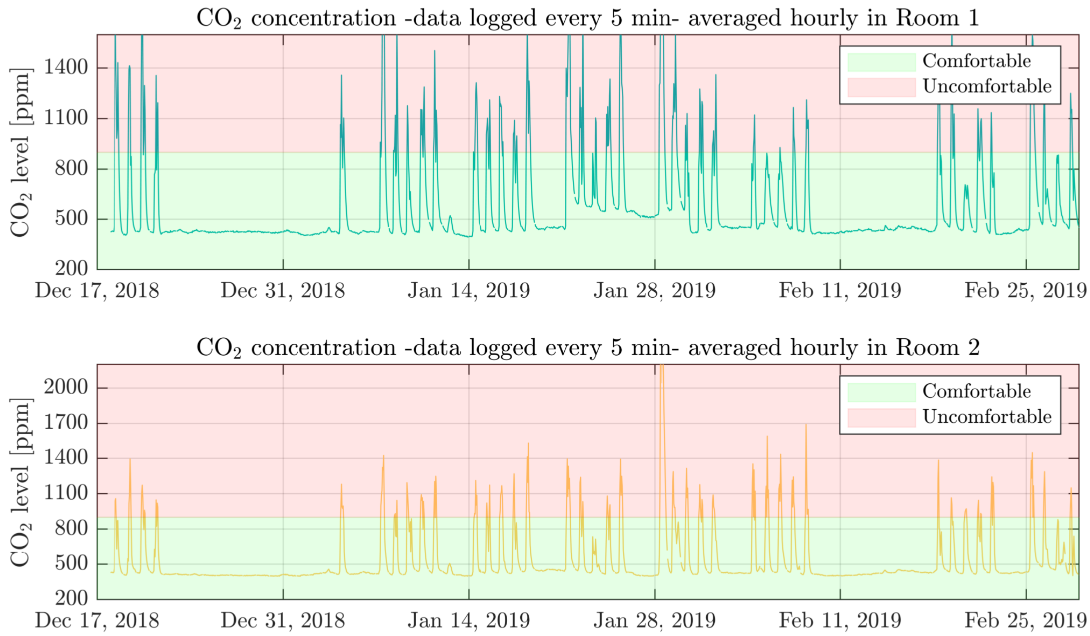

Figure C.5: CO2 levels in both rooms hourly averaged.

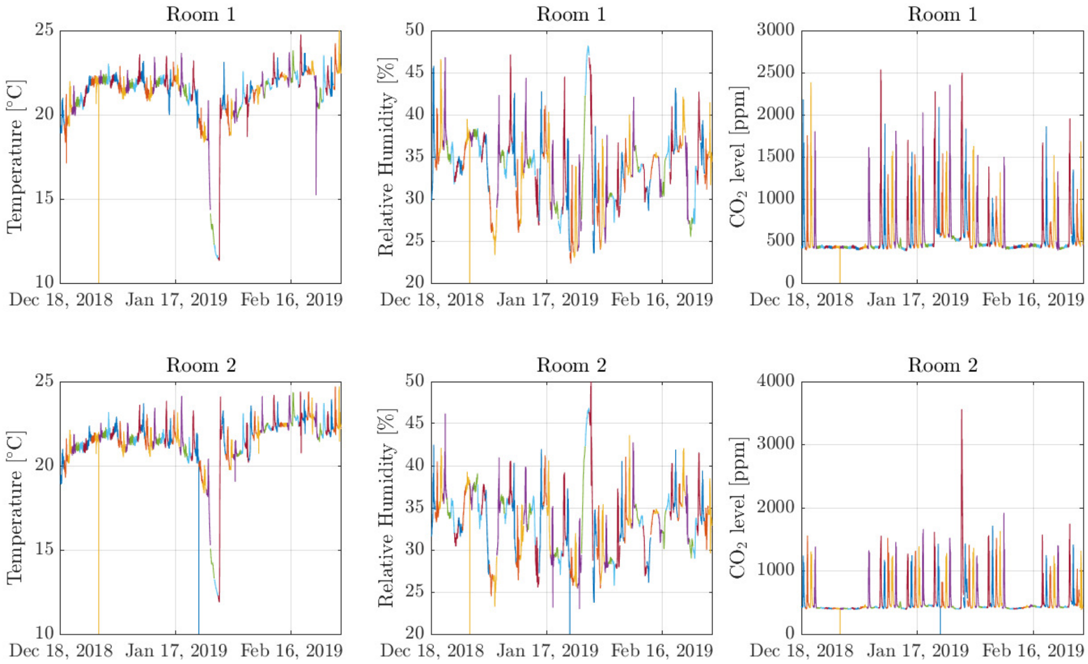

Figure C.6: IC all every 5 min

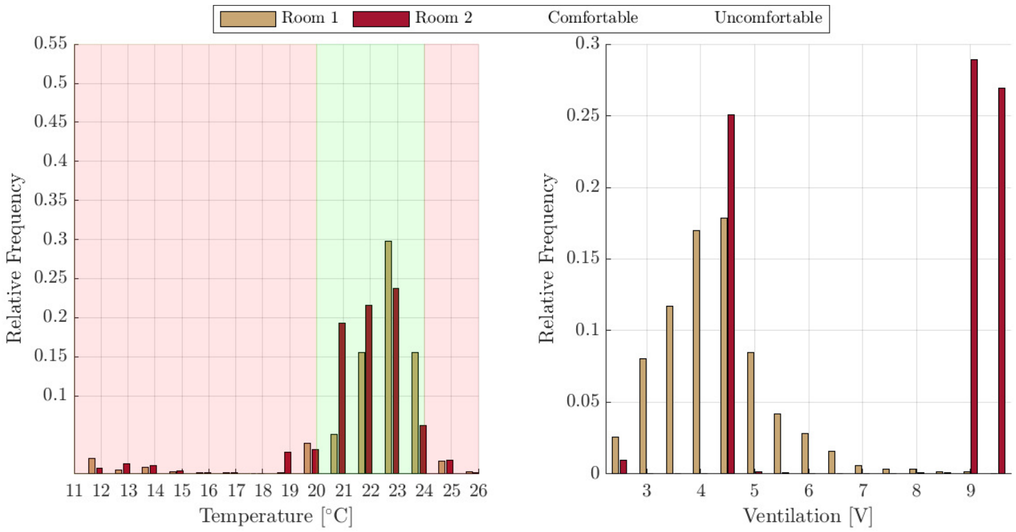

Figure C.7: Lindab histogram of temperature and air flow extracted from each room..

Air Flow Calculations

Kapacitetsskema for Horn Air-flowventiler til Ventilationsvinduet

HORN GROUP

Ventiltyper			Luftmængder i m3/time,				
Gnsn. kapacitet er angivet ved +15 ude-, +20 indetemperatur.			Naturligt diff.tryk		Mek. Aftræk - Behovsstyret		
Konfiguration:	Komplet ventilsæt med 1-3 air-flowventiler		4 pa	8 pa	10pa	20pa	50pa
CWT01:		m3/t	9,9	14,1	15,7	22,4	35,4
Indb. mål 520mm		Antal m2 bolig	9,2	13,1			
CWT02		m3/t	19,9	28,1	31,4	41,5	65,1
Indb. mål 690mm		Antal m2 bolig	18,4	26,2			
CWT03		m3/t	29,8	42,2	47,1	63,9	100,5
Indb. Mål 995mm		Antal m2 bolig	27,6	39,0			

Alle oplyste kapaciter er dokumenteret af Fraunhofer Inst.

V/naturligt aftræk anvendes 4 pa.
V/mek. Hjulpet aftræk anvendes 8 pa. Eller mere.

Min. breddemål til Horn Ventilationsvindue type 2000: alle mål i mm				Type 1900
Fast karm 44mm	Fast karm 55mm	Topstyret 44mm	Topstyret 55mm	Sidehængt:
608,0	630,0	684,0	704,0	720,0
778,0	799,5	853,5	873,5	889,5
1083,0	1105,0	1159,0	1179,0	1195,0

Henviser til Revitt fil.

Ventiltyper			Luftmængder i Liter/Sek,				
Gnsn. kapacitet er angivet ved +15 ude-, +20 indetemperatur.			Naturligt diff.tryk		Mek. Aftræk - Behovsstyret		
Konfiguration:	Term. Aktuator og air-flow ventiltromle		4 pa	8 pa	10pa	20pa	50pa
CWT01:		l/sek	2,8	3,9	4,4	6,2	9,8
Indb. mål 520mm		Antal m2 bolig	9,2	13,1			
CWT02		l/sek	5,5	7,8	8,7	11,5	18,1
Indb. mål 690mm		Antal m2 bolig	18,4	26,2			
CWT03		l/sek	8,3	11,7	13,1	17,7	27,9
Indb. Mål 995mm		Antal m2 bolig	27,6	39,0			

Min. breddemål til vindue type 2000: alle mål i mm				Type 1900
Fast karm 44mm	Fast karm 55mm	Topstyret 44mm	Topstyret 55mm	Sidehængt:
608,0	630,0	684,0	704,0	720,0
778,0	799,5	853,5	873,5	889,5
1083,0	1105,0	1159,0	1179,0	1195,0

Figure C.8: Available air flow rate from different valve combinations provided by *VentilationsVinduet.*

C.3 Visual Comfort

C.3.1 Visual Comfort-Simulations

This table summaries the properties of the materials used for the DIALux simulation in the rooms.

Table C.1: Room elements characteristics set in DIALux to run DF simulations.

Parameter	Material	Reflection factor	Reflective coating	Light Transmittance
Walls	Default	50 %	0 %	-
Ceiling	Default	70 %	0 %	-
Floor	Thick concrete	43 %	0 %	-
Upper side of the slat	-	90 %	98 %	-
Bottom side of the slat	-	28 %	4 %	-
Window's Glass	-	17 %	-	78 %

In Table C.2, results verification between the simulation in DIALux and the actual experiment are presented together with the blinds properties and their visual representation.

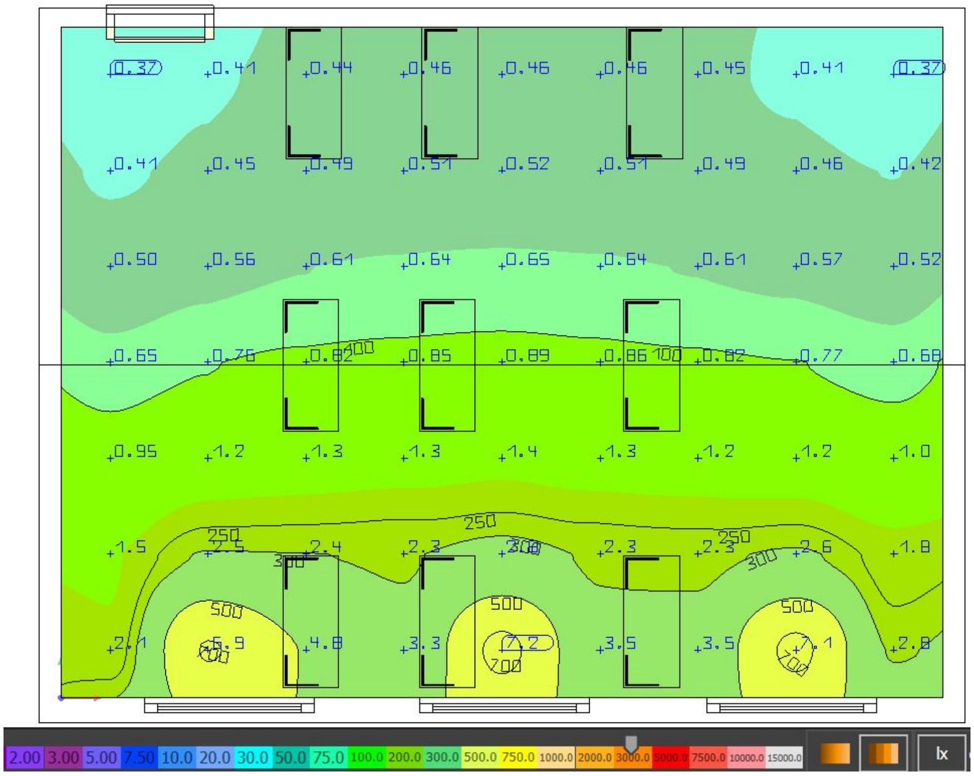

Figure C.9: DF and Lux distribution with blinds up (old windows)

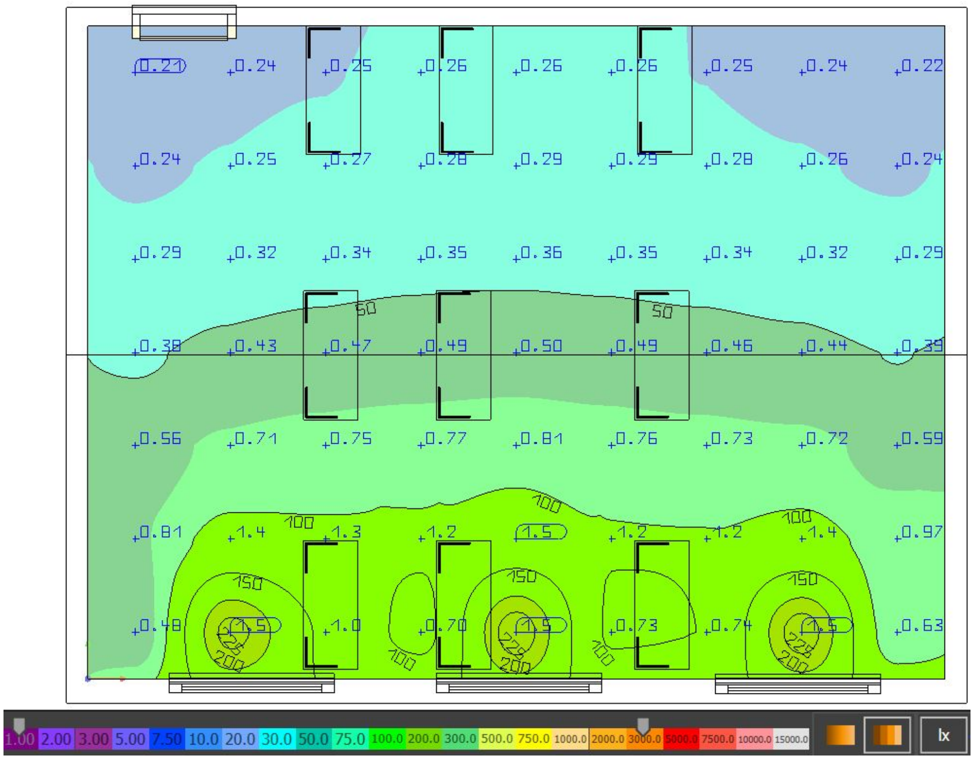

Figure C.10: DF and Lux distribution with blinds down (old windows)

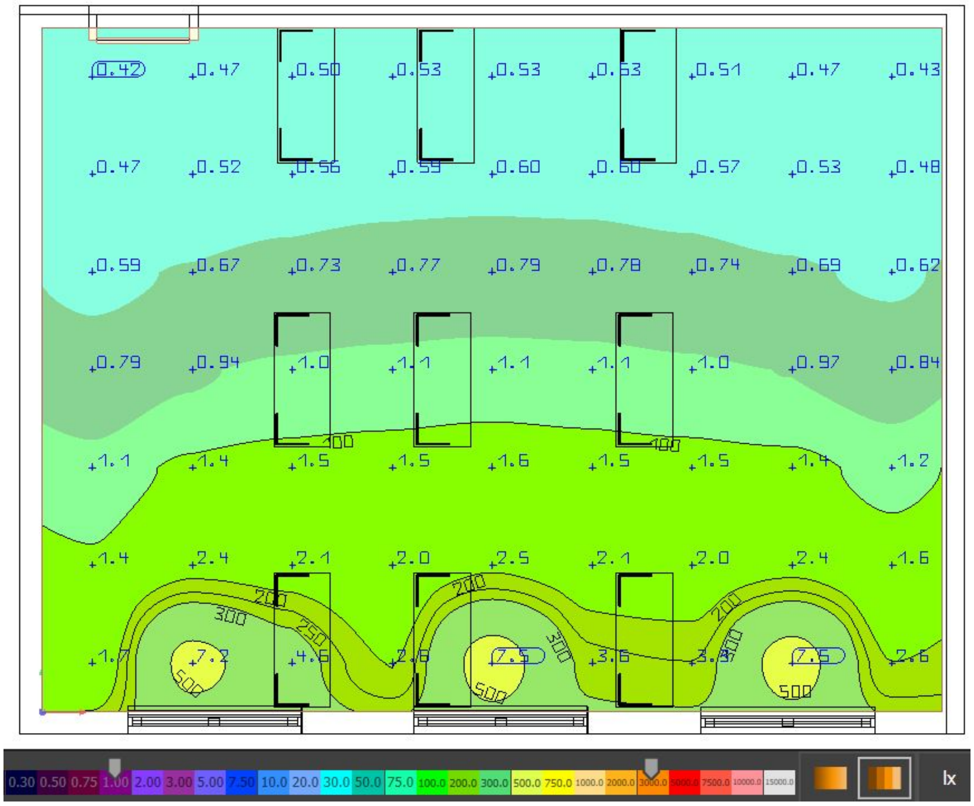

Figure C.11: DF and Lux distribution with blinds at 50% (new windows)

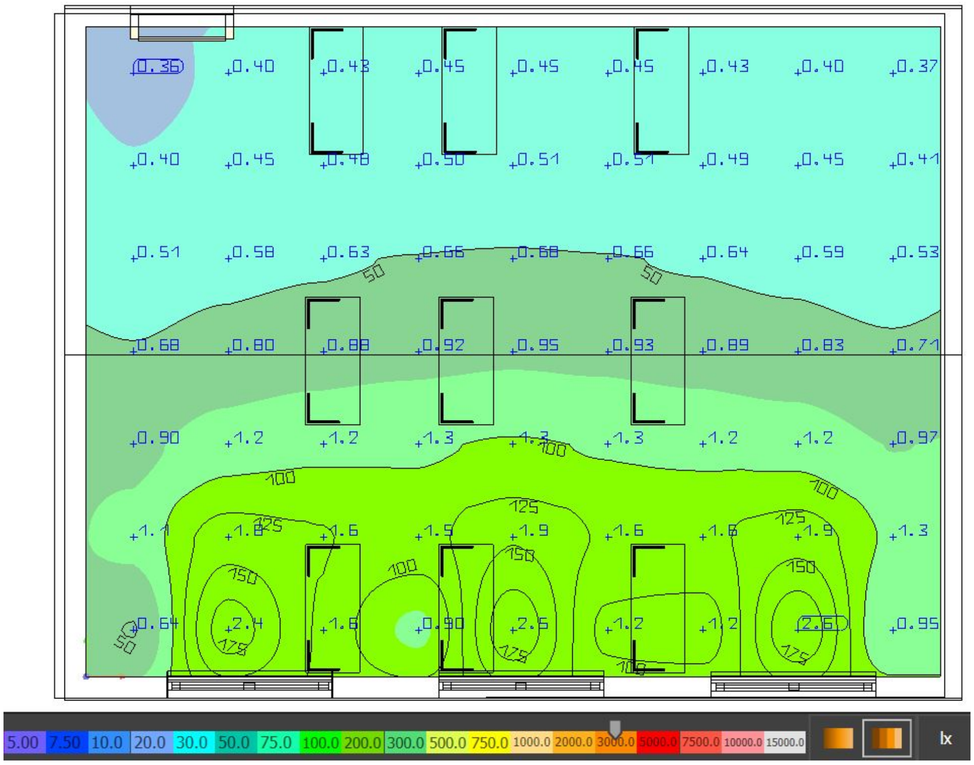

Figure C.12: DF and Lux distribution with blinds down (new windows)

C.4 Outdoor Conditions

An overview of the weather conditions more influential to window performance are showed in Figure C.13 and Figure C.14; External Temperatures and Direct Solar Radiation respectively.

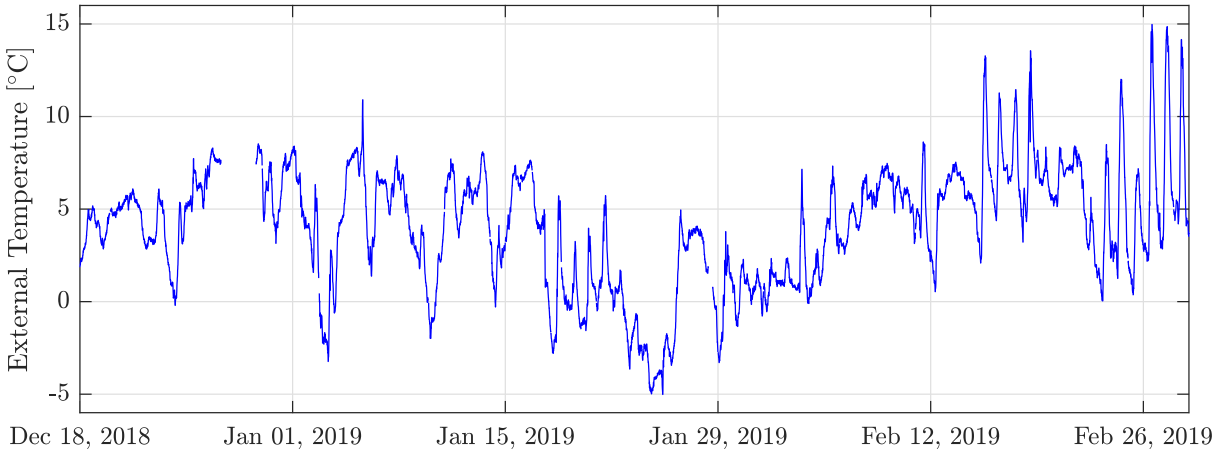

Figure C.13: Outside Temperature distribution - data every 10 min - at Ødis Primary School.

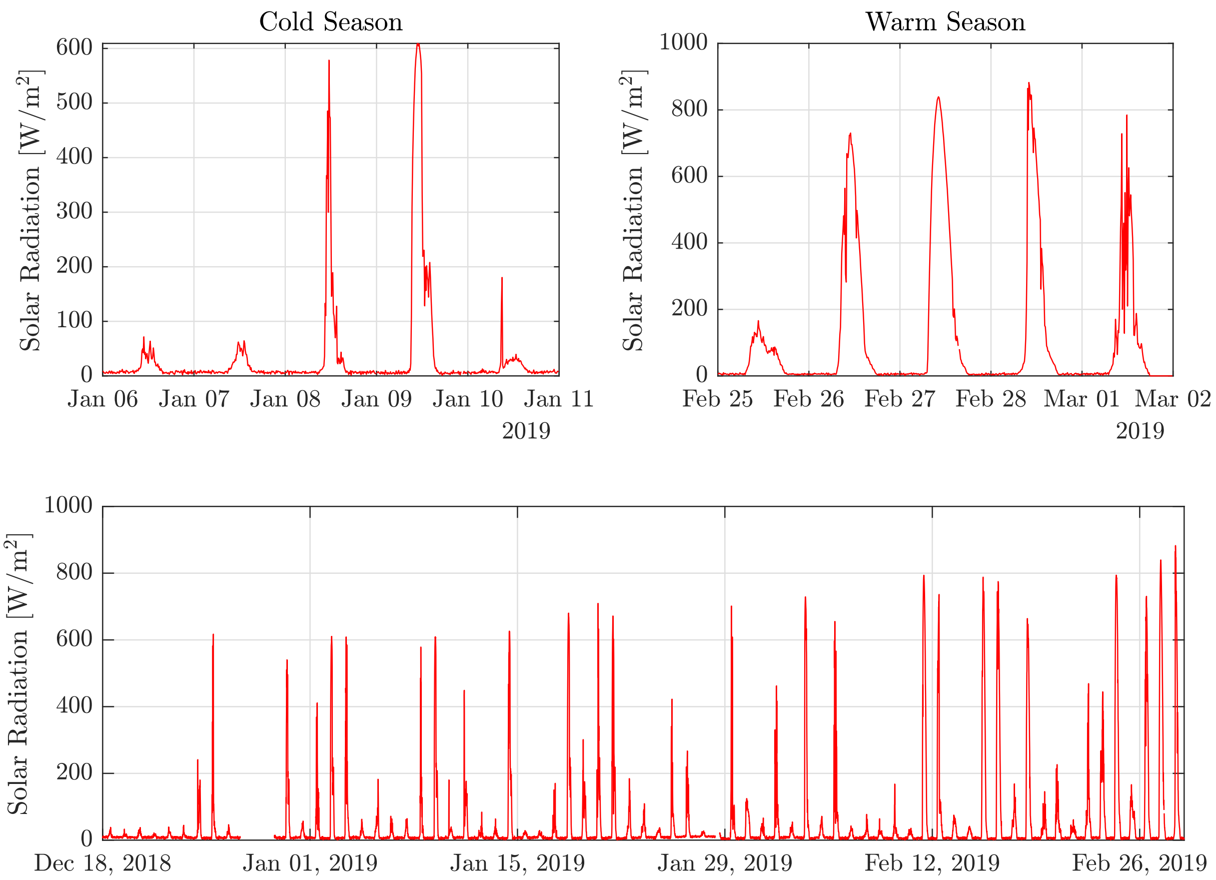

Figure C.14: Solar Radiation distribution - data every 10 min - at Ødis Primary School.

C.5 Visual Comfort WT2

Table C.2: Comparison of the measurements and the simulation for the visual comfort in school.

Sample 1 - RF:28

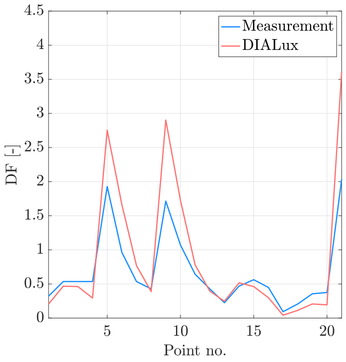

Sample 2 - LT:11 RF:13

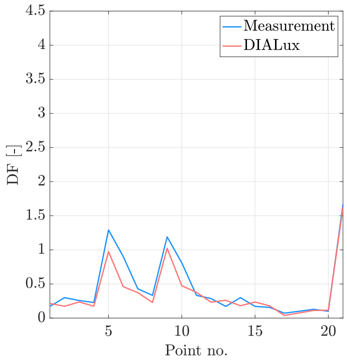

Sample 3 - LT:29 RF:12

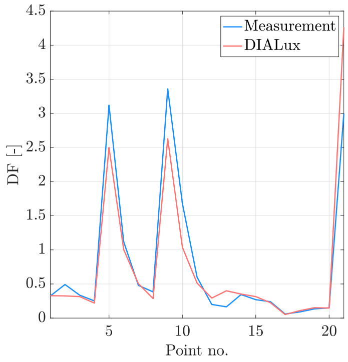

Sample 4 - LT:15 RF:11

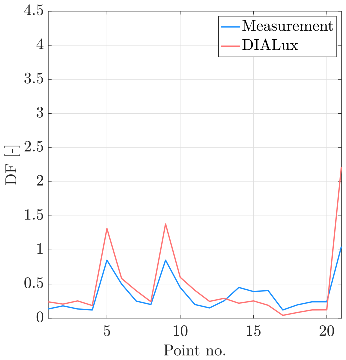

Sample 5 - LT:5 RF:15

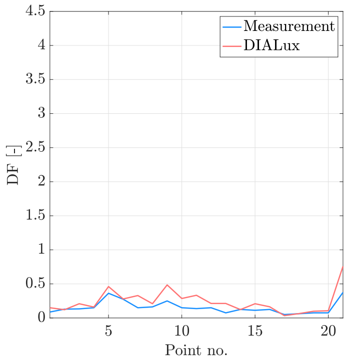

C.6 Passive Heat Recovery

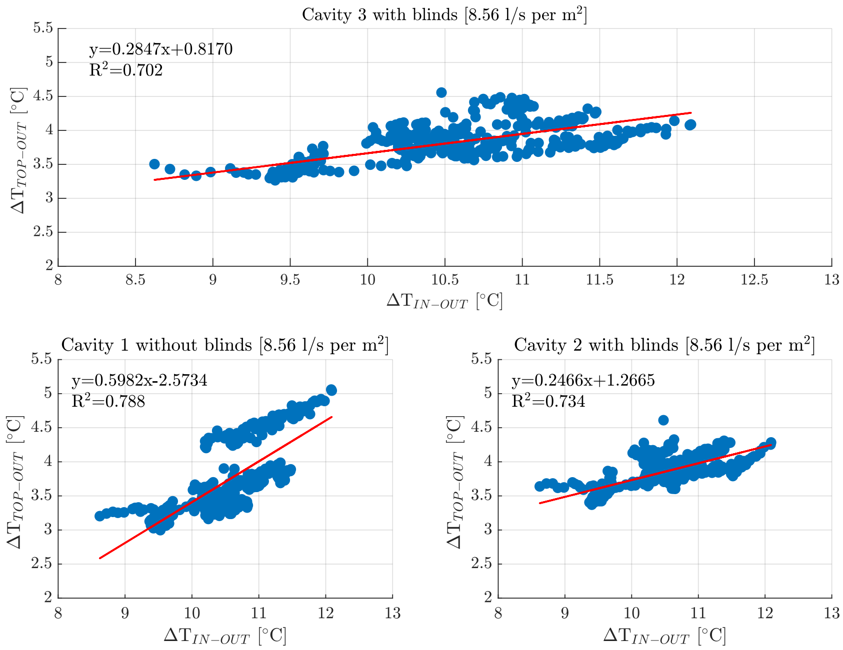

Figure C.15: Passive Heat Recovery for 8.56 l/s per m^2.

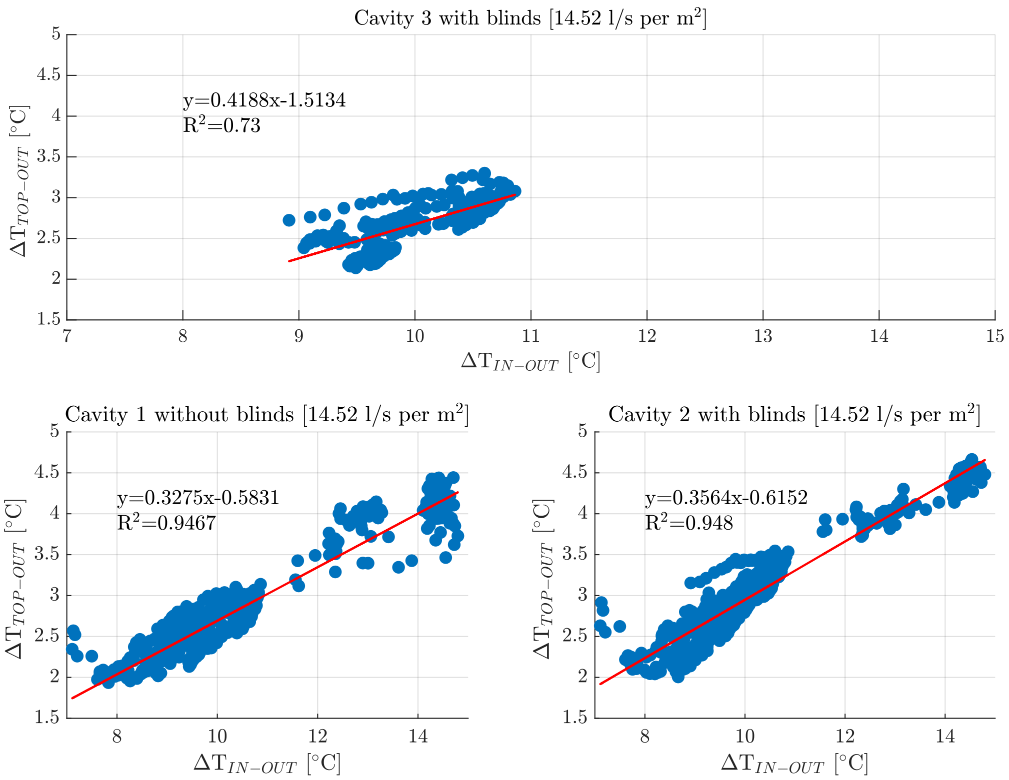

Figure C.16: Passive Heat Recovery for 14.52 l/s per m^2.

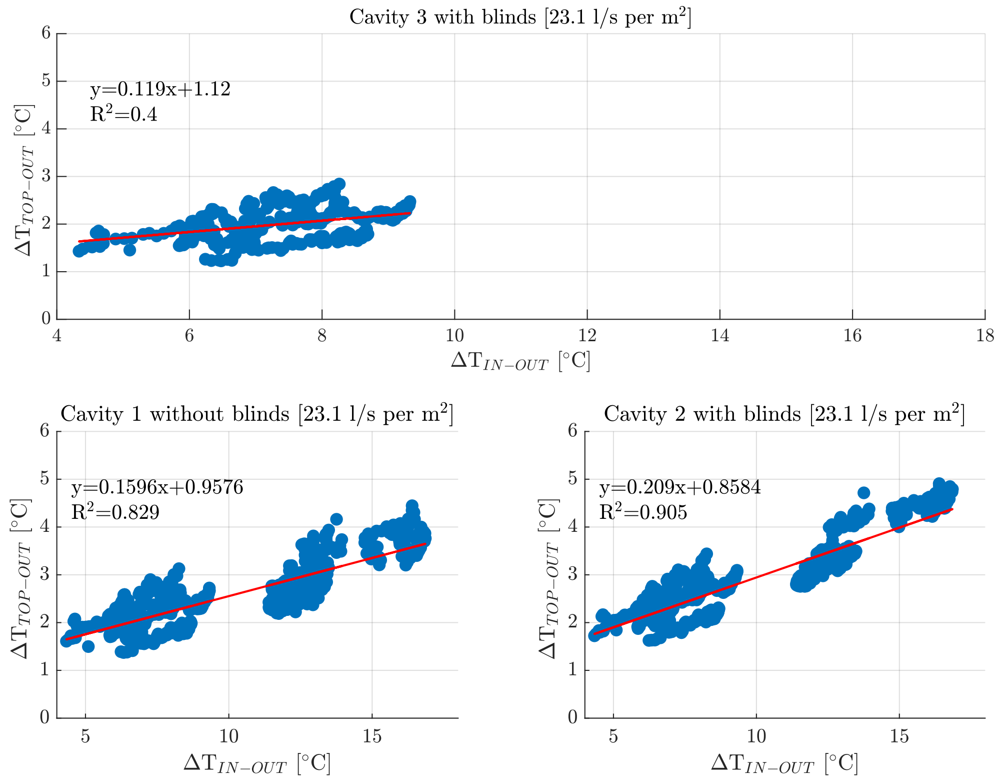

Figure C.17: Passive Heat Recovery for 23.1 l/s per m^2

C.6.1 Active Heat Recovery Test 1

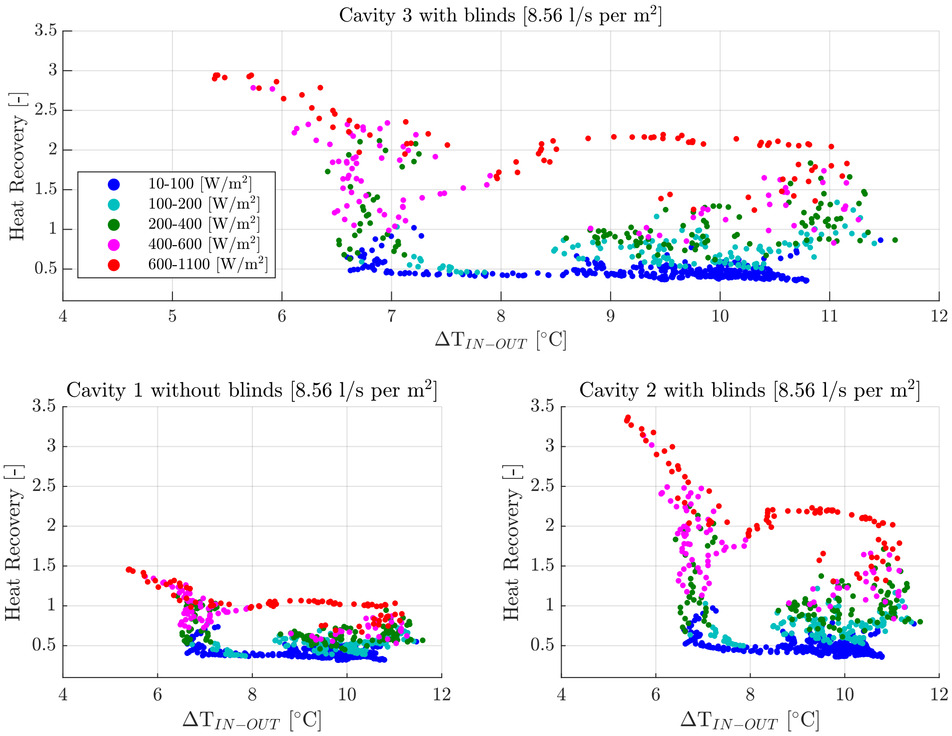

Figure C.18: Active Heat Recovery for 8.56 l/s per m^2.

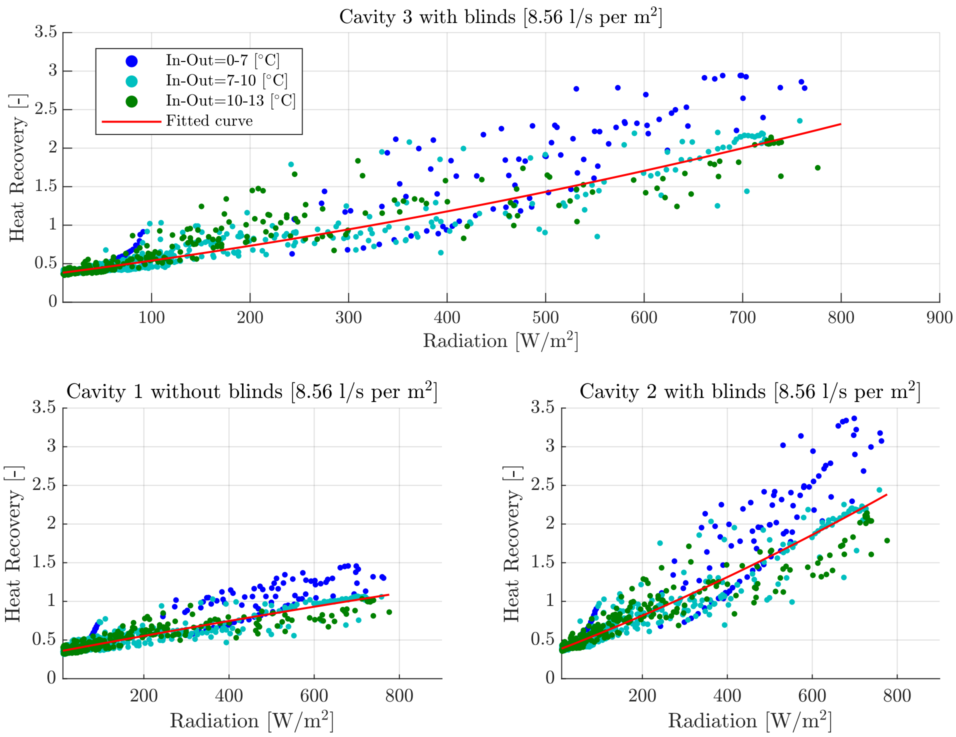

Figure C.19: Active Heat Recovery for 8.56 l/s per m^2.

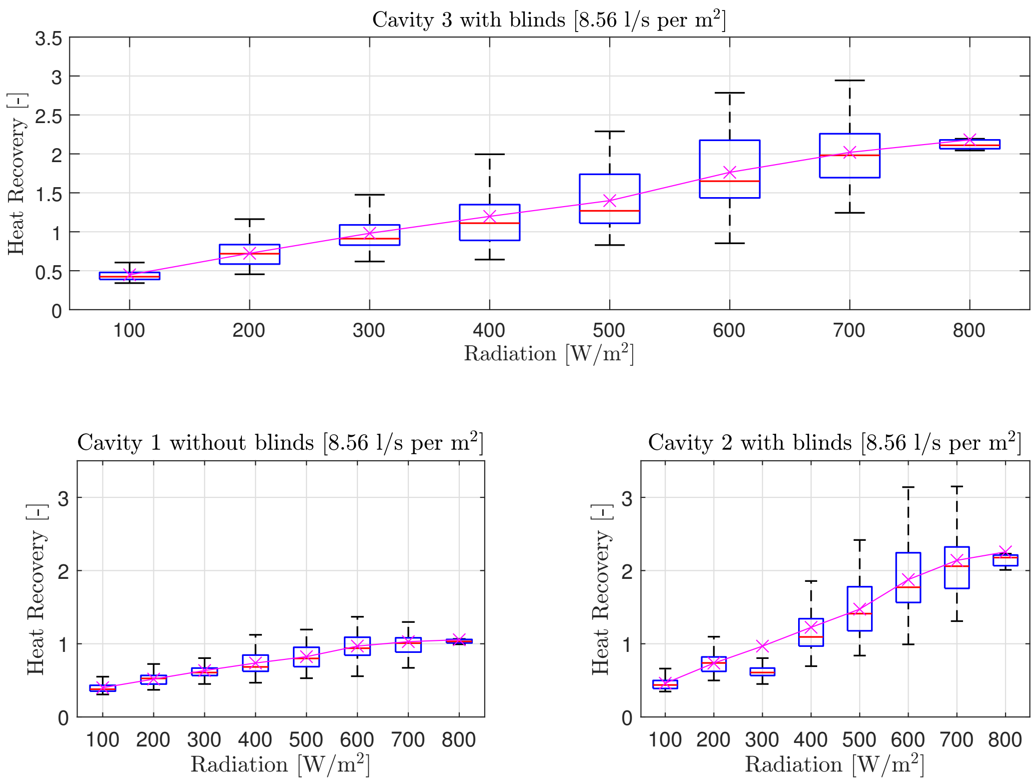

Figure C.20: Active Heat Recovery for 8.56 l/s per m^2.

C.6.2 Active Heat Recovery Test 2

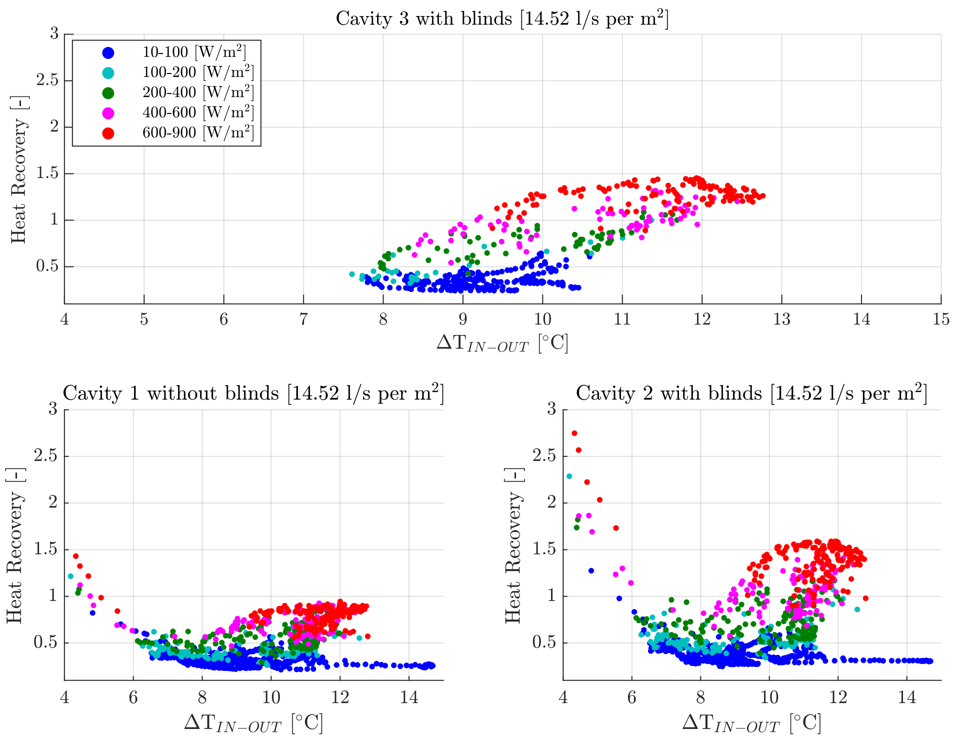

Figure C.21: Active Heat Recovery for 14.52 l/s per m^2

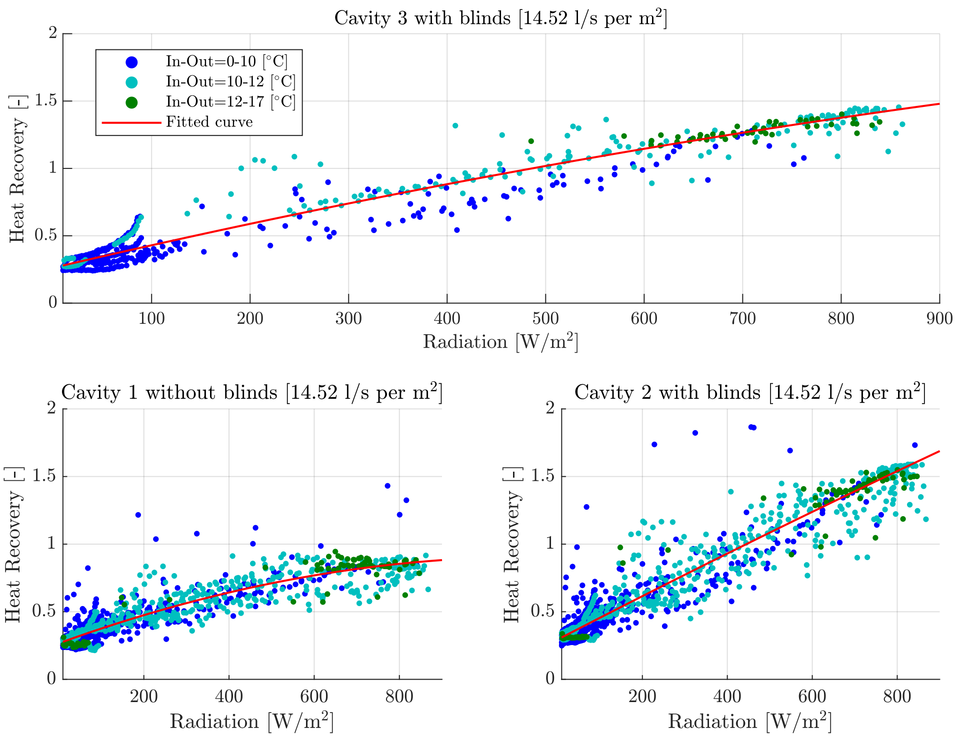

Figure C.22: Active Heat Recovery for 14.52 l/s per m^2.

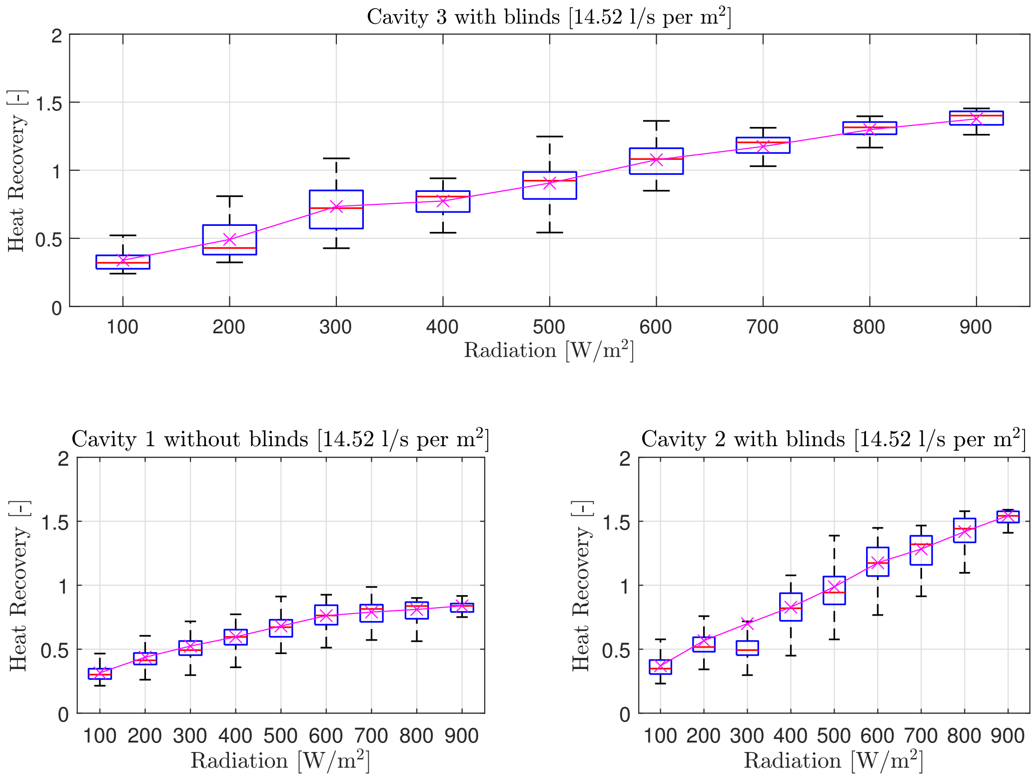

Figure C.23: Active Heat Recovery for 14.52 l/s per m^2.

C.6.3 Active Heat Recovery Test 3

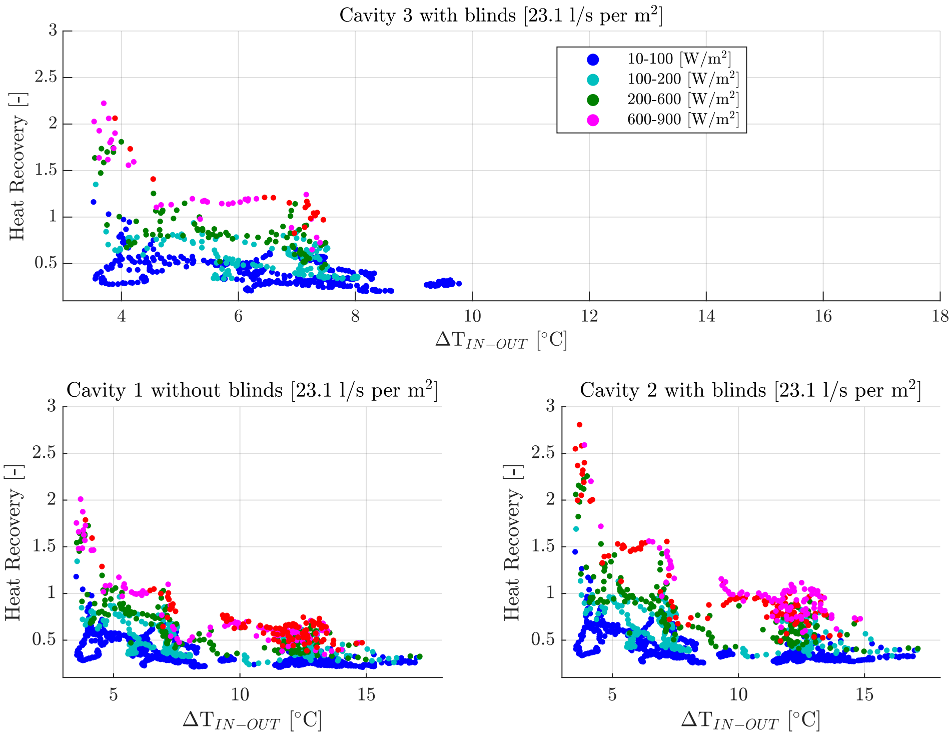

Figure C.24: Active Heat Recovery for 23.1 l/s per m^2.

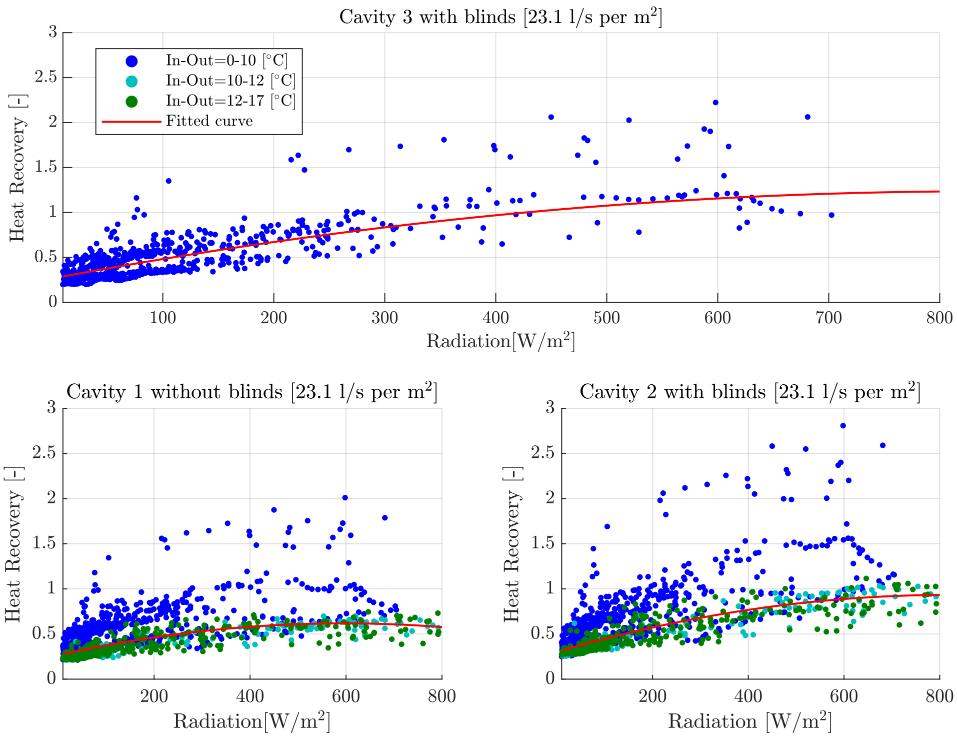

Figure C.25: Active Heat Recovery for 23.1 l/s per m^2.

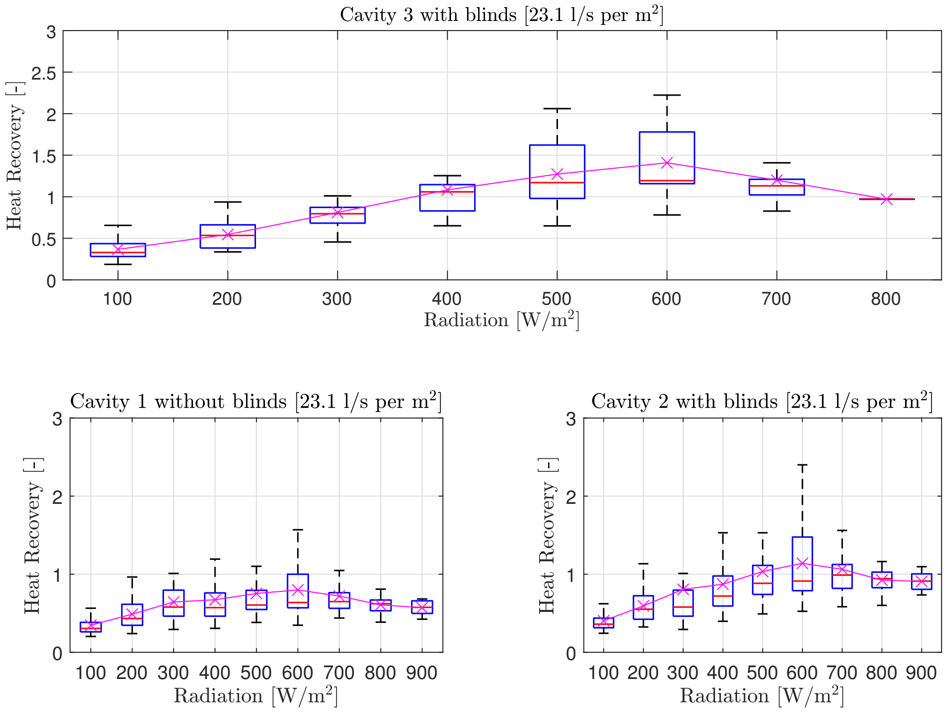

Figure C.26: Active Heat Recovery for 23.1 l/s per m^2.

C.7 Control Design - Node Red

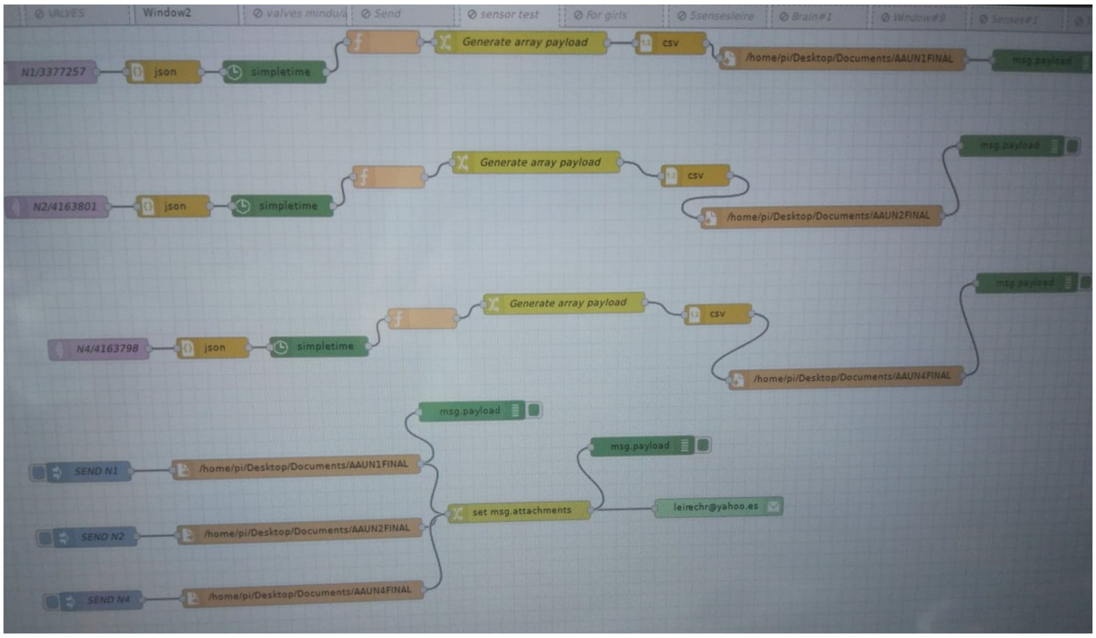

Figure C.27: Node-Red flow chart to make the sensors test.

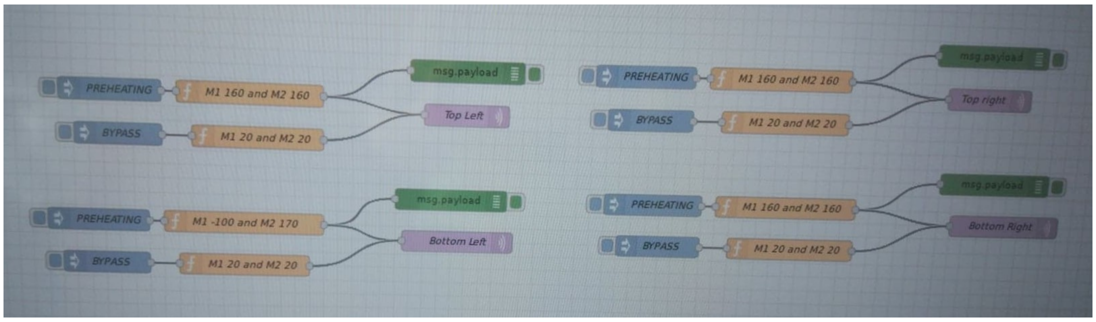

Figure C.28: Node-Red flow chart to change positioning of valves.

D

Request

21 November 2018, Aalborg

GROUP IE9_1-216-2

EMAIL

MARTA BONET ARBOS
mbonet17@student.aau.dk

LEIRE CHAVARRI REMIRO
lchava17@student.aau.dk

ALEKSANDRA MARIA TUTAJ
atutaj17@student.aau.dk

SUPERVISORS

PER KVOLS HEISELBERG
ph@civil.aau.dk

CHEN ZHANG
cz@civil.aau.dk

VENTILATIONSVINDUET
ph@ventilatiosvinduet.dk

Permission request

To whom it may concern,

This request is written on behalf of the students from Indoor Environmental and Energy Engineering at Aalborg University, working on the Master Thesis titled 'Ventilation Window performance and further improvements: a case study in a Primary School' under the supervision of Per Kvols Heiselberg and Chen Zhang with the collaboration of Ventilationsvinduet Company.

The purpose of this project is to test and analyze the performance of the ventilated windows located in two classrooms in Ødis school and provide with the solution that gives an optimal indoor environmental comfort for the occupants and energy savings for the school.

To do so, an experimental case study is required to measure several factors, such as CO_2, that will influence the indoor comfort and well-being of the students.

Therefore, in each classroom, 2 web cameras - model Logitech c920 will be installed to monitor the opening/closing of the window/door and the number of students located in the classrooms.

The pictures will be taken with low resolution and with no possibility to recognize the faces of the people in the classroom, as visible on the example below.

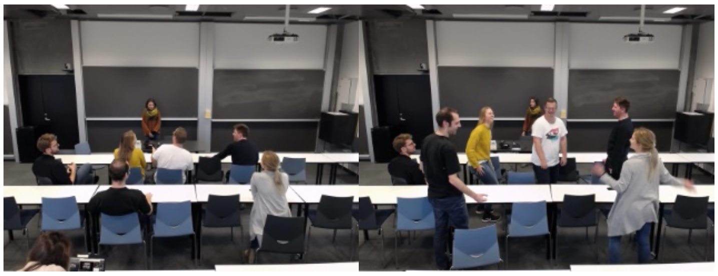

Figure 1 - Example images.

The cameras will take pictures every 5 minutes during the occupied hours (8-16), saved on a private computer located in the school and erased after the analysis is performed. The measurements are expected to be taken during the period between December 2018 – April 2019.

The University is committed to use the images only for educational proposes. They will be used as a part of an evaluation of the indoor environmental in the classrooms.

We ensure not to install and record images of the students without asking first your consent. If you agree to provide us with permission, please sign this letter and return one copy to us by email.

We would be grateful if you would return this form by 28/11/18 the latest.

We appreciate your consideration.

Sincerely,

Aleksandra Tutaj, Leire Chavarri and Marta Bonet

I agree, subject to the conditions set out above, to allow to take images of the students during school activities, to be used by Aalborg University for educational purposes.

Name

Signature

Date